

AD-A040 940

VANTAGE ENGINEERING FRENCHTOWN N J
A THEORY FOR HANDLING QUALITIES WITH APPLICATIONS TO MIL-F-8785--ETC(U)
OCT 75 R H SMITH

F/6 1/3

F33615-74-C-0035

AFFDL-TR-75-119

NL

UNCLASSIFIED

1 OF 2

AD
A040 940



AFFDL-TR-75-119✓

Q B.S.

AD A 040940

A THEORY FOR HANDLING QUALITIES WITH APPLICATIONS TO MIL-F-8785B

VANTAGE ENGINEERING, 410 239
FRENCHTOWN, NEW JERSEY

OCTOBER 1976

TECHNICAL REPORT AFFDL-TR-75-119
FINAL REPORT FOR PERIOD FEBRUARY 1974 TO JULY 1975

Approved for public release; distribution unlimited

AU NO. _____
DDC FILE COPY

AIR FORCE FLIGHT DYNAMICS LABORATORY
AIR FORCE WRIGHT AERONAUTICAL LABORATORIES
AIR FORCE SYSTEMS COMMAND
WRIGHT-PATTERSON AIR FORCE BASE, OHIO 45433

DDC
JUN 23 1977
RESOLVED
C

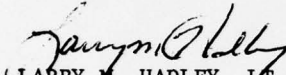
NOTICE


When Government drawings, specifications, or other data are used for any purpose other than in connection with a definitely related Government procurement operation, the United States Government thereby incurs no responsibility nor any obligation whatsoever; and the fact that the Government may have formulated, furnished, or in any way supplied the said drawings, specifications, or other data, is not to be regarded by implication or otherwise as in any manner licensing the holder or any other person or corporation, or conveying any rights or permission to manufacture, use, or sell any patented invention that may in any way be related thereto.

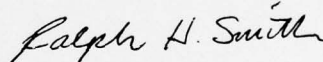
This report has been reviewed by the Information Office (OI) and is releasable to the National Technical Information Service (NTIS). At NTIS it will be available to the general public, including foreign nations.

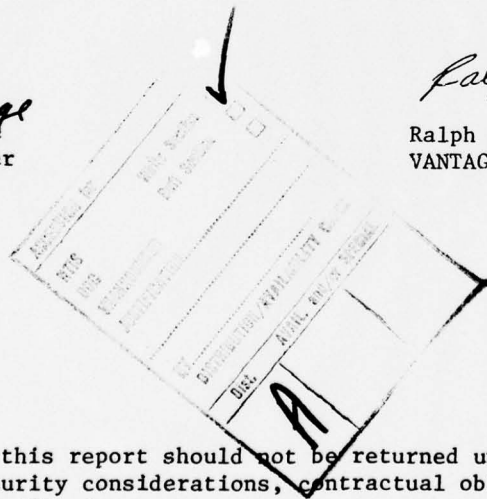
This technical report has been reviewed and is approved for publication.

FOR THE COMMANDER


LARRY M. HADLEY, LT COL, USAF
Chief, Flight Control Division


Frank L. George
Project Engineer


Ralph H. Smith, Author
VANTAGE ENGINEERING



Copies of this report should not be returned unless return is required by security considerations, contractual obligations, or notice on a specific document.

UNCLASSIFIED

SECURITY CLASSIFICATION OF THIS PAGE (When Data Entered)

REPORT DOCUMENTATION PAGE		READ INSTRUCTIONS BEFORE COMPLETING FORM	
1. REPORT NUMBER	2. GOVT ACCESSION NO.	3. REPORT'S CATALOG NUMBER	
18 AFFDL-TR-75-119			
4. TITLE (and Subtitle)	5. TYPE OF REPORT & PERIOD COVERED	6. PERFORMING ORG. REPORT NUMBER	
6 A Theory for Handling Qualities with Applications to MIL-F-8785B,	9 Final Report 11 Feb 74 - 30 Jul 75		
7. AUTHOR(s)	8. CONTRACT OR GRANT NUMBER(s)		
10 Ralph H. Smith	15 F33615-74-C-0035		
9. PERFORMING ORGANIZATION NAME AND ADDRESS	10. PROGRAM ELEMENT PROJECT, TASK & WORK UNIT NUMBERS		
Vantage Engineering Star Route Box 26-A Frenchtown, New Jersey 08825	PE 62201F Project 8219 Work Unit 82190414		
11. CONTROLLING OFFICE NAME AND ADDRESS	12. REPORT DATE	13. NUMBER OF PAGES	
AFFDL/FGC Wright-Patterson Air Force Base, Ohio 45433	14 October 1975		
14. MONITORING AGENCY NAME & ADDRESS (if different from Controlling Office)	15. SECURITY CLASS. (of this report)	15a. DECLASSIFICATION DOWNGRADING SCHEDULE	
12 185p.	UNCLASSIFIED		
16. DISTRIBUTION STATEMENT (of this Report)			
Approved for public release; distribution unlimited.			
17. DISTRIBUTION STATEMENT (of the abstract entered in Block 20, if different from Report)			
18. SUPPLEMENTARY NOTES			
19. KEY WORDS (Continue on reverse side if necessary and identify by block number)			
Flying qualities Flying quality specifications Pilot models Manual control			
20. ABSTRACT (Continue on reverse side if necessary and identify by block number)			
This report hypothesizes a model for pilot-airplane system dynamics which, it is claimed, will unify existing theories, explain peculiarities in available human response data, and permit the prediction of pilot opinion rating (POR) for tasks of interest to the assessment of aircraft flying qualities. The hypothesized model structure is multiple loop with essential nonlinearities. The proposed pilot model is further hypothesized to account for much that has been identified as pilot adaptation in past work. An attempt to parameterize			

DD FORM 1 JAN 73 1473

EDITION OF 1 NOV 65 IS OBSOLETE

UNCLASSIFIED

SECURITY CLASSIFICATION OF THIS PAGE (When Data Entered)

410239

UNCLASSIFIED

SECURITY CLASSIFICATION OF THIS PAGE(When Data Entered)

the proposed model by a trial and error digital computer simulation produced promising but inconclusive results. However, comparison of the proposed pilot model with known forms of measured pilot dynamics for a wide range of aircraft dynamics suggested a metric for the correlation and prediction of POR that appears to be physically related to activity at a particular point within the central nervous system. This metric was evaluated for certain available data sets and was shown to be a consistent and sensitive measure of POR. It was then used to evaluate the short-period requirements of the flying qualities specification MIL-F-8785B. Several general and specific changes to the specification are recommended as a result of this study.

UNCLASSIFIED

SECURITY CLASSIFICATION OF THIS PAGE(When Data Entered)

FOREWORD

This report represents a portion of an effort to up-date MIL-F-8785B, the flying qualities specification for piloted, military airplanes, and to extend its applicability in a continually changing state-of-the-art of flight control system design. This research was performed on-site at the Air Force Flight Dynamics Laboratory under Contract AF33615-74-C-0035 as part of Air Force Project 8219, Task 821904. The AFFDL project engineer was Mr. Frank L. George (AFFDL/FGC). All work was performed by the author, Ralph H. Smith, of Vantage Engineering, Frenchtown, New Jersey, during the period February 1974 through July 1975. The draft of this report was submitted in September 1975.

The author gratefully acknowledges the interest and support given to this work by several members of the AFFDL engineering staff. Among these, Messers Charles B. Westbrook, Robert J. Woodcock, and Frank L. George were instrumental in electing to permit the author to pursue a high-risk approach to a chronic problem of manned flight control. The author is further indebted to Mr. Ronald O. Anderson for his timely assistance in the compilation of available handling qualities data for use in this study, and to Captain Jerry B. Callahan for his considerable help with the computational aspects of this effort. Finally, the contributions of Major James Dillow of the Air Force Institute of Technology are acknowledged. He made it possible to test the theory of pilot rating prediction by providing the necessary computer programs and instructing the author in their use.

TABLE OF CONTENTS

SECTION	TITLE	PAGE
I.	INTRODUCTION.....	1
II.	A UNIFIED MODEL FOR PILOT DYNAMICS IN SINGLE LOOP TRACKING. PART 1: THEORY AND BASE-LINE ANALYSIS	
	A. Background.....	6
	B. Two Hypotheses.....	11
	C. A Nonlinear Time Delay Model.....	12
	D. Candidate Models For Pilot Dynamics.....	19
	E. Requirements For Model Validation.....	22
	F. Spectral Analysis.....	23
	G. Servo vs. Nonlinear Pilot Model Comparisons.....	29
III.	A UNIFIED MODEL FOR PILOT DYNAMICS IN SINGLE LOOP TRACKING. PART 2: COMPUTER SIMULATION AND PARAMETER SEARCHES	
	A. The Approach.....	41
	B. Model Configurations Tested.....	42
	C. Results.....	44
	D. Conclusions.....	47
IV.	PREDICTION OF PILOT OPINION RATING	
	A. General Comments.....	49
	B. Implications of the Nonlinear, Multiple Loop Pilot Model.....	51
	C. A Metric for Rating Prediction in Single Loop Tracking.....	53
	D. Validation of the Rating Metric for Single Loop Tracking.....	56
	E. Rating Differences: In-Flight vs. Fixed-Base....	63
	F. Rating Prediction in Multiple Loop Tracking.....	66
	G. Comments on Multiple Axis Rating Prediction.....	73
	H. Re-examination of the Paper Pilot Concept.....	74
V.	IMPLICATIONS TO MIL-F-8785B	
	A. General Comments.....	82
	B. Selected Airframe Dynamic Configurations.....	82
	C. Investigation of Short-Period Requirements.....	84
	D. Turbulence Effects.....	86
	E. Motion Cue Effects.....	90
	F. Conclusions and Recommendations.....	91

TABLE OF CONTENTS (CONTINUED)

SECTION	TITLE	PAGE
APPENDIX A	A COMPUTER MODEL FOR A NONLINEAR TIME DELAY.....	94
APPENDIX B	A SUBROUTINE FOR THE ESTIMATION OF DESCRIBING FUNCTIONS.....	102
REFERENCES.....		169

LIST OF ILLUSTRATIONS

NUMBER		PAGE
1.	The Servo Model for Pilot Dynamics (The Precision Pilot Model).....	133
2.	The Optimal Control (Kleinman) Model for Pilot Dynamics	134
3.	Latency Time Delay for Visual Rate Detection vs. Rate of Object Motion.....	135
4.	Time Response Properties -- Nonlinear Delay.....	136
5.	Generic Amplitude Properties of Closed Loop System Dynamics.....	137
6.	Model for Evaluation of Nonlinear Delay Dynamics.....	138
7.	Measured Describing Functions for a Nonlinear Delay: Effects of σ_i and $Y_c(s)$	139
8.	Measured Describing Functions for a Nonlinear Delay: Effect of Input Bandwidth.....	140
9.	Nonlinear Model for Pilot-Vehicle System Dynamics.....	141
10.	A Special Closed Loop System.....	142
11.	Special Case #1; Block Diagram Reduction ($x_i = dy_i/dt$, $x = dy/dt$).....	143
12.	Special Case #2; Block Diagram Reduction ($x_i = 0$).....	144
13.	Phase Margin Variations.....	145
14.	Computer-Measured Neuromuscular System Dynamics.....	146
15.	Measured Controlled Element Dynamics, $Y_c = 11.9$	147
16.	Measured Controlled Element Dynamics, $Y_c(s) = 11.9/s$...	148
17.	Measured Controlled Element Dynamics, $Y_c(s) = 11.9/(s-2)$	149
18.	Measured Controlled Element Dynamics, $Y_c(s) = 11.9/s^2$..	150
19.	Measured Controlled Element Dynamics, $Y_c(s) = 11.9/s(s-2)$	151

LIST OF ILLUSTRATIONS (CONTINUED)

NUMBER		PAGE
20.	Comparison of Predicted vs. Experimental $Y_p(j\omega)$	152
21.	Comparison of Predicted vs. Experimental $Y_p(j\omega)$	153
22.	Pilot Rating vs. σ_{β_x} -- Generic.....	154
23.	Equivalent Kleinman-Dillow Model (Converged) for the Arnold Experiment.....	155
24.	Variation of Pilot Opinion Rating With the Proposed Rating Metric.....	156
25.	Correlation of Pilot Opinion Rating With Arnold's Rating Expression.....	157
26.	Variation of McDonnell's and Onstott's, et al, Rating Data With the Proposed Rating Metric.....	158
27.	Comparison of Simulation and Flight Test Pilot Ratings	159
28.	Variations of Pilot Opinion Rating With σ_{β_x} & σ_{β_q} for Multiple Loop Tracking (Miller-Vinje Data).....	160
29.	Rate Signal Activity Measure With a Mode-Switching Model for Pilot Dynamics -- Multiple Loop.....	161
30.	Variation of Pilot Opinion Rating With σ_{β_x} for Multiple Loop Tracking (Teper Data).....	162
31.	Variation of Pilot Opinion Rating With σ_{β_q} for Multiple Loop Tracking (Teper Data).....	163
32.	Short-Period Frequency and Damping Requirements; MIL-F-8785B; Category A.....	164
33.	Comparison of Predicted POR With MIL-F-8785B; Case 1 (CAP=Parameter); $\sigma_{w_g} = 10$ f/s.....	165
34.	Comparison of Predicted POR With MIL-F-8785B; Case 2 (ω_{sp} =Parameter); $\sigma_{w_g} = 10$ f/s.....	166
35.	Comparison of Paper Pilot Rating Prediction and Actual Pilot Ratings for Arnold's Experiment.....	167
36.	Comparison of Paper Pilot Rating Prediction and Actual Pilot Ratings for McDonnell's Experiment.....	168

LIST OF TABLES

NUMBER		PAGE
1.	System Input (From Reference 4).....	108
2.	Longitudinal Dynamic Configurations Tested in Arnold's Experiment.....	109
3.	Kleinman-Dillow Model Parameters for the Arnold Data...	110
4.	Kleinman-Dillow Model Parameters for the McDonnell Data	111
5.	Paper Pilot Parameters for the Onstott Data (After Johnson).....	112
6.	Kleinman-Dillow Model Parameters for the Arnold/Neal-Smith Configurations.....	113
7.	Performance Comparison: Measured vs. Kleinman-Dillow Model Predictions (Miller-Vinje Data).....	114
8.	Conversion of Miller-Vinje POR to the Cooper-Harper Scale.....	115
9.	Kleinman-Dillow Model Parameters for the Miller-Vinje Data.....	116
10.	Kleinman-Dillow Model Predictions of Signal Cross-Correlations.....	117
11.	Estimated Rate Control Activity Metrics for Miller-Vinje Cases.....	118
12.	Aircraft Stability Derivative Set; Case 1.....	119
13.	Aircraft Stability Derivative Set; Case 2.....	122
14.	Aircraft Stability Derivative Set; Case 3.....	123
15.	Kleinman-Dillow Model Parameters and Predicted POR; Case 1, $\sigma_{wg} = 10$ f/s.....	124
16.	Kleinman-Dillow Model Parameters and Predicted POR; Case 2, $\sigma_{wg} = 10$ f/s.....	125
17.	Kleinman-Dillow Model Parameters and Predicted POR; Case 3, $\sigma_{wg} = 10$ f/s.....	126

LIST OF TABLES (CONTINUED)

NUMBER	PAGE
18. Kleinman-Dillow Model Parameters and Predicted POR; Case 1, $\sigma_{wg} = 16$ f/s.....	127
19. Kleinman-Dillow Model Parameters and Predicted POR; Case 2, $\sigma_{wg} = 16$ f/s.....	128
20. Kleinman-Dillow Model Parameters and Predicted POR; Case 3, $\sigma_{wg} = 16$ f/s.....	129
21. Kleinman-Dillow Model Parameters and Predicted POR; Case 1, $\sigma_{wg} = 5$ f/s.....	130
22. Predicted Variation of POR With ω_{sp} at Constant $V_{T\theta_2}$ and ζ_{sp} ; $\sigma_{wg} = 10$ f/s.....	131
23. Effects of M_α on Predicted POR.....	132

LIST OF SYMBOLS

a_z	Aircraft normal acceleration measured at the center of gravity, f/s^2 .
a_{z_p}	Aircraft normal acceleration measured at the pilot's station, f/s^2 .
c	Closed loop system command input.
CAP	"Control Anticipation Parameter" = $\omega_{sp}^2 / (n/\alpha)$.
e	Closed loop system positional error.
\dot{e}	de/dt .
$E[x_i x_j]$	Covariance of $x_i(t)$ and $x_j(t)$ over a specified time interval.
$G_M(j\omega)$	Describing function model for neuromuscular system dynamics.
$G_x(j\omega)$	Describing function model for central processor dynamics in rate channel of human pilot model.
$G_y(j\omega)$	Describing function model for central processor dynamics in positional channel of human pilot model.
J	Cost functional for the optimal pilot model.
K	Constant of proportionality in nonlinear time delay model.
K_c	Gain of controlled element transfer function.
K_{D_x}	Equivalent display gain in the x-channel of the Kleinman-Dillow model or the average equivalent gain in the rate channel between x_e and x_w for the multiple loop pilot model.
$K_{E_{x_i}}$	Equivalent x_i -channel gain of the central processor of a mode-switching model for the human pilot.
K_{F_q}	Equivalent Kalman filter gain in the q-channel of the Kleinman-Dillow model.
K_{F_u}	Equivalent Kalman filter gain in the u-channel of the Kleinman-Dillow model.
K_{F_x}	Equivalent Kalman filter gain in the x-channel of the Kleinman-Dillow model.

LIST OF SYMBOLS (CONTINUED)

K_M	Gain of the neuromuscular system dynamic model.
K_P	Gain of the "Precision Pilot Model".
K_{P_x}	Equivalent state predictor gain in the x-channel of the Kleinman-Dillow model.
$K_{P_{x_i}}$	Gain of the x_i -loop of a servo model for human pilot dynamics.
K_q^*	Optimal controller gain in the q-channel of the Kleinman model.
K_K	Average equivalent pilot model gain in the rate channel between the sensed rate and the signal β_x from the rate channel to the neuromuscular system.
$K_T[a_T/G_T]$	Visual and indifference threshold describing function for the "Precision Pilot Model".
K_u^*	Optimal controller gain in the u-channel of the Kleinman model.
K_x	Pilot model gain in the x-channel.
K_x^*	Optimal controller gain in the x-channel of the Kleinman model.
K_{x_o}	Average value of the nonlinear x-channel gain $K_x(x_w)$ in the multiple loop pilot model.
K_y	Pilot model gain in the y-channel.
K_{y_o}	Average value of the nonlinear y-channel gain $K_y(y_T)$, including a describing function representation for visual threshold effects, in the multiple loop pilot model.
M_{δ_e}	Pitching moment control effectiveness derivative; rad/sec^2 (except for the Miller-Vinje data where units are $\text{rad/sec}^2/\text{inch}$).
n/α	Steady state change in aircraft normal acceleration per unit change in angle of attack for a step change in elevator deflection at constant airspeed and Mach number; g's/radian.
p	$d\phi/dt$.
P_1	Weighting on rate error in the switching function.

LIST OF SYMBOLS (CONTINUED)

POR	Pilot opinion rating; the Cooper-Harper scale is assumed unless otherwise specified.
P _{SP}	Neuromuscular system inverse time constant (hypothesized to originate from spindle system dynamics); 1/sec.
q	$d\theta/dt$.
r	$d\psi/dt$.
S or SF	Switching function; used for the determination of the signal in the human pilot model.
s	$\sigma + j\omega$; the complex Laplace transform variable.
t	Time; secs.
TF	Run length in computer simulation of pilot-vehicle system dynamics; secs.
T _I	Lag time constant for the "Precision Pilot Model", secs.
T _K , T _K ⁱ	Low frequency lead and lag time constants in the "Precision Pilot Model"; secs.
T _L	Lead time constant for the "Precision Pilot Model", secs.
T _L _{x_i}	x _i -loop lead time constant of a servo model for human pilot dynamics; secs.
T _{N1}	Time constant of the first-order pole in the neuromuscular system describing function; secs.
T _w	Rate loop washout time constant in human pilot model; secs --or-- numerator time constant of the $\frac{w}{g}$ (s) transfer function (short-period approximation); secs.
T' _w	Rate loop washout time constant in human pilot model, as modified due to effects of rate loop closure; secs.
T _{θ₂}	Numerator time constant of the $\frac{\theta}{\delta e}$ (s) transfer function (short-period approximation); secs.
u	Perturbation of forward velocity measured in a stability axis system; f/s.

LIST OF SYMBOLS (CONTINUED)

U_o	Aircraft nominal airspeed (stability axes); f/s.
v_g	Lateral gust-induced velocity perturbation (stability axes); f/s.
W	Aircraft weight; lbs.
w	Perturbation of the vertical velocity component of aircraft velocity due to gust or control (stability axes); f/s.
w_g	Vertical gust velocity (stability axes); f/s.
x	Closed loop system rate of response --or-- $\int u(t)dt$ = forward position relative to a fixed spot for VTOL hover control; ft.
$x_d(\tau)$	$x_w(t - \tau)$.
x_e	Closed loop rate error.
$X_i(j\omega)$	Fourier transform of $x_i(t)$.
$\overline{X_i(j\omega)}$	Complex conjugate of $X_i(j\omega)$.
x_i	Closed loop system rate command input = dy_c/dt .
x_s	Rate error as sensed by the human pilot's central processor model.
x_w	Response of the rate washout model.
y	Closed loop pilot-vehicle system's positional response.
$Y_c(s)$	Controlled element (vehicle) transfer function.
$Y_{DL}(j\omega)$	Describing function for the nonlinear time delay model.
y_e	Closed-loop pilot-vehicle system error.
$y_i(t)$	Closed loop system command input.
$Y_p(j\omega)$	Describing function model for pilot dynamics;

$$Y_p(j\omega) = \frac{\Phi_{y_i s}(j\omega)}{\Phi_{y_i y_e}(j\omega)}$$

LIST OF SYMBOLS (CONTINUED)

y_T	Response of threshold in visual position sensor.
Z_w	Dimensional z-force derivative with respect to w; 1/sec.

Greek Symbols

α	Low frequency phase approximation parameter in the "Precision Pilot Model".
α_g	Gust-induced angle of attack; degs.
β	Signal from the central processor of pilot model to the neuromuscular system.
β_q	Signal from the q-channel of the pilot model central processor to the neuromuscular system.
β_x	Signal from the x-channel of the pilot model central processor to the neuromuscular system.
β_y	Signal from the y-channel of the pilot model central processor to the neuromuscular system.
β_u	Signal from the u-channel of the pilot model central processor to the neuromuscular system.
ΔT	Time step size in the computer simulation of pilot-vehicle system dynamics; secs.
δ	Pilot's control response; degrees, radians, or inches.
δ_e	Elevator deflection angle; degs or rad.
δ_N	Damping ratio of second-order component of the neuromuscular system describing function.
δ_{sp}	Damping ratio of the short-period mode.
θ	Pitch attitude; degs (unless otherwise specified).
σ	Real part of complex variable s.
σ_i	RMS value of command or disturbance input to the pilot-vehicle system; inches of displayed error or f/s.

410239

4/8

LIST OF SYMBOLS (CONTINUED)

- σ_{β_q} RMS value of $\beta_q(t)$; the proposed, unified handling quality metric for pitch attitude tracking; inches (unless otherwise specified).
- σ_{β_x} RMS value of $x(t)$; the proposed, unified handling quality metric for any tracking task; inches (unless otherwise specified).
- σ_{x_i} RMS value of any signal $x_i(t)$.
- τ Time delay in the sensation of visual rate, or time delay in the "Precision Pilot Model"; secs.
- τ_N Equivalent time delay in the human pilot describing function for the special case $x_i(t) = 0$; secs.
- τ'_N Equivalent time delay in the human pilot describing function originating due to dynamic coupling between the nonlinear delay and the neuromuscular system dynamics as a result of closed loop control of rate error for the special case $x_i(t) = 0$; secs.
- τ_{NM} Neuromuscular system time delay for the "Precision Pilot Model"; secs.
- τ_o Average value of the nonlinear delay $\tau(x_w)$; secs.
- $\Phi_{x_i x_i}(\omega)$ Power spectral density of the time signal $x_i(t)$.
- $\Phi_{x_i x_j}(j\omega)$ Cross spectral density of the time signals $x_i(t)$ and $x_j(t)$.
- ϕ Aircraft roll angle or the transfer function phase angle; degs.
- ψ Aircraft heading angle; degs.
- ω Imaginary part of the complex variable s ; rad/sec.
- ω_i Bandwidth of command or disturbance input to the pilot-vehicle system; rad/sec.
- ω_k Measurement frequencies for describing function estimation; rad/sec.
- ω_N Undamped natural frequency of second-order component of the neuromuscular system describing function; rad/sec.

LIST OF SYMBOLS (CONTINUED)

ω_{sp} Undamped natural frequency of the short-period mode; rad/sec.

Transfer Function Notation

$$\frac{x_i}{\delta}(s) = \frac{N_{\delta}^{x_i}(s)}{\Delta(s)} = X_{i\delta}(s)$$

$N_{\delta}^{x_i}(s)$ Numerator polynomial of the $\frac{x_i}{\delta}(s)$ transfer function.

$\Delta(s)$ Denominator polynomial of the $\frac{x_i}{\delta}(s)$ transfer function.

SECTION I

INTRODUCTION

This report addresses the problem of how design specifications may be devised to ensure acceptable flying qualities for aircraft having arbitrary airframe and control system dynamics and that are intended to perform either conventional or unconventional flight control tasks requiring precision piloted control.

It is well-known that the current version of the military flying qualities specification MIL-F-8785B (reference 1) is not totally satisfactory for the design of highly augmented aircraft. Its applicability to the design of aircraft employing novel controls or control system mechanizations, or that require unconventional piloting tasks, is questionable. In past design exercises where MIL-F-8785B was strictly inapplicable, it has been used more as a design guide than as a binding contractual specification. The specification backup document (reference 2), used in conjunction with MIL-F-8785B, has been widely praised for such purposes. Its format, scope, and interpretations of available handling quality data bases enable the designer of non-classical aircraft or flight control systems to assess specific designs from a general, state-of-the-art viewpoint. The combined use of MIL-F-8785B and its back-up documentation can, under ideal circumstances, thereby provide the designer with a flexible design approach that may ensure satisfactory flying qualities for aircraft that cannot otherwise be addressed by the handling qualities specification, alone.

There are at least three major difficulties with such an approach to handling qualities design. First, many opportunities can arise for different, equally plausible interpretations of existing handling qualities data bases and their significance in the context of a non-classical system design. Second, the state-of-the-art isn't advanced enough to necessarily enable the a priori specification of satisfactory handling qualities for completely conventional aircraft; the use of available data for unconventional systems design will therefore be even more questionable. Finally, it is difficult to prepare contractual agreements that bind a manufacturer to quantitative design goals when fluid, and somewhat arbitrary, design methods are employed in the development of an aircraft system having non-classical dynamics or that will be used in unconventional ways.

The art of handling qualities is a volatile one. Various limited theories for aircraft handling exist. Handling qualities data bases are limited, sometimes of dubious worth, very expensive to accumulate and extend, and occasionally contradictory. One practical difficulty,

often encountered by those working in the field, is how to successfully coexist with the contradictions posed by the lack of a unifying theory for handling qualities, sparse or conflicting data, and the necessity for the timely accomplishment of aircraft design and development functions. The pressures of system design often demand an expedient treatment of handling qualities considerations during the early design stages. This is unfortunate since it is here that handling quality considerations have their greatest potential benefit to the aircraft system. In future aircraft developments it may prove too costly to system performance and reliability to justify the assumption that basic airframe handling quality deficiencies can be corrected during design of the flight control system. The imposition of global system requirements such as minimizing life-cycle costs or maximizing combat aircraft survivability will, in all likelihood, magnify the importance of the handling qualities discipline relative to the traditional, dominant design technologies. At this time, however, state-of-the-art methods will not support the inclusion of handling qualities within an iterative process of preliminary design optimization such as might be required to meet such design goals. There is, therefore, a strong motivation for seeking a physical theory for aircraft handling qualities that can unify existing data bases obtained from simulation and flight test that is acceptable for predicting handling qualities in circumstances for which empirical data do not exist or are inapplicable, and for integrating handling qualities into the preliminary design process on a more mechanistic, user-oriented basis than is now possible.

It is important to recognize that the present state-of-the-art of handling qualities is fundamentally empirical. Available theories for handling qualities are all based upon a network of empirical data, experiences with classical airframe dynamics, servomechanisms analogies, and conjectural hypotheses which attempt to establish a connection between handling qualities and available models for human pilot dynamics. All these have some demonstrated value for the codification of experimental data and for the design of experiments; none has provided significant insight into the physics of handling qualities (such as, for example, the nature of human subjective response) or has a demonstrated, general capability for reliable a priori prediction of handling qualities.

The elusive, intangible nature of handling qualities has presented a formidable obstacle to the development of a physical theory for the subject. For example, definitions of handling qualities tend to be either personalized and vehicle-centered or general, vague and practically useless. It is conceivable that the nature of handling qualities transcends our abilities to define it in simpler terms. The entire concept of "quality" is involved; reference 27 contains a philosophical and readable discourse on the subject of quality and is recommended to those who view the subject as either trivial or completely obscure.

The lack of a suitable definition does not prevent us from recognizing degrees of handling qualities in practice. The engineering problem is to systematically code these in terms of airframe and control system design parameters -- this requires a suitable handling metric.

Pilot opinion rating (POR) is a widely used and poorly understood metric for handling qualities. It has almost become a de facto substitute for handling qualities through familiarity -- perhaps a classic example of how the measurement can become the thing measured. The dynamic portions of MIL-F-8785B are based on POR data accumulated over many years from diverse sources. It is reasonable to question the policy of basing future handling quality design requirements entirely on POR in view of the changing nature of manned aircraft combat roles. That, however, is beyond the scope of the present work; here, we seek to evolve a better understanding of POR for those flight control tasks and aircraft dynamics that are familiar and are encompassed by MIL-F-8785B. We wish to establish a physical basis for POR, to determine its connection with task, system dynamics and atmospheric disturbances, and to evaluate means for predicting it in those instances where useful data bases for handling qualities do not exist.

POR data often appear to be highly variable and to exhibit unpredictable, systematic biases among the pilot population, and random variations for a given pilot. Such apparent inconsistencies in the handling qualities data bases have been a factor limiting the introduction of handling considerations to aircraft preliminary design. A major tenet of the present work is that anomalies in the POR data base may be illusory. Without a physical theory for handling qualities (and, therefore, for POR) one should not assume that all the factors that parameterize POR are known for a given experimental configuration. Given the typical handling quality experiment -- simulation or flight test -- it is a logical error to classify POR data as inconsistent or variable merely because the same numerical rating was not achieved for two or more data runs with the same vehicle dynamics. For example, it was once widely believed that knowledge of vehicle dynamics would be sufficient for the determination of POR for a prescribed task. Based on this belief it was expected that systematic variations in, for example, short-period dynamics would produce consistent variations in POR for a simulation involving precision tracking of pitch attitude -- regardless of turbulence characteristics. It is now known that this is only approximately true; in fact, variations in turbulence intensity with constant short-period dynamics can produce effects on POR as large as those obtained due to changes in vehicle dynamics with constant turbulence intensity. Before the significance to POR of turbulence was appreciated, the large range of measured POR obtained without experimental control of turbulence intensity was attributed to "pilot variability." We cannot be certain that other effects of similar importance do not still exist. It is clear, however, that we should

dispense with the indiscriminate use of "pilot variability" as a convenient catch-all category for the description of those POR data that do not fit our expectations.

As a practical matter we must expect that POR data obtained from a carefully designed, realistic experiment will exhibit a certain degree of variability. What we need to do, however, is to develop methods for ensuring that the variability is not the systematic result of applying faulty theory or inadequate metrics for the correlation and assessment of POR data. A pilot makes errors in control that we describe as random because they appear to be more-or-less random and because we have no model for otherwise explaining them. It is conceivable that for some vehicle configurations the consequences of such errors to POR are significant, even though pilot-vehicle system dynamics will not be measurably affected. Such configurations, when repetitively evaluated in an experiment, would therefore exhibit apparent random variations in POR. Such variations in POR would not, in fact, be random if the pilot subjectively responds to particular system properties; in that case the POR data might be almost perfectly consistent with a suitable, but unknown, metric -- in other words it is conceivable that it is the engineering analyst and not the pilot who establishes the level of variability in POR data! Of course the pilot is not a machine-like evaluator; run-to-run variations in POR of a genuinely random nature probably must be expected. The Cooper-Harper scale for POR is not perfect and must be interpreted against the experimental conditions by the evaluation pilot. The present state-of-the-art requires that such effects be minimized by averaging sufficient POR data. We should insist, however, that such data be uncontaminated by effects that are within our capability to understand and control. This is not always so easy to accomplish.

To reiterate, the apparent inconsistency or variability that can occasionally be seen in POR data may, to a great extent, result from attempts to establish correlations between POR and various ad hoc, arbitrary metrics when, in fact, such one-to-one correlations may not physically exist. In this report it is assumed that POR data -- properly obtained -- are based on objective criteria (that may be unknown) and can only be understood or correlated with an appropriate model for pilot dynamics and rating prediction.

The prediction of pilot rating is presumed here to depend upon the availability of a reasonable quantitative model for human pilot dynamics in the handling qualities context. There are presently two principal models for pilot dynamics that have recieved general acceptance as working tools for the study of pilot-vehicle system behavior. Principally, these should be regarded as interpolative schemes for rationalizing certain available pilot dynamic and tracking performance data. Neither the servo model (reference 4) nor the optimal control

model (reference 5) is of particular value for explaining the physical nature of known trends in pilot-vehicle system dynamic behavior. Either is capable of accounting for known trends a posteriori through adjustment of model parameters (e.g., equalization in the servo model or cost functional weighting in the optimal control model). The servo model emphasizes man-machine system dynamics; the optimal control model is based upon matching man-machine system performance (e.g., mean-square tracking error).

A physical model for pilot-vehicle systems analysis, which subsumes the servo and the optimal control models, and which is consistent with available human response data, will -- it is anticipated -- lead in a natural manner to a rational theory for understanding and predicting POR. It is further anticipated that a theory based upon such a physical model will not be marred by the limitations of empiricism or controller task that plague the Paper Pilot approach to POR prediction (as embodied in reference 3).

A candidate, unified model for pilot dynamics will be introduced and discussed in this report. It will be shown how this conceptual model leads to a metric for the correlation and prediction of POR. This metric will be used to explore the nature of rating differences between flight and simulator experiments and to examine the significance of attitude tracking to more general flying qualities tasks. A series of demonstrations will illustrate how revisions may be developed to MIL-F-8785B.

It should be noted that, throughout this report, the pilot output is expressed in terms of control deflection rather than control force. This has been done merely for compatibility with the principal data sources for human pilot dynamics as they presently exist. Most measurements of pilot dynamics have been obtained from fixed-base simulation experiments with rudimentary controls for which deflection and force were proportional. For some data, there was no control restraint and we must express the pilot's response as a deflection. In those numerical examples in Sections IV and V, using the Kleinman model, the control system displacement gain (the ratio of surface to control stick deflections) is assumed to be combined with the control effectiveness derivative; it is the overall pitching moment-to-control stick gain that is assumed to be optimized prior to estimation of the POR metric proposed in this report. It is probably true that no general theory for handling qualities can neglect the force-displacement interactions between the pilot's neuromuscular system and the aircraft feel system; that has been done in this report only because it is believed that the necessary data, mathematical models, and physical understanding of neuromuscular-feel system interactions do not yet exist. The potential importance of the feel system to the prediction of handling qualities has been appropriately emphasized at various points throughout this report.

SECTION II

A UNIFIED MODEL FOR PILOT DYNAMICS IN SINGLE LOOP TRACKING
PART 1: THEORY AND BASE-LINE ANALYSIS

A. BACKGROUND

There has, since WWII, been sustained interest in quantifying the contributions of a pilot to the overall closed loop pilot-vehicle system's dynamic response. Research in this area has produced two outstanding models for human pilot behavior in a closed loop system. The first and most thoroughly documented is the servo model. It has received wide attention and has enjoyed a record of successful applications in several areas of aircraft system analysis and design. Reference 6 is a recent summary of the general state of the art of pilot-vehicle systems analysis which emphasizes the significance of the servo model. Applications of state-space formalisms and the principles of optimal control have produced the more recent optimal control model for pilot-vehicle systems analysis (reference 5). Both models have their particular merits and adherents. Both are linear, time-invariant, and tend to be of about equal value for analysis when applied by experts in their usage.

The approach that produced the servo model was to hypothesize a servo-like operation on a single stimulus (system error) by the human pilot, parameterize a servo-mechanism model for his dynamic response, conduct a program of simulation and measurement, and extract the servo model parameters from these data for each control configuration tested. The classic experiments documented in reference 4 were conducted using a sequence of exemplary vehicle dynamics that were hypothesized to encompass the dynamic character and range of airplane - control system dynamics of interest to manned flight. The result of this program was a catalog of pilot model and closed loop system parameters as functions of system input and controlled element dynamics - - all for the single piloting task of continuous closed loop tracking with a single visual display of tracking error (figure 1). A set of "adjustment rules" were developed to guide the user in the selection and adjustment of pilot model parameters according to the specifics of a particular application.

The servo model for human pilot dynamics was originally developed under a set of severe restrictions which are almost never entirely satisfied in practical flight control tasks. These include:

1. The system input is of low bandwidth and is random appearing with invariant statistics.
2. The airplane/display system dynamics are linear and time-invariant.

3. The system has a single input with a compensatory display of system error.

4. The pilot's response is through a single controller.

5. The pilot's task is to track system error in some sense analogous to minimizing mean square error.

6. The pilot's cues are entirely visual.

Ad hoc assumptions are often used to extend the servo theory to encompass a broader range of conditions of more practical interest. These include multiple loop control tasks (e.g. hover over a spot, approach and landing control, etc.), tracking without command inputs, effects on pilot dynamics of vehicle motion, use of multiple controls, and control of multiple axes of vehicle motion.

There is a two-fold difficulty with the ad hoc approach to pilot modeling and its application to handling quality analyses. First, there has been an historic tendency by the handling qualities community to view the representation of human controller functions with differential equations as a sheer novelty and to uncritically accept even small successes in human operator modeling without concern for unity of modeling and understanding. The effect of this atmosphere is to remove any sense of urgency for a more critical search for alternative explanations for human pilot behavior that might lead to broader, more unified understanding; it is safer to promote and sponsor low-risk (and low payoff) research. Second, the permissive attitude that embraces the ad hoc philosophy leads inevitably to the misuse of carefully documented baseline theory such as reference 4 and to the development of faulty theory for the prediction of handling qualities. In mathematics, an hypothesis is rejected for all time if it is shown to fail for one test case. This same logic is seldom applied in the development of a theory for handling qualities. Failure of pilot opinion rating to satisfy a prescribed theoretical metric for its correlation is inevitably blamed on the "variability" of pilots and almost never on the metric, its underlying theory, or the experimental design.

Methodical extensions of the single loop servo theory for pilot-vehicle dynamics to multiple loop control tasks or to account for motion effects have been attempted. These have not met with the same degree of success as has the single loop theory. In fact, a consistent, methodical approach which addresses all the conceivable effects of input, display, controller, task, and vehicle parameters may be impractical within the context provided by the servo theory for pilot dynamics. We lack a scheme for rationalizing all the conceivable higher order control situations of practical interest and for parameterizing a pilot model suitable for all. In short, the problem has too many dimensions to lend itself to a direct experimental study. The state-of-the-art of the servo model is now such that it can be

extended to more general control tasks only by strapping-on additional ad hoc complications. One wonders whether a simpler and more fundamental approach might not exist.

A more mechanistic, if not simpler, approach to human pilot modeling is described in reference 5. The optimal control model for pilot-vehicle dynamics -- widely known as the Kleinman model after its principal originator -- is based upon the assumption that human controller response is near-optimum in some sense and is essentially linear. The character of optimization theory led in a natural manner to formulation of the governing system equations in terms of state variables. The state vector components are selected by the analyst to simulate the various feedback cues actually available to the human pilot. Normally, these include vehicle attitudes and attitude rates for visual, fixed-base tracking and rotational or linear accelerations if motion cue effects are to be modeled. The modeling of multiple loop tracking tasks will usually require that trajectory variables and their higher order derivatives, as may be sensible by the human pilot, be included within the state vector. In the simplest fixed-base tracking task, with a visual display of system error, the Kleinman model will usually be chosen such that the information vector is system error and error rate (figure 2).

It should be noted that, even in single loop visual tracking, the Kleinman model treats the information available to the human pilot model as a vector quantity for convenience; i.e., it is consistent with state space formalisms. There is no evidence that any physical importance was initially attached to this assumption. Rather, it was done to provide continuity with the servo model's lead equalization requirements. That is, the generation of lead by the servo model is considered to be synonymous with the feedback of error rate in the Kleinman model. This does not necessarily have to be true but need not concern us at this point in this report. What is of concern here is the possibility that control information is assimilated by the human pilot as though it were a vector quantity -- that is, the formal treatment of operator input by the Kleinman model may be a reasonable model for the physical process (at least in a linearized sense).

The Kleinman model delays each feedback variable by an amount τ seconds which must be pre-set by the analyst. An "observation noise," linearly uncorrelated with system input, is injected into each feedback variable. Each noisy feedback, delayed by τ seconds, is then fed to a Kalman filter, which estimates the feedback state in the presence of noise, and then to a predictor which uses all feedback variables to predict the value of each state variable at the time $t + \tau$ (i.e. it tries to remove the effect of the time delay). The injection of "observation noise" is essential if the model's predictions of system performance are to be realistic. If it were omitted, then the Kalman filter and the predictor would yield a perfect estimate of the system's state for use by the optimal controller and the model's performance

would be far superior to the human pilot's. The predictor yields a vector of perceived state variables which is operated on by the optimal controller algorithm to produce the optimum feedback gains, $K_x(i)$. A final noise component, "motor noise," is injected at the control point to account for the remainder of the human pilot's nonlinear or non-stationary dynamics.

The optimal controller operation in the Kleinman model adjusts the feedback gains to minimize a cost functional (e.g. see figure 2). In practical applications, the cost functional is a linear combination of mean-square values of various system signals. The weights in the cost functional are selected to yield the best match between model-predicted and experimental values of system performance measures (usually mean-squared tracking error).

A principal area of concern in applying the Kleinman model is that the cost functional weights must be varied according to changes in vehicle dynamics, display mechanization, vehicle disturbance, or task requirements. If this were true, then the model would be of little real value for predictions of system behavior in the absence of an extensive data base. Fortunately, this may not be the case. Reference 25 suggests that, for the same or similar task constraints, weights derived for one reliable data source may be invariant. This matter will be re-examined later in this report (Section IV).

The choice of either the servo or the Kleinman model for the analysis of single loop tracking tasks (such as those shown in figures 1 or 2) is, to some extent, a matter of personal preference. It is true, however, that the servo model was developed as a tool for explaining the pilot's role in influencing closed loop system dynamics. It was believed that understanding of pilot-vehicle system dynamics gained from applications of the servo model would lead to a theory for handling qualities that would permit quantitative predictions of his subjective evaluation of system suitability. The Kleinman model, on the other hand, was developed as a tool for predicting tracking performance of a closed loop pilot-vehicle system without particular regard for system dynamics. However, the Kleinman model can be used for the prediction of system dynamics and the servo model is usable for predicting system performance. Nevertheless, the initial selection and adjustment of model parameters is usually done on the basis of matching system dynamics with the servo model and system performance with the Kleinman model.

Applications of the servo model to the analysis of handling quality tasks involving higher levels of control such as multiple loop or multiple axis tracking requires considerable familiarity and skill with the single loop servo model plus a certain amount of artistry. For such tasks a major part of the analysis problem is to select a reasonable structural form for the pilot model (e.g. What are the feedback variables? What are the equalization requirements? What control cross-feeds apply? etc.?).

It was indicated earlier in this section that the modeling process for the more complex tasks entails a certain ad hoc flavor. Models resulting from this process are not necessarily unique. Further, experiments are not necessarily an aid to the development of more extensive and accurate servo descriptions of human pilot dynamics. It is often not possible to directly measure the servo model elements by experiment, as can be done in single loop tracking, because of uniqueness difficulties (reference 7). By contrast, it has already been indicated that the Kleinman model may be applied to such tasks with relative ease (at least in concept) without procedural or structural change beyond the addition of new state variables and introducing new observation noise components for each.

In fact, the practical situation is such that either the servo or the optimal control model can be applied to the same problem with about equal probability for success and with about the same result. Both are linear models. Both are parameterized to replicate different features of the same experimental data base. Many experimental programs over the past two decades have established the essential validity of the linearity assumption for the pilot's dynamic response in exemplary tracking tasks. The vehicle, display, and trajectory dynamics are typically linear, or nearly so. An optimality criterion exists to permit the dynamics of any linear system to be "explained" with an optimal control model. Thus, the "adjustment rules" for the parameterization of the servo model can be visualized as the frequency domain equivalents of the cost functional and its weights in the Kleinman model.

There is a tendency by those working in the handling qualities field to forget that these models are fundamentally empirical. Both were derived as expedient tools for assessment of empirical relationships between the pilot and his control environment. Neither is necessarily a physiologically acceptable model for human behavior. No philosophical basis for the correctness of either model has yet to be established on rigorous grounds. Both models depend for their successful application upon the existence of base-line data for their parameterization. In this sense, they are interpolative models. What we require for handling quality applications, especially for examining design specification requirements, are predictive models for use in the absence of data.

The remainder of this section will address the problem of how our understanding of human pilot dynamics may be unified by developing a new model which subsumes the servo and optimal control descriptions of his behavior in manual tracking. The point in doing this is not to develop better techniques for predicting pilot dynamic response, per se. Rather, we anticipate that a physically realistic model for human pilot dynamics will suggest a method for the prediction of pilot opinion rating.

B. TWO HYPOTHESES

The following two hypotheses, with a discussion of each, are presented here as guides in the search for a unified theory for human pilot dynamics. Neither hypothesis has been entirely validated. The reader may draw his own conclusions about their value after digesting the remainder of this report.

HYPOTHESIS 1

The servo and the optimal control models for human pilot dynamics are linearizations of a more fundamental nonlinear model. The measurable variations in servo or optimal control model parameters with changes in controlled element or forcing function can be partly explained as operating state changes in the nonlinear model rather than by attributing them entirely to manual adaptation, per se.

HYPOTHESIS 2

A model for human pilot dynamics that structurally matches the human physiology involved in the tracking process will lead to a natural measure for pilot opinion rating.

DISCUSSION

Neither the servo nor the optimal control model offers an explanation for why the model or closed loop parameters vary with system changes. It is known, for example, that closed loop phase margin and cross-over frequency vary systematically with controlled element (vehicle) dynamics and that this, in some way, reflects task difficulty. Forcing function bandwidth has a strong, consistent effect on phase margin. The portion of the human controller's response that is not linearly correlated with system input, the remnant, appears to be dependent upon both input statistics and controlled element dynamics. Increasing input cut-off frequency beyond about 80 percent of the cross-over frequency produces a discontinuous reduction in system cross-over frequency (the so-called ω_c regression phenomenon). The distribution of control stick motions becomes notably bi-modal, indicative of controller "pulsing," for certain controlled elements; the effect is modeled with either the servo or optimal control model as an increase in remnant. The generation by a human operator of lead equalization, as required in the servo model and accounted for in Kleinman's model with a rate feedback path, is intuitively acceptable to most of us. However, lag generation, which the servo model description requires for a particular class of controlled elements (pure gain), is not intuitively satisfactory to this author.

Reference 4 documents all these, and other, empirical trends for the single loop tracking task within the context of the servo theory. No similar experimental program of the comprehensiveness of that described in reference 4

has ever been accomplished for the optimal control model - - although spot-checks have been made.

Empirical models for the data base provided by reference 4 have, as previously indicated, proven very useful for predicting system dynamics and performance in many practical applications. However, it is reasonable to expect that a model capable of explaining the physical origins of the data trends will readily lend itself to identification of the limits of applicability of the servo and optimal control models and to establishing the necessary and sufficient conditions for their use. That is, if the servo and Kleinman models are reasonable, parochial descriptions for human pilot dynamics, then a more fundamental model will subsume these. In addition, a pilot model that is more accurate than these in physiological details should permit a more rationalized and less artistic approach to including effects due to higher order control tasks, motion cues, effects of turbulence intensity, and so forth.

There is reason to believe that at least some of the variations in human pilot dynamics are the result of nonlinear physical mechanisms internal to the human system. It is reasonable, then, to invent the first hypothesis. If it can be validated, it would permit the decoding of the process of manual adaptation to an extent not heretofore possible. It would also provide a model for the automatic prediction of human pilot remnant (or at least a large part of it) as well as providing a unified, predictive model applicable to very general flight control tasks and to the evolution of a realistic theory for handling qualities.

Any usable theory for handling qualities must incorporate a method for the quantitative prediction of pilot opinion rating. It is not enough to predict system dynamics and tracking performance. The prediction of opinion ratings must, however, derive from a sound physical basis and hopefully be closely tied with a reliable model for human pilot dynamics. It is not sufficient to base the prediction method on statistical models, devised with a set of experimental data, in the absence of a general physical theory for the nature of the rating process. The second hypothesis formalizes this philosophy and re-affirms the author's belief that a rational and physically-oriented basis exists for the pilot's "manufacture" of his opinion rating.

C. A NONLINEAR TIME DELAY MODEL

It was once suggested to the author that the classification by mathematicians of differential equations into the two categories of "linear" and "nonlinear" would be analogous to the classification by zoologists of animals as "elephants" and "everything else." The parallel does emphasize the special character of linear systems analysis and suggests the magnitude of the difficulties that await the analyst foolhardy enough to trespass too deeply into the waters of nonlinear modeling of physical systems. Nevertheless,

the viewpoint here is that a unified model for human pilot dynamics is attainable only if one is prepared to address the possibility that a human controller's nonlinearities are at the root of his most interesting, useful, yet most baffling behavior. Still, where does one begin the search for a suitable nonlinear model?

A systematic search for a unified nonlinear model for human dynamics that considers all possible nonlinearities without consideration for known physical properties of the human mechanism or of the describing function (servo model) data base as it exists is not likely to succeed. There are too many possibilities to consider and the behavior of even simple nonlinearities is too difficult to systematize in the absence of guideline physical criteria.

Certain general properties of the human controller in closed loop tracking tasks are known and can be used to evaluate candidate nonlinear pilot models. For example, the combinations of system input and controlled element dynamics that guarantee closed loop stability are generally known (and here we purposely ignore the problem of catastrophic pilot-induced oscillations) or can be deduced with the aid of the servo model for pilot-vehicle systems analysis. Provided one is familiar with the experimental data base for manual tracking experiments, then the general character of the human controller's response is known as a function of controlled element dynamics; e.g. we have general knowledge about whether his response should be smooth or pulse-like, what the distribution of control deflection will be, and of the frequency content of the control response.

The arguments used by this author to justify the approach documented on these pages are quite circular and involve more than a little intuition. The essential defense offered for this approach is that it is the result of several years of study of the reference 4 data base and appears to be self-consistent. That is, each nonlinearity introduced here appears to offer the potential for rationalizing some facet of the experimental data without creating new inconsistencies or requiring additional assumptions.

A nonlinear multiple loop model for pilot dynamics will be proposed later in this section. A nonlinear time delay in the rate sensor mechanism will comprise an essential nonlinearity in this model. The attributes of an amplitude-dependent time delay will be discussed in the remainder of this article.

Brissenden (reference 8) measured the latency time delays incurred in human sensation of visual rate. The experiment described in that reference is not directly applicable to the problem of closed loop tracking; it does, however, establish that the time delay involved in the detection by a human of a rate stimulus, given only a visual display, is generally dependent upon the stimulus magnitude. Representative data from reference 8 are shown on figure 3. These data are unfortunately not quantitatively suitable for further analysis.

The data of reference 8 prompted the derivation of a model for the direct visual sensation of rate in reference 9. Insofar as possible, this model considers the physiology of the physical process in visual detection of a stimulus' rate of change. Its principal value is to establish a physical basis for an amplitude-dependent time delay in rate detection.

Both references 8 and 9 are consistent in their indication of a hyperbolic variation of time delay with rate amplitude. This variation was determined for step changes in rate; however, it is possible to show by example that the detailed relationship between rate x and time delay τ probably isn't of qualitative importance to system time response characteristics so long as τ decreases with increasing x and vice versa. In all the work discussed in this report the hyperbolic variation is assumed:

$$\tau = \frac{K}{|x|}, K = \text{constant}$$

No discussion of the general properties of a nonlinearity of this form exists, to the author's knowledge, in the literature. Figure 4 indicates some of the more basic time response effects that can be produced by a nonlinear delay.

It is assumed that the delay is symmetrical with respect to the sign of the rate change. Thus, the pulse width of a stimulating rate is preserved by the nonlinearity.

A sequence of pulses will be transformed, such that the delayed response contains a decreased spacing between successive stimulus peaks when the rate amplitudes successively increase and vice versa (2a of figure 4). However, the amplitudes of the stimulus pulses are unaffected by the transformation. If one stimulus pulse is followed closely enough by another having a significantly greater amplitude then the delay will invert the order of the input pulses as shown in 2b of figure 4. It will be assumed in the present work that the physical interpretation of this behavior is that the smaller pulse is never detected by the human sensor.

A sinusoidal rate stimulus will be transformed by a delay of this form into a periodic signal that looks much like a square wave (sketch 3 of figure 4). A sinusoidal describing function for the nonlinearity would be a unit gain (since response and stimulus amplitudes are equal) plus a phase lag

$$\phi = \omega\tau, \text{ radians}$$

where τ is the delay between input and response peaks as indicated in sketch 3 of figure 4.

Any continuous input can be represented as a series of pulse inputs.

From the above discussion it should be obvious that a nonlinear delay of the form assumed will:

1. introduce discontinuities in the output when large, high-frequency changes occur in the input,
2. steepen input ramps,
3. elongate input "tails",
4. not affect input amplitudes, except possibly in a local sense when small peaks may be eliminated due to the pulse inversion process discussed above and,
5. produce an input-output phase angle relationship that is dependent on the local time delay.

It is believed and is hereby postulated that a nonlinear time delay of the above or similar form will serve as a principal factor in explaining the origins of certain of the data trends shown in the data base of reference 4. In particular, it is reasonable to expect that a nonlinear delay will account for:

1. the pulse-like character of control response for certain of the controlled elements that are classified as difficult to control (the amplitude distributions of control contain a bimodal component for these cases).
2. the production of remnant that, in reference 4 and elsewhere has been attributed to random fluctuations in reaction time delay.
3. the variations in effective time delay with the controlled element or input descriptions.
4. the variations of closed loop phase margin with input statistics and controlled element dynamics.
5. certain of the inter-operator differences previously attributed to "style."
6. the lagging low-frequency phase angles that appear in almost all describing function measurements of human operator dynamics.

The nonlinear delay will, of course, be imbedded in a closed loop system which purports to model pilot-aircraft system dynamics. The input to the delay element will be the closed loop system's error rate. This signal will be shaped by the nonlinearity allied with the dynamic response of the remaining system elements. In general, if the system were entirely linear with good tracking dynamics and with low frequency command or

disturbance inputs, the closed loop equations would indicate that the power content in closed loop error rate is most significant at frequencies from slightly below crossover to the effective bandwidth of system input and much smaller at lower or higher frequencies. This observation is depicted in the generic sketches of figure 5. The system input power spectral density illustrated in figure 5 is representative of those used in the servo model validation experiments documented in reference 4 as well as in many subsequent programs of analysis or experiment.

A closed loop system having poor servo performance will tend to have more error power content at frequencies below the crossover frequency. This will magnify the peak in the error rate spectra and substantially increase the error rate signal level for a constant input spectrum.

It is plausible, based on the closed loop observations above, to speculate that the frequency-dependent amplitude of the error rate spectral components together with the amplitude-dependent time delay, could account for the data trends noted above provided the overall model for pilot-vehicle system dynamics can be appropriately structured. The connection between the Bode amplitude plot $|e_c(j\omega)|$ and the corresponding phase relation between $\dot{e}(t)$ and $c(t)$ should be noted, in particular. In regions where $|e_c(j\omega)|$ is small (e.g. the low and high frequency regions depicted in Figure 5) the nonlinear delay will be large and the equivalent phase lag will be substantial. It should also be evident that when the closed loop error rate response is near-periodic as, for example, when the system phase margin is very small, the time delay produced by the nonlinear delay will be nearly constant.

The mathematical treatment of an amplitude-dependent time delay is extremely complicated and beyond the scope of this report. For present purposes it is sufficient to present a digital computer model for the delay and use it in the simulation of candidate nonlinear models for the human pilot. The details of this development, with a flow-chart and a program listing, are given in Appendix A.

The innocuous appearance of a hyperbolic variation of delay with error rate magnitude belies the complexity involved in its simulation with a digital program. Basically an output file must be created, given the input to the delay, and updated according to whether or not the output storage is to be overwritten as in case 2b of figure 4. The response from the delay is then determined by interpolation on the output file at the time of entry to the delay element.

A major programming difficulty is to ensure compatibility between the delay model and that for the rest of the pilot-vehicle system. In particular, the requirements peculiar to the numerical integration algorithm must be carefully considered. A predictor-corrector scheme was used in the present work. Thus, the nonlinear delay model incorporates features

to permit changes in time step size and to allow the back-spacing of simulation time as is occasionally necessary with such an integrator. Special checks are also required in the model to ensure that sufficient storage exists in the output file to permit the numerical interpolation required to calculate the actual output at a given time.

The final model documented in Appendix A is believed to be a reasonable representation of the physical process discussed above. It is, however, tailored to operate in a closed loop environment and could possibly be improved in detail; further experimental resolution of the physiology of visual rate detection will undoubtedly be required if a higher-fidelity computer model for the process is to be developed.

At this point we wish to consider the character of the dynamics of the nonlinear delay as a function of controlled element dynamics or system input intensity and bandwidth. This, however, is to be done within the framework of a representative configuration for the pilot-aircraft system model. This will require that we jump ahead somewhat in the presentation since no detailed description of a suitable pilot model has yet been made. Figure 6 presents such a model together with reasonable parametric values for its use. A more detailed description of this model will be made in the next Article.

For present purposes it is sufficient to consider the pilot model of figure 6 as though it were equivalent to the Kleinman model previously discussed and shown in figure 2 for the single loop, visual tracking task. In fact, the two models are very similar. The primary difference, other than the presence of nonlinearities, is in the use of a switch to select either rate or positional control - - but not both simultaneously - - in the model of figure 6. The parametric values given in figure 6 are applicable only to two controlled elements as follows:

1. $\gamma_c = 11.9 / s^2$
2. $\gamma_c = 11.9 / s(s-2)$

This model for pilot-vehicle system dynamics will be discussed in the next Article. It will be concluded there that it is a reasonable model for the identical experimental configurations documented in reference 4 using human controllers.

The pilot-vehicle model was simulated on a CDC 6600 digital computer and allowed to operate for controlled time periods during which the describing function for the nonlinear time delay was measured. This was done using the ratio of Fourier coefficients estimated at each of the

discrete input frequencies for the delay's input and response. The Fourier coefficients were estimated using the computer program documented in Appendix B. It is noted in Appendix B that the low frequency measurements of describing function amplitude and phase angle are unreliable, in general, and that the overall measurement fidelity is affected by the measurement time and the sample interval. The latter were selected as 240 seconds (as in the reference 4 experiments) and 0.025 seconds, respectively, based on prior simulation studies which established their validity for providing unbiased estimates of the describing function amplitude and phase angle.

Measured describing function $Y_{DL}(j\omega)$ are shown in figure 7 for two controlled elements, for three levels of command input, and for constant input bandwidth. Note that the amplitude $|Y_{DL}(j\omega)|$ should equal unity at all measurement frequencies; accordingly, the three lowest frequency data points of figure 7 should be disregarded as unreliable for the cases $Y_c(s) = 11.9/s^2$. The phase angle contributions for two linear delays of 0.16 and 0.08 seconds are shown for comparison. For $Y_c(s) = 11.9/s^2$ it appears that a linear delay of 0.16 seconds provides an excellent fit to the nonlinear delay's describing function at frequencies greater than about 1.0 rad/sec. Similarly, the 0.08 second delay provides a good match with the phase data for $Y_c(s) = 11.9/s(s-2)$. If the suspect three lowest frequency data points are disregarded then the remaining data indicate a tendency for the development of lagging, low-frequency phase, as postulated, for both controlled elements. It is therefore plausible that either a nonlinear delay or another essential nonlinearity having similar closed-loop dynamic effects could be responsible for the empirical variations with controlled element of equivalent time delay, phase or gain margin and cross-over frequency as documented in reference 4. A unified explanation for these measured variations has never been offered. No consistent effect of input amplitude is discernible for the $Y_c(s) = 11.9/s^2$ data of figure 7.

Figure 8 illustrates the sensitivity of $Y_{DL}(j\omega)$ to input bandwidth ω_i . For these data the rms input amplitude is constant ($\sigma_{y_i} = 0.5$ inches of displayed error) and the controlled element is $Y_c(s) = 11.9/s^2$. The case $\omega_i = 4.0$ rad/sec corresponds to a condition of regressed cross-over frequency ω_c (reference 4). For $\omega_i < 4.0$ these data suggest that increasing input bandwidth creates an increase in higher frequency phase angles. There is no clear effect of ω_i on low frequency phase lag when $\omega_i < 4.0$. For the regressed case ($\omega_i = 4.0$ rad/sec) it can be seen that significant phase angle reductions occur at all measurement frequencies other than the suspect lowest frequency points. These results are merely the manifestation of the general shift to higher frequencies of the dominant spectral components of error rate when the input bandwidth is increased. The degree to which this occurs is, in general, a function of the controlled element dynamics and the loop gains.

As an aside, it is interesting to speculate about the physical nature of the ω_c regression phenomenon in view of the sensitivity of $Y_{DL}(j\omega)$ to changes in input bandwidth. The phenomenon has been attributed to gross, self-adaptive changes in the human operator's control technique for the purpose of minimizing the variance of system error (reference 4). Here, we see that any technique change due to input bandwidth changes may only be apparent; the measured changes in system dynamics may result from nonlinear phenomena rather than from a true adaptive control change, conscious or unconscious.

It is, at this stage, impossible to compare these trends with the phase lag data measured in the reference 4 experiments. We have no guarantee that the pilot model shown in figure 6 is satisfactory in structure or parameterization as an explanation for these experimental data. The point of this presentation has been merely to establish that the contribution of the nonlinear delay to system dynamics is a function of controlled element dynamics and input characteristics. It should be clear that it is the spectral shape of the error rate that is important to the determination of the nonlinear delay's response. Consequently, the describing function $Y_{DL}(j\omega)$ will also be a very strong function of the pilot model gains K_x and K_y (especially K_y) since these affect the qualitative nature of the closed loop system response. It is also apparent from the data of figures 7 and 8 that the nonlinear delay could, in the region of closed loop crossover, be replaced with a linear delay and a remnant. These would vary with input and controlled element exactly as suggested by the "precision" pilot model summarized in reference 4.

D. CANDIDATE MODELS FOR PILOT DYNAMICS

There are two fundamental differences between the character of the pilot models proposed here and that of the state-of-the-art models (i.e. servo or optimal control models). First, the proposed models are essentially nonlinear for reasons that have already been discussed. Second, they are multiple loop; their properties can only be understood within a context provided by multiple loop analysis methods. There is a correlation between the multiple loop model parameters and those of the servo or Kleinman models; this will be established in a following article.

All modeling discussions in this section are directed toward the task of manual control in fixed-base tracking with a visual display of system error and with a single control. The multiple-loop pilot model structure is, however, hypothesized to permit extension to more complicated control tasks.

There are various physical sensor mechanisms within the human body which provide environmental stimuli to the central nervous system. A fundamental assumption of this work is that each of these serves as a potential point for the feedback of stimulus information to the human controller.

It is further assumed that no equalization is permitted of any feedback variable. That is, no lead or lag may be generated within any signal path. Instead, if the servo description of the human pilot requires that lead be generated for the control of a particular controlled element, then the multiple loop model will require the feedback of error rate through the visual rate sensor. The manner by which the multiple loop model provides lag equalization will be discussed in a subsequent article.

The general structure of the hypothesized pilot-vehicle model is shown in figure 9. This is a generalization of figure 6. The model contains a feedback of position y and of position velocity $\dot{y} = \frac{dy}{dt}$. A command input $y_i(t)$ is used with system error y_e and system error rate \dot{y}_e displayed to the pilot. The generation of error rate requires the creation of a rate command \dot{y}_i such that $\dot{y}_i = \frac{dy_i}{dt}$ (this is to avoid having to differentiate $y_i(t)$). A rate washout is used for reasons that will be discussed later. A threshold nonlinearity is used at the point of position error detection to simulate a visual threshold of perception or one due to a pilot's indifference to small errors. The loop gains on rate K_x and position K_y are assumed to be nonlinear, single-valued functions of the delayed rate \dot{y}_d and the perceived error y_r . The block labeled "S" is intended to represent either a summing junction (i.e. $\beta = \beta_x + \beta_y$) or a nonlinear switch, as in figure 6 (i.e. $\beta = \beta_x$ or β_y).

The model used for neuromuscular system dynamics $G_M(s)$ is the same as that shown on figure 6 and derives from reference 10. Several points are worth noting about this model and its implications.

The experiments documented in reference 10 were of the highest possible quality within the present state-of-the-art; they permitted a direct measurement of neuromuscular dynamics. The authors of that report indicated how neuromuscular dynamics are affected by control feel characteristics; the parameterization of $G_M(s)$ shown in figure 6 is believed to be reasonable for tracking tasks of the sort discussed in reference 4. The measured time delay associated with $G_M(s)$ should be compared with the human operator delay given in the "Precision Pilot Model" of reference 4. It can be seen that they are almost exactly the same. That is, the Precision Pilot Model delay ($\tau = .09$) of reference 4 should, according to reference 10, be attributed entirely to the neuromuscular system. It was this comparison that led to the omission of a time delay in the position control portions of figures 6 and 9.

It was rather authoritatively stated in reference 4 that the lagging low frequency phase in measurements of the human pilot describing function is attributable to the neuromuscular system; a model for muscle spindle dynamics was derived (discussed in reference 11) and offered in later work as a theoretical basis for this conclusion. However, the direct measurement of neuromuscular system dynamics as documented in reference 10 appears to contradict this conclusion; no evidence is shown to support the assignment of low frequency phase lags to the neuromuscular system. The authors of reference 10, in fact, attributed the phenomenon to "retinal and central equalization"! It is hoped that the introduction in this report of a multiple loop pilot model structure and nonlinearities in the rate sensor will eventually resolve the matter.

As an aside, it is worthwhile to note that rather unexpected closed loop oscillations were observed by Teper in his fixed-base hover simulation of V/STOL control (reference 12). These were lightly damped control oscillations at frequencies from 4 to 6 radians/second. Teper attributed these to the neuromuscular system and accounted for them in his servo model characterization and measurements. No explanation for their unusually low frequency was offered, however, nor is one apparent vis-a-vis the servo or optimal control models or from the neuromuscular system dynamics of reference 10. It is plausible to expect that a closed loop mode of that sort could originate as a multiple loop effect - - possibly one involving the nonlinear delay.

The pilot model, as originally proposed, did not employ a switching function between the two feedback paths. Instead, the signals β_x and β_y were summed to represent coordinated control activity. It was determined by trial, however, that large thresholds in both the rate and position loops tended to create lagging low frequency phase angles in the measured pilot model describing function. There was no compelling physical justification for large dual thresholds; however, the character of their effect was such as to almost always yield either rate or positional control, but not both. This suggested that a time-sharing model for pilot dynamics would be a physically reasonable alternative and one consistent with the recent work of Onstott for multiple axis tracking (reference 15). For that reason, the switching function was devised and evaluated as a candidate nonlinearity.

The system input $y_i(t)$ was chosen to match those of reference 4. These were formed as the sum of ten non-synchronous sine waves with frequencies and component amplitudes (suitably scaled) chosen to replicate the experimental situation of reference 4; these are listed in Table 1. The input spectrum is illustrated on figure 6.

An explanation for the incorporation of rate washout in the pilot model is difficult to make at this point. In Article F of this section,

however, it will be shown that the rate command $x_i(t) \approx 0$ is sufficient if the multiple loop model is to account for the lag equalization required by the servo model for a pure gain controlled element. In general $x_i(t)$ is nonzero when a command input exists; however, $x_i(t) = 0$ can be achieved in a practical sense when the command input bandwidth is low frequency provided a low frequency washout is inserted in the rate sensor location. This was the essential reason for its introduction. Such a filter is physically reasonable since it is unlikely that a human pilot is responsive to very low frequency rate errors -- he would merely try to null the position error. It is also possible that rate washout dynamics can contribute to explaining the origins of the low frequency phase lags.

The controller gains K_x and K_y were chosen to be nonlinear functions of amplitude in an attempt to duplicate certain pilot behavior that has been identified in the literature as "adaptive." Specifically, it was hoped that one set of pilot model parameters could be determined that would permit control of several controlled elements without further adjustment.

E. REQUIREMENTS FOR MODEL VALIDATION

The pilot model form proposed in the last article must, in some manner, be validated as an adequate theory for rationalizing part or all of the available data base for human pilot dynamics. A twofold problem must be addressed by the validation program. First, the proposed model is incomplete in detail; only its structure is defined and even that is variable according to whether or not the model is to incorporate a switch between the control of error and error rate. Consequently the validation effort must resolve the form desired of each nonlinear element to be included within the model. Second, the model's parameters must be quantified to simulate actual system response to acceptable levels of fidelity.

It would be relatively easy to select the elements of figure 9 to model pilot-vehicle system dynamics and performance for a particular combination of input and controlled element. The concern here, however, is that the resulting model provide a unified, physically acceptable theory for the explanation of empirical trends. The principal data base available for model comparisons is provided by reference 4. The general requirements to be imposed on the pilot model are that it provide stable closed loop system response, with time histories qualitatively equal to what one would expect from experiment, and yield describing function measurements $Y_p(j\omega_k)$ in agreement with those summarized in reference 4. Additional requirements are that the model-predicted distributions of control motion, the control's power spectral density, the remnant, and the correlation coefficients all substantially

agree with the reference 4 data. Further, it is desired that the final pilot model require a minimum number of parametric changes to account for the entire range of controlled element and system input combinations which constitute the data base. That is, insofar as is practical and physically acceptable, the model should exhibit the qualities usually attributed to self-adaptation. This is a self-imposed restriction introduced because it seems to be a plausible approach to rationalizing our understanding of human controller dynamics. Such a model would also contribute to simplified practical applications by non-specialists since it would be self-adaptive to a large degree.

F. SPECTRAL ANALYSIS

In this section we wish to develop some basic signal properties for the pilot-vehicle model of figure 9. These will be used in the next article to establish comparisons between the nonlinear, multiple loop model and the conventional servo model descriptions of the human pilot.

Consider the two loop, two input, single controller system of figure 10. The signals n_x and n_y are assumed to be noise injection processes and are assumed to be uncorrelated with x_i or y_i . In the following analysis, consider the system signals to be expressed in terms of their Fourier transforms where appropriate. The total system response to x_i , y_i , n_x and n_y is:

$$y = \left(\frac{y}{y_i}\right)'' y_i + \left(\frac{x}{x_i}\right)'' \frac{N_{\delta}^y}{N_{\delta}^x} x_i + \left(\frac{y}{y_i}\right)'' n_y + \left(\frac{x}{x_i}\right)'' \frac{N_{\delta}^y}{N_{\delta}^x} n_x$$

$$x = \left(\frac{x}{x_i}\right)'' x_i + \left(\frac{y}{y_i}\right)'' \frac{N_{\delta}^x}{N_{\delta}^y} y_i + \left(\frac{x}{x_i}\right)'' n_x + \left(\frac{y}{y_i}\right)'' \frac{N_{\delta}^x}{N_{\delta}^y} n_y$$

where

$$\left(\frac{y}{y_i}\right)'' = \frac{G_y G_M Y_{\delta}}{1 + G_y G_M Y_{\delta} + G_x G_M X_{\delta}} \triangleq H_y$$

$$\left(\frac{x}{x_i}\right)'' = \frac{G_x G_M X_{\delta}}{1 + G_y G_M Y_{\delta} + G_x G_M X_{\delta}} \triangleq H_x$$

Other closed loop signals are:

$$\delta = \frac{y}{Y_{\delta}} = \frac{x}{X_{\delta}}$$

$$y_e = y_i - y$$

$$x_e = x_i - x$$

Cross-spectral density expressions may be developed as follows:

$$\begin{aligned}
 \Phi_{x_i \delta}(j\omega) &= \overline{X_i(j\omega)} \delta(j\omega) \\
 &= \frac{1}{X_\delta} \overline{X_i(j\omega)} \left[H_x X_i(j\omega) + H_y \frac{N_\delta^x}{N_\delta^y} Y_i(j\omega) + H_x n_x + H_y \frac{N_\delta^x}{N_\delta^y} n_y \right] \\
 &= \frac{H_x}{X_\delta} \Phi_{x_i x_i} + \frac{H_y}{X_\delta} \frac{N_\delta^x}{N_\delta^y} \Phi_{x_i y_i} = \frac{H_x}{X_\delta} \Phi_{x_i x_i} + \frac{H_y}{Y_\delta} \Phi_{x_i y_i} \quad (1)
 \end{aligned}$$

$$\begin{aligned}
 \Phi_{x_i x_e}(j\omega) &= \overline{X_i(j\omega)} X_e(j\omega) = \overline{X_i(j\omega)} X_i(j\omega) - \overline{X_i(j\omega)} X(j\omega) \\
 &= \Phi_{x_i x_i} - X_\delta \Phi_{x_i \delta} = \Phi_{x_i x_i} - H_x \Phi_{x_i x_i} - \frac{X_\delta}{Y_\delta} H_y \Phi_{x_i y_i} \\
 &= (1 - H_x) \Phi_{x_i x_i} - \frac{N_\delta^x}{N_\delta^y} H_y \Phi_{x_i y_i} \quad (2)
 \end{aligned}$$

$$\Phi_{x_i x}(j\omega) = \overline{X_i(j\omega)} X(j\omega) = \Phi_{x_i x_i} - \Phi_{x_i x_e} = H_x \Phi_{x_i x_i} + \frac{N_\delta^x}{N_\delta^y} H_y \Phi_{x_i y_i} \quad (3)$$

$$\begin{aligned}
 \Phi_{x_i y_e}(j\omega) &= \overline{X_i(j\omega)} Y_e(j\omega) = \overline{X_i(j\omega)} Y_i(j\omega) - \overline{X_i(j\omega)} Y(j\omega) \\
 &= \Phi_{x_i y_i} - H_y \Phi_{x_i y_i} - H_x \frac{N_\delta^y}{N_\delta^x} \Phi_{x_i x_i} \\
 &= (1 - H_y) \Phi_{x_i y_i} - H_x \frac{N_\delta^y}{N_\delta^x} \Phi_{x_i x_i} \quad (4)
 \end{aligned}$$

$$\Phi_{x_i y}(j\omega) = \overline{X_i(j\omega)} Y(j\omega) = H_y \Phi_{x_i y_i} + H_x \frac{N_\delta^y}{N_\delta^x} \Phi_{x_i x_i} \quad (5)$$

$$\begin{aligned}
\Phi_{y_i \delta}(j\omega) &= \overline{Y_i(j\omega)} \delta(j\omega) = \frac{1}{Y_\delta} \overline{Y_i(j\omega)} Y_i(j\omega) \\
&= \frac{H_Y}{Y_\delta} \overline{Y_i(j\omega)} Y_i(j\omega) + \frac{H_X}{Y_\delta} \frac{N_\delta^y}{N_\delta^x} \overline{Y_i(j\omega)} X_i(j\omega) \\
&\quad + \frac{H_Y}{Y_\delta} \overline{Y_i(j\omega)} n_Y(j\omega) + \frac{H_X}{Y_\delta} \frac{N_\delta^y}{N_\delta^x} \overline{Y_i(j\omega)} n_X(j\omega) \\
&= \frac{H_Y}{Y_\delta} \Phi_{y_i y_i} + \frac{H_X}{X_\delta} \Phi_{y_i x_i} \tag{6}
\end{aligned}$$

$$\begin{aligned}
\Phi_{y_i y_e}(j\omega) &= \overline{Y_i(j\omega)} Y_e(j\omega) = \overline{Y_i(j\omega)} Y_i(j\omega) - \overline{Y_i(j\omega)} Y(j\omega) \\
&= \Phi_{y_i y_i} - H_Y \Phi_{y_i y_i} - H_X \frac{N_\delta^y}{N_\delta^x} \Phi_{y_i x_i} \\
&= (1 - H_Y) \Phi_{y_i y_i} - H_X \frac{N_\delta^y}{N_\delta^x} \Phi_{y_i x_i} \tag{7}
\end{aligned}$$

$$\Phi_{y_i y}(j\omega) = \overline{Y_i(j\omega)} Y(j\omega) = H_Y \Phi_{y_i y_i} + H_X \frac{N_\delta^y}{N_\delta^x} \Phi_{y_i x_i} \tag{8}$$

$$\Phi_{y_i x}(j\omega) = \overline{Y_i(j\omega)} X(j\omega) = H_X \Phi_{y_i x_i} + H_Y \frac{N_\delta^x}{N_\delta^y} \Phi_{y_i y_i} \tag{9}$$

$$\Phi_{y_i x_e}(j\omega) = \overline{Y_i(j\omega)} X_e(j\omega) = \overline{Y_i(j\omega)} X_i(j\omega) - \overline{Y_i(j\omega)} X(j\omega)$$

$$= \Phi_{y_i x_i} - \Phi_{y_i x} = (1 - H_x) \Phi_{y_i x_i} - H_y \frac{N_{\delta}^x}{N_{\delta}^y} \Phi_{y_i y_i} \quad (10)$$

$$\Phi_{\delta\delta}(j\omega) = \overline{\delta(j\omega)} \delta(j\omega) = \frac{1}{|X_{\delta}|^2} \overline{X(j\omega)} X(j\omega)$$

$$|X_{\delta}|^2 \Phi_{\delta\delta}(j\omega) = |H_x|^2 \Phi_{x_i x_i} + \overline{H_x} H_y \frac{N_{\delta}^x}{N_{\delta}^y} \Phi_{x_i y_i} + \overline{H_y} H_x \frac{N_{\delta}^x}{N_{\delta}^y} \Phi_{x_i y_i}$$

$$+ |H_y \frac{N_{\delta}^x}{N_{\delta}^y}|^2 \Phi_{y_i y_i} + |H_x|^2 \Phi_{n_x n_x} + \overline{H_x} H_y \frac{N_{\delta}^x}{N_{\delta}^y} \Phi_{n_x n_y}$$

$$+ \overline{H_y} H_x \frac{N_{\delta}^x}{N_{\delta}^y} \Phi_{n_x n_y} + |H_y \frac{N_{\delta}^x}{N_{\delta}^y}|^2 \Phi_{n_y n_y} \quad (11)$$

There are two special cases of interest in the development of comparisons between the servo model of figure 1 and the nonlinear model of figure 9 that may be derived from the above equations.

Special Case #1

$x_i(t)$ and $y_i(t)$ are linearly correlated according to the following rules:

$$x_i(t) = \frac{dy_i}{dt} \quad \& \quad x = \frac{dy}{dt}$$

The first five equations are then specialized as follows:

$$\Phi_{y_i \delta} = \Phi_{y_i y_i} (j\omega \frac{H_x}{X_\delta} + \frac{H_y}{Y_\delta}) \quad (1)'$$

$$j\omega \Phi_{y_i y_e} = \Phi_{y_i y_i} [j\omega (1 - H_x) - H_y \frac{N_\delta^x}{N_\delta^y}] \quad (2)'$$

$$j\omega \Phi_{y_i y} = \Phi_{y_i y_i} (j\omega H_x + H_y \frac{N_\delta^x}{N_\delta^y}) \quad (3)'$$

$$\Phi_{y_i y_e} = \Phi_{y_i y_i} (1 - H_y - j\omega H_x \frac{N_\delta^y}{N_\delta^x}) \quad (4)'$$

$$\Phi_{y_i y} = \Phi_{y_i y_i} (H_y + j\omega H_x \frac{N_\delta^y}{N_\delta^x}) \quad (5)'$$

Equations 6 - 10 are redundant. Observe that since

$$j\omega \frac{H_x}{X_\delta} + \frac{H_y}{Y_\delta} = (j\omega H_x \frac{N_\delta^y}{N_\delta^x} + H_y) \frac{1}{Y_\delta} = (j\omega H_x + H_y \frac{N_\delta^x}{N_\delta^y}) \frac{1}{X_\delta}$$

then the same grouping of H_x and H_y occurs in all five equations; i.e. H_x and H_y occur only as the linear combination

$$H_T \triangleq H_y + j\omega \frac{N_\delta^y}{N_\delta^x} H_x$$

Therefore, only one of equations 1' - 5' is independent. (It would be possible to generalize this result to n-inputs and m-controls by introducing vector notation). For this special case,

$$X_\delta = j\omega Y_\delta$$

therefore

$$H_T = H_Y + H_X$$

$$H_T(j\omega) = \frac{(G_X G_M j\omega + G_Y G_M) Y_\delta}{1 + (G_X G_M j\omega + G_Y G_M) Y_\delta}$$

But

$$H_T = \frac{Y_{OL}}{1 + Y_{OL}}$$

where Y_{OL} is an equivalent open loop describing function.

$$Y_{OL}(j\omega) = (G_X j\omega + G_Y) G_M Y_\delta = \frac{Y}{Y_e}(j\omega) = Y_\delta \frac{\delta}{Y_e}(j\omega)$$

$$\delta(j\omega) = (G_X j\omega + G_Y) G_M Y_e(j\omega) + f(n_x, n_y)$$

$$\Phi_{y_i \delta}(j\omega) = (G_X j\omega + G_Y) G_M \Phi_{y_i y_e}(j\omega)$$

$$\boxed{\frac{\delta}{Y_e}(j\omega) = (G_X j\omega + G_Y) G_M = \frac{\Phi_{y_i \delta}}{\Phi_{y_i y_e}}} \quad (12)$$

It is understood that $\delta/Y_e(j\omega)$ is a describing function in the above analysis. The sequence of block diagram reductions by which the general system of figure 10 is specialized for this case is shown in figure 11.

Special Case #2

The X-channel command is identically zero; i.e. $x_i(t) \equiv 0$. Then equation (6) and (7) become

$$\Phi_{y_i \delta} = \frac{H_Y}{Y_\delta} \Phi_{y_i y_i}$$

$$\Phi_{y_i y_e} = (1 - H_Y) \Phi_{y_i y_i}$$

Equations (8), (9) and (10) are redundant. Then

$$\begin{aligned} \frac{\Phi_{y_i \delta}}{\Phi_{y_i y_e}} &= \frac{1}{Y_\delta} \frac{H_Y}{1 - H_Y} = \frac{G_Y G_M Y_\delta}{1 + G_Y G_M Y_\delta + G_X G_M X_\delta - G_Y G_M Y_\delta} \\ &= \frac{G_Y G_M}{1 + G_X G_M X_\delta} \end{aligned}$$

However, this is just the closed loop describing function

$$\left[\frac{\delta}{y_e}(j\omega) \right]_{x \rightarrow \delta} = \frac{G_v G_M}{1 + G_x G_M X_\delta} = \frac{\Phi_{y;\delta}}{\Phi_{y;y_e}} \quad (13)$$

The notation $\left[\frac{\delta}{y_e}(j\omega) \right]_{x \rightarrow \delta}$ indicates that the describing function is the equation resulting from closed loop control of x with δ . The reduction of this case to an equivalent single loop control system is demonstrated in figure 12. It is noted that equation 13 is true regardless of any possible correlation between x and y ; it only requires $X_\delta \neq 0$. Equations 12 and 13 are directly applicable to the pilot-vehicle system model of figure 9 for the two special cases.

G. SERVO V. NONLINEAR PILOT MODEL COMPARISONS

The most thoroughly researched and documented dynamic description of the human pilot, embodied in the "precision pilot model" of reference 4, is illustrated in figure 1. A set of "adjustment rules" for selecting the model parameters given the input and controlled element is an integral part of the model. This empirical model is based on the notion that pilot-vehicle system dynamics are single loop in structural form with lead or lag compensation in the pilot model according to the character of the controlled element dynamics. The servo description of pilot dynamics can be measured as the ratio of cross-spectral densities; viz.

$$\gamma_p(j\omega) = \frac{\Phi_{y;\delta}(j\omega)}{\Phi_{y;y_e}(j\omega)}$$

We wish to make heuristic comparisons between the servo model and the nonlinear, multiple loop model proposed in this report and shown in figure 9. This Article will address the plausibility of the nonlinear model as an alternative explanation for the experimental data base of reference 4 and offer suggestions for why the servo model parameters vary with the experimental configuration in the manner codified in the "adjustment rules." At this point, the detailed structure of the nonlinear model has not been established nor are its nonlinearities known in sufficient detail to support an in-depth analysis. Consequently, describing function representations of the nonlinear model will be used for analytical comparisons.

An underlying assumption of the servo model is that the visual display of closed loop error constitutes a scalar input of information to the human pilot. The nonlinear model is based on the notion

that information is perceived by the human as a vector quantity; in particular a compensatory, visual display is assumed to provide both error and error rate information through physically distinct sensor paths. The direct sensation of visual rate by the multiple loop model and lead equalization by the precision pilot model are strictly equivalent only under very specialized conditions. In particular, there must be no significant nonlinearity or dynamic element that is peculiar to only one of the two information paths. Also, the transmission time delays must be equal for both paths. The literature of human dynamics, by implication, has historically treated rate feedback and lead generation as equivalent processes.

It was indicated earlier in this report that the servo and optimal control models are equivalent. Here it should be noted that the Kleinman model structure (figure 2) is very similar to that of the nonlinear model (figure 9). They differ principally in that the same time delay is assumed for both rate and position information in the Kleinman model, whereas the rate delay is functionally dependent upon the nonlinearity and the error rate amplitude spectrum in the nonlinear model. Also the Kleinman model treats the neuromuscular system dynamics in a very expedient, non-physical manner that may, for certain controlled element dynamics, be a bit too crude; this, however, is not a matter of first-order importance. Here we merely wish to indicate the similarity between the Kleinman and the nonlinear models and to note that comparisons drawn in this Section between the servo and nonlinear models apply equally well to the Kleinman model.

The closed loop system of figure 10 may be considered to be a random input describing function representation of the proposed nonlinear pilot model of figure 9. The describing function G_x , for example, represents the linear portion of the response to closed loop errors in rate of the visual and central processor dynamics. The transfer function Y_d is identical to the controlled element transfer function $Y_c(s)$ of figure 9.

It was shown in the last article that the closed loop system of figure 10 reduces to the corresponding single loop form of figure 11 for the special case where \dot{x}_i and \dot{x} are the time derivatives of y_i and y , respectively (Special Case #1). Comparison of figures (1) and (11) indicates that when the signals \dot{x} and y are linearly correlated according to the assumptions of the nonlinear pilot model, the relation between the human pilot describing function from the servo theory, and that from the nonlinear theory is

$$Y_p(j\omega) = (j\omega G_x + G_y) G_M$$

However, the describing functions G_x and G_y are unknown (since neither

the nonlinearities nor the detailed structure of the multiple loop model is known). By comparison of figures 9 and 10, it seems reasonable to assume that

$$G_x = \frac{K_{x_0} T_W s}{T_W s + 1} e^{-\tau_0 s}$$

$$G_y = K_{y_0}$$

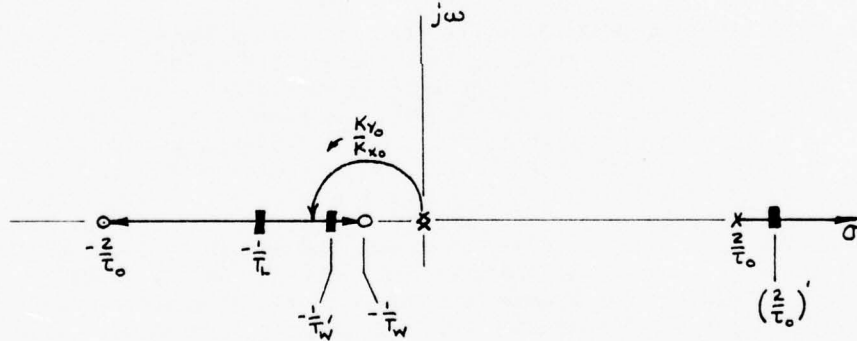
where, for convenience in manipulation, $j\omega$ has been replaced by the complex variable s ; K_{x_0} , K_{y_0} and τ_0 are the statistical averages of K_x , K_y and τ , respectively. The visual threshold describing function has been incorporated in K_{y_0} . With a first approximation for $e^{-\tau_0 s}$

$$sG_x + G_y = \frac{-K_{x_0} s^2 (s - \frac{2}{\tau_0})}{(s + \frac{1}{T_W})(s + \frac{2}{\tau_0})} + K_{y_0}$$

The zeros of $sG_x + G_y$ are roots of $F + 1 = 0$, where, by definition

$$F = -\frac{K_{y_0}}{K_{x_0}} \frac{(s + \frac{1}{T_W})(s + \frac{2}{\tau_0})}{s^2 (s - \frac{2}{\tau_0})}$$

The roots of $F + 1 = 0$ vary with $\frac{K_{y_0}}{K_{x_0}}$ in the manner depicted in the following root locus sketch:



A plausible form for $sG_x + G_y$, for nominal values of K_{y_0} and K_{x_0} , is then seen to be

$$sG_x + G_y = K_{x_0} (s + \frac{1}{T_L}) \left(\frac{s + \frac{1}{T_W'}}{s + \frac{1}{T_W}} \right) e^{-\tau_0 s}$$

where the first order Padé approximation has been replaced by the transform for a constant delay (this assumes that $\frac{2}{\tau_0} \approx \frac{2}{\tau_0'}$). From reference 10

$$G_M(s) = \frac{K_M \left(\frac{s}{P_{sp}} + 1 \right) e^{-\tau_{NMS}}}{(T_{N1}s + 1) \left[\left(\frac{s}{\omega_N} \right)^2 + \frac{2\xi_N}{\omega_N} s + 1 \right]}$$

Then

$$Y_p(j\omega) = (j\omega G_x + G_y) G_M = K_p e^{-j\omega\tau_o} (T_L j\omega + 1) \left(\frac{T_W' j\omega + 1}{T_W j\omega + 1} \right) \left\{ \frac{(\frac{j\omega}{P_{SP}} + 1) e^{-j\omega\tau_{NM}}}{(T_{N1} j\omega + 1) \left[(\frac{j\omega}{\omega_N})^2 + \frac{2\zeta_N}{\omega_N} j\omega + 1 \right]} \right\} \quad (14)$$

Equation 14 is nearly the same form as the Precision Pilot Model, (references 4 and 10), repeated here for the reader's convenience:

$$Y_p(j\omega) = K_p K_T \left[\frac{a_T}{\sigma_T} \right] e^{-j\omega\tau} \left(\frac{T_L j\omega + 1}{T_I j\omega + 1} \right) \left(\frac{T_K j\omega + 1}{T_M' j\omega + 1} \right) \left\{ \frac{(\frac{j\omega}{P_{SP}} + 1) e^{-j\omega\tau_{NM}}}{(T_{N1} j\omega + 1) \left[(\frac{j\omega}{\omega_N})^2 + \frac{2\zeta_N}{\omega_N} j\omega + 1 \right]} \right\} \quad (15)$$

Note that the terms $(T_W' j\omega + 1)$ and $(T_W j\omega + 1)$, constituting a lag-lead pair in the multiple loop model, appear to be compatible with the low frequency factors $(T_K j\omega + 1)$ and $(T_K' j\omega + 1)$ from the Precision Pilot Model. Equation 14 contains a lead term $(T_L j\omega + 1)$ as required by the servo theory for pilot equalization. However, it contains no lag term equivalent to $(T_I j\omega + 1)$ of equation 15.

The servo theory, embodied in the Precision Pilot Model (equation 15) and the "adjustment rules," requires that the analyst select the pilot model parameters according to (primarily) the controlled element dynamics $Y_c(s)$. Generally, either T_L or T_I is nearly zero according to whether lag or lead equalization is required to satisfy the closed loop system dynamic requirements. Later, an explanation will be offered of how the nonlinear model can produce lag equalization. Now we wish to discuss the multiple loop model, equation 14, vis-a-vis the servo model, equation 15. Note, however, that both models are "servomechanism" descriptions (e.g. compare the structure of figures 1 and 6). The "servo model," however, has become synonymous in the literature with the Precision Pilot Model (equation 15); the generic term is used here in that parochial sense. Furthermore, we wish to establish that the nonlinear, multiple loop theory need not be rooted in the framework of assumptions that force the human pilot model to be analogous to a linear, time-invariant servomechanism as in the "servo" theory.

Comparison of equations 14 and 15 indicates several important points:

1. The visual and indifference threshold $K_T \left[\frac{a_T}{\sigma_T} \right]$ from equation 15 is not explicitly present in equation 14. However, if the full effects

of the nonlinear time delay were considered then it is reasonable to expect that, in accordance with previous discussions, an apparent threshold would exist due to the rate sensor. Therefore, measurements of $Y_p(j\omega)$ from experimental tracking data would contain a remnant effect that could reasonably be attributed to an error threshold due to the linear correlation of error and error rate.

2. The time delay τ_o in equation 14 originates in the hypothesized rate sensor nonlinearity. It is equivalent to the delay τ in equation 15 when the neuromuscular delay τ_{NM} is included. The magnitude of the delay τ_o is, however, dependent in some as yet unknown fashion upon the level of the closed loop error rate signal. This, in turn, will be a function of the pilot model gains (notably K_{y_o}), the controlled element dynamics, $Y_c(s)$, and the spectral properties of the system input. Therefore it is plausible that a nonlinear delay, properly parameterized, could rationalize the experimental variations of τ (from equation 15) as they are known to exist and are documented in reference 4.

3. Equation 14 suggests that the dominant effects of the nonlinear time delay on the pilot model will occur serially with the term $e^{-j\omega\tau_o}$. This could account, in part, for the lagging low frequency phase angles measured and documented in reference 4 and modeled in the Precision Pilot Model by the factor

$$\frac{T_K j\omega + 1}{T_K' j\omega + 1}$$

in equation 15. The nonlinear model suggests, however, that the lagging low frequency phase will result from the combination of the nonlinear delay with the washout dynamics. The low frequency lead time constant T_W' is dependent upon the washout time constant T_W , the error rate signal amplitude level (and hence τ_o), and the relative gains for error and error rate control K_{y_o}/K_{x_o} .

4. The low frequency lag-lead pair in the Precision Pilot Model discovered in the reference 4 experimental program was attributed to neuromuscular system dynamics in that report. In reference 10 the effect was conclusively shown not to result from direct neuromuscular dynamics, and the terms were attributed to "central processes." Here the terms

$$\frac{T_W' j\omega + 1}{T_W j\omega + 1}$$

in equation 14 are seen to be the result of rate sensor dynamics (modeled as a rate washout because no information is known to exist to permit further refinement) together with a multiple loop model structure which treats error and error rate as distinct components of an information input vector.

5. Any wholesale attempt to interpret and rationalize the behavior of the Precision Pilot Model parameters shown in equation 15 from the basis of a conventional single loop servo theory description of the human pilot (as in figure 1) would be extremely confusing if the nonlinear model (figure 9) is, in fact, more physically appropriate. To illustrate, the nonlinear model, embodied in equation 14, indicates that the time constants τ_o , τ_L , τ_w and τ_w' are all interrelated in an orderly way. There is no physical model for this behavior in the single loop servo model.

6. The parameters K_p , τ_o , τ_L and τ_w' of equation 14 are all input-dependent to the extent that this affects the level of error rate and, hence, the nonlinear delay's response. Controlled elements which tend to produce highly oscillatory closed loop responses can therefore be expected to demonstrate the most sensitivity of these parameters to input level. If the nonlinear model is a suitable description of the human controller's actual behavior, then the comment applies to the parameters K_p , τ , τ_L and τ_K of equation 15.

7. An experimental program to measure $Y_p(j\omega)$ cannot, in general, distinguish which of the two candidate pilot models (the single loop model or the nonlinear model) is correct. Both describing functions are given by the ratio of cross-spectral densities:

$$\underbrace{Y_p(j\omega)}_{\text{single loop}} = \underbrace{(G_x j\omega + G_y) G_M}_{\text{multiple loop}} = \underbrace{\frac{\Phi_{y;\delta}}{\Phi_{y;y_e}}}_{\text{experiment}}$$

The nonlinear model offers a physical model for explaining experimental phenomena that are treated empirically within the single loop servo theory. This in turn may be of benefit for establishing the validity of the nonlinear model.

But what of the Precision Pilot Model's requirement for lag equalization ($\tau_L j\omega + 1$)? Consider the following:

1. The lag equalization shown in equation 15 was determined to apply when the controlled element dynamics were essentially a pure gain at low frequencies, i.e. $Y_c(s) = K_c$.

2. A pure gain controlled element produces no attenuation of closed loop modes present in the control stick response.

3. The lag equalization was determined to exist by Elkind, reference 14, for low-frequency, low-amplitude command inputs; his data do not confirm its presence for his more unconventional, high-

frequency inputs. The reference 4 experiments confirmed Elkind's results with low-bandwidth inputs.

The postulated nonlinear rate sensing leads one to suspect that for controlled element dynamics similar to those of a pure gain, with low bandwidth inputs, the error rate signal perceived by the human operator may be dominated by the response rate of the controlled element; that is, the rate command may be essentially zero. If this is assumed then the closed loop system of figure 10 reduces to the special case #2 discussed in the last article and shown in figure 12. For this case, the multiple loop pilot model, if valid, will reduce to the corresponding form given by the Precision Pilot Model. That is, from equation 13 with $X_c = j\omega Y_c$,

$$Y_p(j\omega) = \frac{G_y G_m}{1 + j\omega G_x G_m Y_c} \quad (16)$$

where $Y_p(j\omega)$ should be compatible with equation 15. Once again, the describing functions $G_x(j\omega)$ and $G_y(j\omega)$ are unknown. For the purpose of demonstrating the suitability of the nonlinear multiple loop model as an alternative to the Precision Pilot Model, and for consistency with the rationale for equation 14, assume

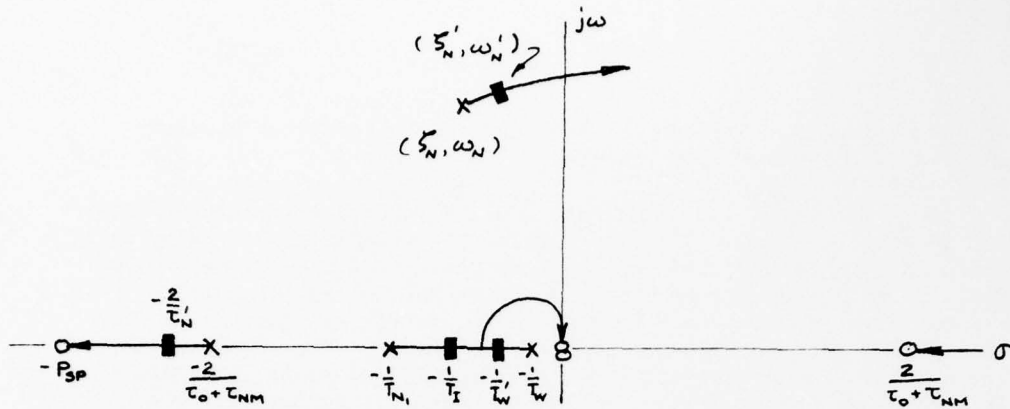
$$G_x = \frac{K_{x_0} T_w s e^{-\tau_0 s}}{T_w s + 1}$$

$$G_y = K_{y_0}$$

where for notational simplicity, $j\omega$ has been replaced by the complex variable s ; K_{x_0} , K_{y_0} and τ_0 represent average values, in some undefined sense, of K_x , K_y and τ respectively. Use the previous expression for $G_m(s)$ and the first-order Pade approximation for the time delay terms. Define

$$F = s G_x G_m Y_c = \frac{K_{x_0} K_c K_m T_w s^2 \left(-\frac{\tau_0 + \tau_{NM}}{2} s + 1\right) \left(\frac{s}{P_{SP}} + 1\right)}{(T_w s + 1)(T_{N1} s + 1) \left[\left(\frac{s}{\omega_N}\right)^2 + \frac{2\zeta_N}{\omega_N} s + 1\right] \left(\frac{\tau_0 + \tau_{NM}}{2} s + 1\right)}$$

Roots of $F+1 = 0$ are poles of Y_p . They vary as a function of $K_{x_0} K_c K_m T_w$ in the manner shown on the following root locus sketch. The particular pole-zero configuration shown is believed to be consistent with the known data base for neuromuscular system dynamics (reference 10) and with the washout dynamics hypothesized in this report.



Then

$$1 + BG_x G_M Y_c = \frac{(\tau'_N s + 1)(\tau_I s + 1) \left[\left(\frac{s}{\omega'_N} \right)^2 + \frac{2\xi'_N}{\omega'_N} s + 1 \right] (\frac{\tau'_N}{2} s + 1)}{(\tau_N s + 1)(\tau_{NI} s + 1) \left[\left(\frac{s}{\omega_N} \right)^2 + \frac{2\xi_N}{\omega_N} s + 1 \right] (\frac{\tau_o + \tau_{NM}}{2} s + 1)}$$

To a first approximation, $\tau'_N = \tau_o + \tau_{NM}$. The cancellation of time delay terms appearing in the final expression for $Y_p(j\omega)$ will not be precise. However, the phase contribution to $Y_p(j\omega)$ due to the time delay-derived term

$$\left(\frac{\tau_o + \tau_{NM}}{2} j\omega + 1 \right) / \left(\frac{\tau'_N}{2} j\omega + 1 \right)$$

can be approximated by $e^{-j\omega\tau_o}$. Finally,

$$Y_p(j\omega) = K_p e^{-j\omega\tau_o} \left(\frac{1}{\tau_I j\omega + 1} \right) \left(\frac{\tau_N j\omega + 1}{\tau'_N j\omega + 1} \right) \left[\frac{\left(\frac{j\omega}{P_{sp}} + 1 \right) e^{-j\tau_{NM}\omega}}{\left(\frac{j\omega}{\omega'_N} \right)^2 + \frac{2\xi'_N}{\omega'_N} j\omega + 1} \right] \quad (17)$$

Equation 17 is an approximation to the nonlinear, multiple loop pilot model provided that the rate and position loop nonlinear effects are adequately represented by the forms assumed for the describing functions G_x and G_y . However, equation 17 is a valid representation for human dynamic response if and only if it is completely consistent with the Precision Pilot Model (equation 15) which, of course, is merely an analytical fit to the available manual tracking data base.

Equation 17 may be directly compared with the Precision Pilot Model. No low-frequency lead equalization term $(\tau_L s + 1)$ appears in equation 17; this term, however, is not necessarily present in the Precision Pilot Model for pure gain controlled elements with low-frequency command inputs. The low-frequency ratio

$$(\tau_N j\omega + 1) / (\tau'_N j\omega + 1)$$

is seen to be lead-lag in form (i.e., $T_w > T_w'$) instead of lag-lead as prescribed by the Precision Pilot Model of equation 15. This is not regarded as a serious issue here since the data base for pure gain controlled elements (chiefly reference 4 and 14) does not permit high quality resolution of the low frequency phase lag. The lag-lead explanation for this phase lag in the Precision Pilot Model is empirical and based on the assumption of a single loop pilot model structure with constant time delay. The multiple loop theory attributes the phase lag to two sources: the washout dynamics coupled with other system dynamics and the nonlinear delay, directly. Equation 17 does not contain a first-order neuromuscular system lag. This, also, is not a matter of concern here since the lag is of little significance to closed loop system dynamics and since the data base for pure gain controlled elements does not permit its resolution with any accuracy (i.e. it may not, in fact, exist for pure gain controlled elements). Elkind's measurements did not extend to the neuromuscular range and the reference 4 experiments purposely did not address the pure gain controlled element to any depth.

Equation 17 does contain the first-order lag term ($T_I s + 1$) required by the Precision Pilot Model. This term, according to the multiple loop theory, originates from coupling between the neuromuscular system time constant T_{N1} and the washout time constant T_w due to rate feedback! This is a complete departure from the conventional viewpoint regarding its origins and is - - at least to this author - - a much more palatable explanation than the assumption of premeditated lag equalization by a single loop human pilot. The origin of the lag term in the multiple loop model may be seen much more clearly if the neuromuscular system dynamics are neglected. A low frequency approximation is then

$$Y_p(j\omega) = \frac{G_Y}{1 + j\omega G_X K_C} = \frac{K_{Y_0}}{1 + j\omega K_{X_0} K_C} = \frac{K_{Y_0}}{1 + T_I j\omega}$$

where $T_I = K_{X_0} K_C$. This is overly simplified, perhaps, but it clearly demonstrates that the lagging equalization is the result of the inner (rate) loop closure of figure 12.

The possibility must be accepted that this same form for $Y_p(j\omega)$ can apply to controlled elements other than pure gains. The multiple loop theory suggests that the applicability of equation 16 will depend upon the system input as much as upon the controlled element dynamics due to the hypothesized rate sensor nonlinearity. Until the structure and component descriptions of figure 9 are resolved in detail, it will not always be possible to make an a priori deduction of the correct form for $Y_p(j\omega)$ given arbitrary combinations of controlled elements and input.

The simplified analysis above can be applied to other controlled elements with effect. Assume $G_M = 1$;

1. $Y_c(s) = \frac{K_c}{s}$: it is well-known that control of such dynamics is "easy" and "pleasant." The closed loop response is not oscillatory. For low bandwidth command or disturbance inputs it is reasonable to assume $G_x = 0$ (i.e. no rate feedback). Then

$$Y_p(s) = sG_x + G_y = K_{y_0}$$

That is, a low frequency approximation to Y_p is a pure gain - - in agreement with the Precision Pilot Model. It is interesting to point out that when no command input exists ($x_i(t) = y_i(t) = 0$) then

$$Y_p(s) = \frac{G_y G_M}{1 + sG_x G_M Y_c}$$

would appear to apply regardless of the controlled element. For the K_c/s controlled element, assuming $G_M = 1$, this form will reduce to:

$$Y_p = \frac{K_{y_0}}{1 + K_{x_0} K_c} = K_p \quad - - - \text{a pure gain!}$$

That is, this viewpoint suggests that an inner loop rate feedback only serves to modify the gain of the outer-loop equivalent controlled element. Consequently, there is no rigid requirement on the level of rate control required to create a satisfactory loop closure.

2. $Y_c(s) = \frac{K_c}{s^2}$; this is known to be a "difficult" system to control. Assume the correct model form is

$$Y_p = sG_x + G_y \cong K_{y_0} \left(\frac{K_{x_0}}{K_{y_0}} s + 1 \right)$$

The alternative possibility (for no rate command input, at least) is

$$Y_p = \frac{G_y}{1 + G_x K_c / s} \cong \frac{s K_{y_0}}{s + K_{x_0} K_c}$$

Either of these forms is plausible; the first, however, probably best agrees with the experimental evidence.

These three examples suggest that change in controlled element dynamics from the form K_c/s to K_c to K_c/s^2 requires a progressive increase in the level of rate loop control to satisfy the overall closed loop requirements. It seems reasonable to expect that highly unstable controlled elements will require additional increments of rate control. At this point it should be noted that the unified ranking of these controlled elements with respect to their equalization requirements is possible only because the proposed model treats error and error rate as distinct stimuli within a multiple loop structure. The lag required

in the conventional theory for $Y_c(s) = K_c$ simply doesn't "fit" with a ranking of controlled elements according to their lead equalization requirements.

In summary, the simplified treatment above has established the plausibility that all controlled elements may be classified according to their requirements for rate feedback "activity." Namely, the K_c/s controlled element requires no or minimum rate feedback, K_c requires more, and K_c/s^2 requires more yet. Unstable controlled elements may be expected to fit within this ranking in an orderly fashion; e.g. $Y_c(s) = K_c/(s-\lambda)$ will probably require more rate feedback than will $Y_c(s) = K_c$ but less than $Y_c(s) = K_c/s^2$ - - at least for λ less than about 4.0. Similarly, $Y_c(s) = K_c/s(s-\lambda)$ will probably require more rate control than will $Y_c(s) = K_c/s^2$. When one considers that typical pilot opinion ratings vary uniformly from optimum for K_c/s - like controlled elements to very poor for highly unstable ones, then the potential for correlation of rate feedback "activity" measures with pilot opinion ratings is unmistakable.

The single loop servo theory for human dynamics offers no explanation for the origin of control stick "pulsing" that is known to occur in tracking experiments with controlled elements similar in form to K_c/s^2 or for certain unstable ones. The best the Precision Pilot Model can offer for these situations are rules for selecting the lead requirements in the model and advice about the level of remnant required to yield reasonable estimates of closed loop signal levels (e.g. see references 15 and 16 for a discussion of empirical remnant data). The model cannot replicate the distributions of control motion - - which are typically bimodal. Examination of the nonlinear pilot model structure (figure 9) suggests an immediate explanation. The controlled elements for which control pulsing is known to occur are those for which the closed loop response is highly oscillatory. The phase margins measured for closed loop systems of this sort would be minimum and approach zero in extreme cases (see figure 13 which is a summary of phase margin measurements from the reference 4 experiments). The closed loop error rate for these systems would be quite periodic, although not exactly sinusoidal. The periodic content of error rate would, however, be sufficient to evoke a pulsing type response from the nonlinear delay with pulse amplitudes proportional to rate amplitudes. This nonlinear response would then become the "bimodal" content of the control response $\delta(t)$.

More comparisons between the nonlinear model theory and the data base with its single loop servo model explanation are possible. However, it is clear from the above discussions that a more detailed model for the nonlinear elements of figure 9 would be of considerable benefit to such a comparison. The nonlinear model's structure

and the candidate nonlinearities can create a number of possible forms for $Y_p(s)$; these can serve to obscure comparisons almost as much as to provide enlightened understanding of experimental behavior.

It is important to understand that the human operator does not select the form of $Y_p(s)$ to apply given a combination of input and controlled element. According to the nonlinear model hypothesis his feedback system structure is fixed. The specific feedback nonlinearities create system responses which require $Y_p(s)$ forms of the sort shown above for their explanation in classic terms. In other words, the classic lag or lead equalization may only be apparent. Both can originate with rate feedback control. Whether the rate control is identified as a lead or a lag activity depends, in certain cases (e.g. $Y_c(s) = K_c$), upon how the analyst chooses to visual a model for human controller dynamics.

If one is to extend the parallel between the nonlinear and single loop theories, it is necessary to restrict the controlled element to those that are adequately modeled by linear, constant coefficient differential equations and to require that the system input (command or disturbance) be a near-gaussian process. These restrictions are necessary to stay within the framework of the servo and optimal control descriptions of the human pilot. The data base for pilot dynamics is, in the main, characterized by these same limitations. The reader should note, however, that these restrictions need not apply to the multiple loop, nonlinear model. No assumptions of that sort are required in its development. Nevertheless, if one wishes to consider nonrandom inputs or time-varying, nonlinear aircraft responses, it is necessary that appropriate models for physical processes be provided within the model. For example, the rate sensor dynamics may not be the same for discrete inputs as for continuous ones; the criteria for control in maneuvering flight, with no external inputs, are not always known a priori but must be modeled. With regard to the latter possibility, it must be recognized that not all human controller activity can be modeled in a genuinely predictive manner, nor should we worry about this. Our concern should be to devise adequate, predictive models for controller behavior (including his verbal rating) that is of direct interest to aircraft system design and design optimization.

SECTION III

A UNIFIED MODEL FOR PILOT DYNAMICS IN SINGLE LOOP TRACKING. PART 2: COMPUTER SIMULATION AND PARAMETER SEARCHES

A. APPROACH

Available experimental data were used for the resolution of the postulated nonlinear, multiple loop pilot model in structure and detail. Detailed analytical comparisons were attempted between the pilot model parameters predicted using the linearized model shown in figure 10 and the experimental results of reference 4 - - plus those of reference 14 to a minor extent. This was an attempt to quantify the average gains, K_{x_0} and K_{y_0} , and the constant of proportionality k in the nonlinear time delay model:

$$\tau = \frac{K}{|X_w|}$$

It was a general conclusion of this work, however, that the analytical approach was not likely to permit quality resolution of the sort required over all the data ranges.

Another difficulty faced in the validation of the proposed model was the dearth of time response data available for comparison with model predictions. The reference 4 data base is presented entirely in the frequency domain. Hence, the choice was made to program the pilot model and the controlled element, both suitably parameterized, on a digital computer, use sums of sine waves to generate a command input, mechanize an analyzer for the estimation of the pilot model describing function $Y_p(j\omega)$, and adjust model parameters until a match could be obtained of $Y_p(j\omega)$ with those documented in reference 4 together with physically reasonable system time responses. In the actual trials the emphasis was on obtaining qualitatively reasonable time responses, both in amplitude and temporal character. The measurement of $Y_p(j\omega)$ was used as a final, quantitative check on the validity of the model. The system input used was precisely that of the reference 4 experiment - - tabulated in Table 1.

The original intent was to iterate on pilot model parameters until a match was also achieved between predicted and measured values of remnant, correlation coefficients, signal amplitude distributions, and power spectral density of the control δ . This, however, was never accomplished due to failure to succeed with the primary objectives.

The decision was made to perform all parameter searches manually

from an intercom terminal with a scope presentation of system time responses, describing functions and signal statistics. In this way a particular baseline combination of nonlinear element parameters was selected for a given input and controlled element; the program would then be activated, and the results displayed at the terminal. Variations in the system parameters were made depending on the character of the system response. This was done by the author in a trial and error fashion. Insight provided by analytical approximations, such as those presented in the previous article, provided useful clues to assist the parameter iteration.

It was assumed at the outset that the nonlinearities in the multiple loop model could be configured to simulate human response dynamics for specific controlled elements. For example, selecting $G_x \approx 0$ and $G_y = K_y e^{-\tau_0 s}$ (K_y and τ_0 are constants) would be guaranteed to basically satisfy the validation requirements for $Y_c(s) = K_c/s$ or $K_c/(s-\lambda)$. The introduction of an error threshold or a tailored amplitude-dependent gain $K_y = K_y(\gamma_r)$ would not be expected to qualitatively affect the simulation fidelity. The problem, however, was to devise one such model that would, with minor variation (preferably in G_y), simulate all five pilot-vehicle systems under consideration. Almost all the effort was directed toward this goal.

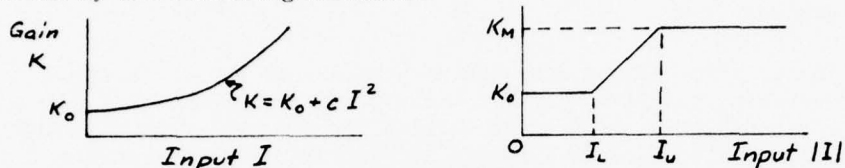
B. MODEL CONFIGURATIONS TESTED

There are an infinity of possible nonlinearities and ways for combining them that could be considered in a program to resolve and validate the proposed model for human pilot dynamics (figure 9). The successful comparisons between the linearized version of this model (figure 10) and the Precision Pilot Model, as discussed in the last section, indicated that the number and nature of required nonlinearities is probably limited. These nonlinearities were introduced in the last section.

There were two principal classes of model configurations tested: coordinated control of error and error rate for which $\beta = \beta_x + \beta_y$ (figure 9) and mode switching between control of either error or error rate, exclusively. These will be described here in sufficient detail to indicate their general character, only.

Both the switching and non-switching models were tested with and without rate washout or an error threshold. Variable and constant gain models for K_x and K_y were tested for each of these combinations. An error rate threshold was introduced in one set of trials for the non-switching model with constant gain values for K_x and K_y . One trial was made in which the nonlinear delay was placed in the error loop with constant loop gains and no switching. Another trial eliminated

rate feedback entirely and, instead, introduced a functional dependence of the position gain on x_D and y_T ; viz., $K_y = K_{y0} + p x_D y_T$, where $p = \text{constant}$. Two types of variable gain parameterization were used as shown by the following sketches:



Eight switching schemes were used in the evaluation of the merits of the switching model. These are listed below. The first was the nominal one, used for most simulations:

1. $S = p_1 x_D^2 - y_T^2$; $\beta = \beta_y (S < 0)$; $\beta = \beta_x (S > 0)$.
2. $S = p_1 x_D^2 - y_T^2$, as above determined the control mode when $|y_T| \leq y_L$ (an arbitrary value). Otherwise $\beta = \beta_y$.
3. $S = p_1 x_D^2 - y_T^2$ determines the control mode when $|y_T| > y_L$. Otherwise $\beta = \beta_y$.
4. $S = p_1 x_D^2 - y_T^2$ determines the control mode when $y_L < |y_T| < y_u$; $\beta = \beta_y$ when $|y_T| \leq y_L$; $\beta = \beta_x$ when $|y_T| \geq y_u$. Both y_L and y_u are arbitrary parameters that are intended to reflect the nearness of the closed loop state (error and error rate) to unacceptable levels of stability or to display saturation.
5. $\beta = \beta_x$ when $|x_D| > x_M$ (an arbitrary parametric value); $\beta = \beta_x + \beta_y$ when $|x_D| \leq x_M$.
6. $\beta = \beta_y$ when $|x_D| \leq x_M$; $\beta = \beta_x + \beta_y$ when $|x_D| > x_M$.
7. $\beta = \beta_x$ when y_T and x_D have the same sign; otherwise, β is determined as in (1) when $|x_D| \leq x_M$ and $\beta = \beta_x$ when $|x_D| > x_M$.
8. $\beta = \beta_x$ when $|x_D| > x_M$; otherwise, β is determined as in (1).

The neuromuscular system dynamic model was that obtained from reference 10; viz.,

$$G_M(s) = \frac{K_M \left(\frac{s}{30} + 1 \right) e^{-0.09s}}{\left(\frac{s}{10} + 1 \right) \left[\left(\frac{s}{15} \right)^2 + \frac{2(1)}{15} s + 1 \right]}$$

The gain K_M was set to 1.0 in all simulations for want of better information. No neuromuscular system parameters were varied during the course of the simulations.

All computer simulations were conducted on the CDC 6600 computer at Wright-Patterson Air Force Base, Ohio.

C. RESULTS

The accuracy of the measurement system used for estimation of the describing function $Y_p(j\omega)$ was of concern. Therefore, preliminary runs were conducted to examine the quality of the measurement system (discussed in Appendix B) and to establish suitable values for time step sizes and run lengths to avoid the introduction of systematic errors in the measurement process. Certain of these data sets will be shown later. It was found that run lengths of at least 40 seconds and time steps of about .0125 to .025 seconds were usually sufficient to ensure a reasonable measurement of system dynamics. The exception was at the very lowest measurement frequencies where errors (especially in phase) are practically impossible to eliminate - - at least with the Fourier coefficient measurement scheme.

A check was made on the fidelity of the neuromuscular system model. The neuromuscular system equations were excited with the sums of sine waves input, the input and response were Fourier transformed by the analyzer described in Appendix B, and the transfer function $G_M(j\omega)$ was estimated as the ratio, at each input frequency, of the output to input Fourier coefficients. The results are shown on figure 14. Both the amplitude and phase estimates are seen to be in excellent agreement with the analytical values when the run length is 40 seconds. Note the absence of scatter and compare this result with measurements made later with a mode switching pilot model.

Further checks were made of the measurement technique and of the programming fidelity by measuring, in situ, the dynamics of the various simulated controlled elements. This was done by selecting parameters for the pilot model which yielded a stable and reasonable closed loop response, running the pilot-vehicle simulation for a prescribed time period, and estimating the ratios of Fourier coefficients for the controlled elements' output and input. The results are shown in figures 15-19. The pilot models used for the controlled elements $Y_c(s) = 11.9$, $Y_c(s) = 11.9/s$, and $Y_c(s) = 11.9/(s-2)$ all used coordinated control of error rate and error (i.e., $\beta = \beta_x + \beta_v$) rather than mode switching. Mode switching models for pilot dynamics were used for measurements of $Y_c(s) = 11.9/s^2$ and $Y_c(s) = 11.9/s(s-2)$. In all five cases constant gain models were used.

The measured data for $Y_c(j\omega)$ are interesting and deserve comment.

There is a qualitative difference between the results obtained for the coordinated control pilot models (figures 15-17) and those for the mode switching models (figure 18 and 19). With the coordinated control models, the measured $\gamma_c(j\omega_k)$ converge toward the theoretical values as the step size is decreased and as the running time is extended. This is not necessarily the case for the mode switching pilot models. For these, considerable variation in measured $\gamma_c(j\omega_k)$ - especially the low frequency phase - is obtained with changes in running time or step size. Further, there is no clear trend toward convergence, particularly for the case $\gamma_c(s) = 11.9/s(s-2)$. An exception to these remarks occurs in the mid-frequency region near the expected crossover frequency. There, the variability in measured phase and amplitude is virtually nonexistent for all conditions shown.

In reference 4, it is noted that considerable variability in the measured human operator describing function is usually obtained for a number of trials with the same subject or between different subjects. In the experiments this variability was found to be minimum, however, near the crossover frequency. Reasons for this have never been determined, but the authors of reference 4 suggested that the crossover frequency has an important bearing on system stability and performance; therefore, all subjects will be constrained in their dynamic response near the crossover condition - hence the low variability of measurements near crossover. It was further suggested that variability in measurements at other frequencies reflects operator "style" variations which, by and large, aren't too important to system dynamics and performance. Here, in the measurement of controlled element dynamics, we see a similar sort of measurement result that would be difficult to attribute to "style" of the computer pilot! The matter, however, will not be considered further in this report.

It was generally difficult to select parameters for the pilot model that would produce a stable closed loop system. Stability in a nonlinear system is often difficult to ascertain; these were no different in that respect. The nature of the nonlinearities selected for the pilot model, together with the typical closed loop dynamics sought, tended to produce limit cycles in many of the cases examined.

It was no easy matter to identify observed oscillations as a limit cycle or to diagnose stability due, mainly, to contaminating effects of the system input. The input was replaced, in a few cases, with initial conditions on the motion in order to more easily resolve questions of system stability. This was unsatisfactory, however, since the lack of a continuous input was often sufficient to change the closed loop response in a qualitative way. Thus, the experimental evidence was that the pilot-vehicle system model could not be divorced from the system input when searching for its identifying parameters. A typical problem encountered in the conduct of these parameter searches was that a

combination of model parameters would yield closed loop time responses that were stable for a number of seconds (usually 15 to 20 seconds from problem initiation) and then suddenly diverge.

A general observation from the examination of several hundred system time responses and dozens of measured pilot model describing functions was that $\gamma_p(j\omega_k)$ is not a very sensitive measure for pilot-vehicle system dynamics. It appears that - - at least for systems characterized by figure 9 - - qualitative changes can be created in closed loop time response, due to variations of model parameters, without major change to the describing function.

The original description of the postulated pilot model did not have mode-switching as a candidate nonlinearity. Switching was included in an attempt to create the lagging low frequency phase in measured $\gamma_p(j\omega_k)$. It was found by trial and error that the incorporation of unrealistically large thresholds in both the error and error rate channels would produce a sizable low frequency phase lag. The closed loop time responses were, however, physically unrealistic. An examination of the system's response suggested that error rate was usually large when error was small, and vice versa. Accordingly, the dual thresholds operated like a switch to dictate the control of either error or error rate. A mode switch of the form

$$\begin{aligned} S &= p_1 x_D^2 - \gamma_T^2 \\ \beta &= \beta_x \quad (S > 0) \\ \beta &= \beta_y \quad (S < 0) \end{aligned}$$

was then introduced as a candidate nonlinearity. It is physically reasonable and is easily programmed.

A major thrust of this effort was to devise a set of parameters for the pilot model nonlinearities that would be invariant, or nearly so, with changes in controlled element or input. This goal was not achieved. It was, in fact, difficult to stabilize the "easier-to-control" $\gamma_c(s)$ without forcing error rate control to be near-zero. Levels of rate feedback for $\gamma_c(s) = K_c, K_c/s$ & $K_c/(s-2)$ sufficient to contribute significant power to $\delta(t)$ would almost certainly destabilize the closed loop. The elimination of rate control from these cases was, however, defeating the purpose of the entire program. A potential solution to the dilemma was to introduce nonlinear gains $K_x(x_D)$ and $K_y(\gamma_T)$, configuring these in such a way that the closed loop signal amplitudes would yield the appropriate loop gains for all controlled elements. This was the origin of the nonlinear gain model. Unfortunately, no acceptable configurations were found for the nonlinear gain models $K_x(x_D)$ and $K_y(\gamma_T)$. It was, in fact, often a struggle merely to stabilize the closed loop system with the gain models previously discussed.

A limited amount of success was achieved. The controlled element $Y_c(s) = 11.9/s(s-2)$ was extremely difficult to stabilize; after considerable difficulty, a mode-switching model for the human pilot was devised which would stabilize the closed loop and yield reasonable time responses. This same pilot model, without modification, was applied to the control of $Y_c(s) = 11.9/s^2$. The resulting closed loop system was stable and produced very reasonable signal behavior. The measured $Y_p(j\omega)$ for these two Y_c are shown in figures 20 and 21. The shaded regions on both figures represent the variations obtained in the data measured in the reference 4 experiments. It seemed reasonably clear that with a certain amount of tailoring, the multiple loop pilot model could provide an excellent match to these data. The more important part of the problem, however, was somehow to transform this successful model into one that was equally applicable without change to the other three controlled elements. This was attempted without success.

D. CONCLUSIONS

The results of the trial and error computer experiment were inconclusive. The properties of specific nonlinear pilot models were often such as to entice the author into believing that a major success was within his grasp; but this never materialized. On the other hand, the modeling approach still looks reasonable. No results were obtained that refute the philosophy behind it. However the study has confirmed to this author the truth of tales of manifold horrors that can be encountered in the study of nonlinear systems. In a way, this author is left feeling a little like a virgin: she thinks she knows - - and she does - - but she hasn't the experience.

No indication was found to suggest that a nonlinear pilot model could not account for a considerable portion of what, in past work, has been called "pilot adaptability." Instead, the successful application of one such model, without change, to two controlled elements suggests that hypothesis 1 of Section II is well-founded. However, even if the approach is completely valid, it will probably be exceedingly difficult to resolve the pilot model in detail. Additional data on the modality of visual sensing may be required for this purpose.

The mode-switching model appears to be a very attractive avenue to pursue with future research. The present study showed that it has features that are attractive in single loop tracking. Unfortunately, this study could not say conclusively that mode switching is an appropriate model.

Three possible sources were identified for lagging phase of the pilot describing function $Y_p(j\omega)$ at low frequencies. These are

the closed loop effects of a nonlinear time delay in the rate sensor, a rate loop washout, and a mode switching between control of error to control of error rate and vice versa. In general, it appears that mode switching is partly responsible for low frequency variability in measurements of $\gamma_p(j\omega_k)$. It is plausible to suspect that short-term variations in the nonlinear delay τ due to variations in the peak amplitudes of closed loop error rate are largely responsible for higher frequency variations in experimentally measured $\gamma_p(j\omega_k)$.

The interface provided an analyst by a computer terminal intercom is not sufficient for addressing this problem. A more timely interactive capability is required if a trial and error approach is ever to succeed in defining the details of the postulated pilot model. It would seem that a large-scale hybrid computer could be successfully applied to this problem. Such a facility would permit the nonlinearities (especially the nonlinear delay) to be programmed on the digital portion of the computer; the analog features would provide a capability for the analyst to make potentiometer adjustments while observing system response. This "instant feedback" feature could permit the rapid convergence to acceptable time responses that are required if the postulated pilot model is to receive an exhaustive evaluation.

SECTION IV

PREDICTION OF PILOT OPINION RATING

A. GENERAL COMMENTS

Any discussion of pilot opinion rating prediction, collection, or evaluation will lead sooner or later to the introduction of terms like "pilot variability" or "pilot set." These connote a randomness in a pilot's ability to produce consistent rating of a given task or rating biases that one pilot may display as a result of his personal tastes, prior experiences, whimsy or other factors too elusive to classify. If, indeed, an evaluation pilot's capabilities for objective and quantitative task or configuration ratings are significantly influenced by factors that bear no more than peripheral relation to the task, then useful predictions of pilot ratings may be impossible to achieve in other than contrived circumstances.

However, there is another viewpoint on this matter that has never been systematically addressed. Could not random appearing scatter in rating data result from a simulation or flight test that involves factors beyond the experimenter's control or that are unknown to him? Might not biases in a pilot's rating result from a poorly conceived experiment in which, for example, the operational task to be rated is only tenuously connected with the experiment or for which the specific operational problem is ill-defined to the pilot? Can unbiased ratings be produced by a subject who has limited experience in the purpose and use of the rating scale? We really know very little about the "physiology of ratings" or about whether a physical basis for them exists. Accordingly, it is reasonable to hypothesize that the shortcomings of the current base of pilot opinion rating data reflect our lack of knowledge of rating mechanics as much as the inadequacies, real or imagined, of the pilot as an evaluator of system quality.

With neither a physical theory for pilot opinion rating nor the knowledge that such a theory cannot be devised, it is logically impossible to categorize "inconsistencies" in pilot opinion ratings as apparent or real. An early theory for pilot opinion rating derived from the single loop servo theory for pilot dynamics. This theory, circa 1960, hypothesized that the pilot's equalization requirements, as measured within the context of this control theoretic, would quantify task difficulty and therefore correlate with rating data. Applications established that a correlation did exist but that equalization, as defined by the servo model, was not sufficient for the complete correlation or prediction of pilot ratings. There is something more involved.

An intuitive notion that has long been popular in certain circles is that pilot opinion should correlate with measures of tracking performance in the closed loop system. Numerous experiments, however, have shown that good performance does not necessarily indicate good ratings, and vice versa. Still, the notion persists. It isn't clear, for example, what "performance" might mean to an evaluation pilot; this, of course, has provided another research tangent with which the man-machine community can grapple.

There is something intuitively satisfying about correlating a pilot's rating with how hard he must work to perform the assigned task. The "workload" notion, however, which conceptualizes a metric for quantifying this relation, has introduced another red herring to flying qualities research; the search for a pilot workload measure seems to have become an end in itself.

McDonnell addressed the three topical areas above (viz., pilot dynamics, pilot performance, and task difficulty) plus an important new one - - the pilot opinion rating scale. He considered the general problem of how a scale for the quantification of pilot opinion can contribute to both systematic and random errors in rating data; he suggested an alternate scale derived from the application of psychometric principles. McDonnell did not question the existence of a physical basis for pilot ratings but, by implication, assumed its existence. He concluded that ... "ratings are probably based on performance and the degree of difficulty experienced in maintaining the performance. The difficulty is most easily represented by the pilot equalization required and the vehicle stick characteristics" ... reference 17.

Anderson (reference 3) proposed a formal method for the prediction of pilot opinion ratings. The method is based on the assumption that a pilot will, in some way, adjust his equalization to optimize his own ratings. It requires a "rating functional" which formally connects system performance (typically, expressed as mean-squared error), pilot equalization, and pilot rating. The method, now generically known as "Paper Pilot," provided the first rational treatment of the combined effects on pilot ratings of system performance and pilot dynamics.

There is, however, no known physical basis for the Paper Pilot concept of rating optimization. Like workload, the concept is philosophically interesting, difficult or impossible to disprove, and intuitively satisfying to some. It suffers from two principal limitations. First, a rating functional is required which, when minimized via applications of linear, optimal control theory, will yield a numerical estimate of pilot opinion rating. There is no physical rule for selecting the functional; past applications of the Paper Pilot method have used functionals based on statistical correlations of rating with performance and servo model parameters. Unfortunately the functionals derived for past studies have not been unique; it is difficult or impossible to select

a valid rating functional on any a priori basis. It also seems to be true that the rating prediction is sensitive to the choice of functional.

The second limitation of the Paper Pilot methodology concerns the fidelity with which one can predict the parameters in the servo model for human pilot dynamics. This is, in general, a difficult and somewhat artistic task. When done to the level of detail required by the Precision Pilot Model (reference 4) it is not well suited to the iterative solution methods required for applications of optimal control theory. Simplified and less accurate pilot model forms are normally used - especially for multiple loop control tasks where considerable artistry must be employed in their selection.

It may be that the true value of the Paper Pilot theory is that it represents a new way of thinking about pilot rating data and has carried rating discussion to a new level of sophistication. Further, the occasional success of the theory is cause for real hope that pilot opinion is based on (unknown) physical considerations and may, therefore be predictable. However, no method for the prediction of ratings is of more than academic interest without a self-consistent, physical theory which can bound its limits of validity. An empirically derived model may be perfectly satisfactory for data correlation or for interpolation over a data set; it is of limited value for prediction in the absence of data and of no value for extending the flying qualities specification into areas of novel control methodology or unusual airframe dynamics.

In this section it will be assumed that a physiological basis exists for pilot rating, that its character is suggested by the nonlinear, multiple loop pilot model of Section II, and that this leads to a unique handling quality metric for the prediction of pilot opinion ratings. The metric will be evaluated for a particular set of single loop tracking data. It will also be used for preliminary examination of a multiple loop control task. Generalizations will be made about the metric, its connections with Paper Pilot and some short-comings of the pilot modeling state-of-the-art.

B. IMPLICATIONS OF THE NONLINEAR, MULTIPLE LOOP PILOT MODEL

It appears to be generally true that in single and multiple loop tracking tasks the amount of pilot lead equalization, as determined from the servo model for pilot dynamics, is an indication of good or poor pilot opinion ratings. However, there are situations where poor ratings are obtained while only a small lead is measured, and vice versa. Further, it has been well documented that pilot opinion of a flight control task is as much a function of input intensity as of vehicle dynamics per se. The conventional servo model for human pilot dynamics does not admit variations in pilot equalization with input amplitude.

Thus, lead (or lag) equalization is not a suitable metric for pilot opinion - - at least from the viewpoint provided by the servo model.

Use of the servo model (e.g. figure 1) will seriously handicap any analysis of pilot opinion rating prediction if a physical rating mechanism, internal to the human pilot, exists as assumed here. By present theory we must conclude that the servo model is basically flawed in that it intermixes the effects of proportional and rate control. This, of course, is the result of its treatment of input as a scalar quantity. If pilot opinion rating and task difficulty are related one-to-one, and if pilot equalization is a reasonable measure of task difficulty, then past failures to correlate equalization entirely with rating can reasonably be attributed to shortcomings in the servo description of human pilot dynamics as a model for pilot equalization.

The simplified analyses comparing the properties of the servo and multiple loop models, given in Section II Article G of this report, have established the plausibility that the servo model equalization terms (lead and lag) derive entirely from rate feedback when this is treated as a distinct information path as in the multiple loop pilot model. The significance of this observation is that for a constant input level it appears to permit the relative ranking of controlled elements according to the level of rate feedback required to yield closed loop dynamics as determined by experiment. This ranking is important because it appears to be consistent with the known trend of pilot opinion rating over these same controlled elements. It was indicated in Section II, for example, that in order of increasing rate feedback requirements we would probably have $\gamma_c(s) = \frac{K_c}{s}, K_c, K_c/(s-\lambda), \frac{K_c}{s^2}, K_c/s(s-\lambda)$. A metric which quantifies the level of rate feedback control might also quantify the pilot opinion rating.

Thus, a duality appears to exist between pilot opinion rating and the level of rate feedback required by the multiple loop pilot model for a prescribed control task and with constant input intensity. Furthermore, if it is assumed that the level of rate control "activity" is the harbinger of pilot opinion rating, then it is reasonable to expect that a rating metric based on this property will encompass effects on rating due to input intensity as well as those due to controlled element dynamics. This corollary follows immediately from the multiple loop model structure (figure 9) where it is apparent that, regardless of how one defines rate control "activity," an activity metric will be dependent upon closed loop dynamics (especially the amplitude and frequency of the dominant mode) and input statistics.

C. A METRIC FOR RATING PREDICTION IN SINGLE LOOP TRACKING

The notion of rate loop "activity" introduced in the last article is a bit ethereal and of no more practical value than "workload" or "task difficulty" measures unless it can be quantified in a unique way which derives from a physical, rather than intuitive or statistical, theory. The following two hypotheses are therefore proposed:

HYPOTHESIS: A general, physiological measure for rate control "activity" in single loop tracking is the rate of nerve impulses (or an equivalent physical measure) at the point within the central nervous system where all signals originating due to rate control are summed. The neuromuscular system is postulated to provide a component to this hypothesized signal junction; this component is dependent upon the feel system characteristics and will affect pilot rating. In the remainder of this report the contributions of the feel system to pilot opinion will be discounted by assuming that the control system force and displacement sensitivities are optimized with respect to pilot opinion rating. Then to the extent that the control feel is optimum, the nerve impulse rate due to rate feedback control will be uniquely related to pilot opinion.

HYPOTHESIS: The relation between pilot opinion and nerve impulse rate at the summation point of all signals originating due to rate control is fixed for each pilot. It may depend upon his piloting experiences, training and his personal interpretation of the pilot opinion rating scale. It is independent of controlled element dynamics, input characteristics, and task specifics.

Measurements of central nervous system activity such as that proposed above are not available in the handling qualities literature and, in all probability, are beyond the present state-of-the-art of medical science. Within the context of the multiple loop model (figure 9), what we seek is a measure for the level of the signal β_x (the rate loop output to the neuromuscular system). The root mean square value σ_{β_x} might suffice, but it is not directly measurable. On an average basis terms for which measurement may be possible can be substituted for σ_{β_x} . Observe that, with $x_s = x_w$ in figure 9,

$$\sigma_{\beta_x} = K_R \sigma_{x_s}$$

where x_s is the rate error as sensed by the human pilot and K_R is the average equivalent gain in the rate channel between x_s and β_x . In general, x_s will not equal x_w ; in particular, the visual display may insert nonlinearities or additional dynamics into the rate channel between x_e and x_w . The signal x_s is not measurable. However,

$$\sigma_{x_s} = K_{D_x} \sigma_{x_e}$$

where K_{D_x} is the average equivalent gain in the rate channel between

x_e and x_w - - in effect, a display gain. Finally, the proposed metric for pilot opinion rating is just

$$\sigma_{\beta_x} = K_{D_x} K_R \sigma_{x_e} \quad (18)$$

In accordance with the above discussion, it is hypothesized that a monotonic relation will exist between σ_{β_x} and pilot rating in the manner shown on figure 22.

A principal reason for the work described in Sections II and III on the development of a multiple loop model for the human pilot was to enable the prediction of the gain product $K_{D_x} K_R$. At this writing, however, this has not been achieved. The reader should recall that a basic proposition of this modeling study was that the model sought will unify existing pilot models, viz., the conventional single loop servo model and the Kleinman model. It is contended that both these state-of-the-art models are satisfactory in a limited sense but are subsumed by a nonlinear, multiple loop model similar in structure to that shown in figure 9. Therefore it is reasonable to believe that either the servo or the Kleinman model could be used for the estimation of σ_{β_x} , in lieu of a more accurate model.

If the Kleinman model is used for the estimation of σ_{β_x} , then

$$\sigma_{\beta_x} = K_{D_x} K_x^* K_{F_x} K_{P_x} \sigma_{x_e} \quad (19)$$

where (see figure 2)

- K_x^* = optimal controller gain in the x(rate) channel.
- K_{F_x} = an equivalent gain for the Kalman filter.
- K_{P_x} = an equivalent gain for the state predictor.
- K_{D_x} = an equivalent display gain.

There is a certain risk entailed in the use of the Kleinman model for this purpose. It was devised as a tool for the estimation of system performance. It contains no guarantee that it can accurately predict system properties at the high level of detail required here. Furthermore, it has already been mentioned that the Kleinman model requires the selection of a cost functional and weighting factors for the terms in this functional. We have no physical guarantee that a cost functional and its weights will apply to tasks other than that for which they are tailored to match system performance measures. Another difficulty will arise if the controlled element gain K_c (which is, typically, a control effectiveness derivative such as M_{δ_e}) is non-optimum with respect to pilot opinion rating. The Kleinman model merely adjusts K_x^* to optimize the gain product $K_x^* K_c$ - - i.e., K_x^* is dependent on K_c . The pilot opinion metric σ_{β_x} , however, is independent of K_c . Therefore, when the Kleinman model is used for the estimation of

$\sigma_{\beta x}$ the predicted value of K_x^* must be normalized with respect to the value of K_c for which pilot opinion is optimized. Any subsequent prediction of pilot rating will therefore apply only to those aircraft-controller configurations for which the control feel characteristics have been optimized with respect to pilot opinion rating. Experimental measurements of the terms of equations 18 or 19 can only be correlated with pilot opinion rating if, during the experiment, the control system gain was optimized with respect to pilot opinion at each configuration tested.

It is reasonable to expect that the neuromuscular system contributes (through muscular tension, perhaps) to the nervous system activity at the point where the rate control signals are summed, and that if this effect were included in the estimation of $\sigma_{\beta x}$ then the effects on pilot rating due to non-optimum control feel characteristics could also be predicted. There are insufficient data available for this purpose at the present time; it is also beyond the scope of the present study and will not be considered further.

The remarks concerning the effects of nonoptimum controller gain on pilot opinion rating apply equally well to the single loop servo model for pilot dynamics. If the servo model is used for the estimation of $\sigma_{\beta x}$, then equation 18 is replaced with

$$\sigma_{\beta x} = K_{Dx} K_p T_L \sigma_{xe} \quad (20)$$

The product $K_p T_L$ is the servo model approximation to the rate controller gain. It is a valid approximation to K_x^* in the Kleinman model only for certain conditions that cannot be prescribed a priori. Equation 20 should be used only as a last resort. The problem with the conventional servo model, from the viewpoint of the proposed pilot model, is that it requires no lead and therefore no rate feedback for three broad classes of controlled element configurations, viz., $\gamma_c(s) = K_c$, K_c/s &

$K_c/(s-\lambda)$. For each of these the nonlinear model for pilot dynamics - - which is claimed to more precisely model human physiological process mechanics - - will possibly yield considerable rate feedback activity. Thus, equation 20 is strictly inapplicable when $T_L \approx 0$. The Kleinman model apparently does not suffer from this same limitation. Therefore equation 19 is recommended as an interim formula for the estimation of $\sigma_{\beta x}$.

The metric $\sigma_{\beta x}$ implicitly includes effects on pilot opinion rating due to controlled element dynamics, disturbance or command inputs, or task requirements. It is hypothesized that if the generic relation between pilot rating and $\sigma_{\beta x}$ shown in figure 22 can be quantified for any single loop tracking task, then the result can be used as a calibration of rating vs. $\sigma_{\beta x}$ for any other single loop tracking task! Further, it is hypothesized that if $\sigma_{\beta x}$ could be measured from flight test or

simulation experiments in which pilot ratings are also obtained, then the ratings would be entirely correlated with $\sigma_{\beta x}$ in the sense that a plot of rating vs. $\sigma_{\beta x}$ would yield a single-valued curve of the form shown in figure 22. Then, to the extent that effects on rating due to control feel characteristics have been minimized, $\sigma_{\beta x}$ can be considered as the magical and long-sought workload measure for pilot opinion.

D. VALIDATION OF THE RATING METRIC FOR SINGLE LOOP TRACKING

By above hypothesis the proposed metric for pilot opinion rating $\sigma_{\beta x}$ can be correlated with rating data obtained from any handling quality experiment provided sufficient data are measured to permit the estimation of $\sigma_{\beta x}$. [As an aside, we must estimate $\sigma_{\beta x}$, via the use of experimental data and a model for pilot dynamics, until such time as a technique can be devised for its direct measurement by experiment.] Almost no such data exists.

Reference 18 is the notable exception known to this author. Arnold's pilot opinion rating data were obtained from a fixed base simulation of pitch attitude tracking in turbulence with fighter-type aircraft dynamics. His experiment was conducted using five current service pilots, each of whom had broad operational experience in the type of aircraft and task being simulated. The task definition was prescribed with the aid of the subjects; their principal contribution to the experimental design was to select an attitude display configuration (cathode ray tube simulation of IFR tracking in pitch) and level of turbulence intensity that seemed realistic in an operational sense. Further, the subjects were instructed to fly the simulation just as they would the actual airplane. [This approach to simulation of handling quality problems seems, to this author, to make much more sense than the pedantic one in which all simulation parameters are pre-selected by the analyst. The results from such simulations are, of course, valid in some sense, the question, however, is to determine their meaning in a flight environment.] Arnold's display contained a sizable threshold introduced to promote task realism. The predominant effect of this display was to eliminate the display of small pitch changes about the reference attitude such as, for example, those due to "nose bobble". Fourteen aircraft configurations were evaluated. Each was flown several times by each subject and average pilot opinion ratings were obtained. The configurations selected had previously been flight tested in the USAF variable stability T-33 (reference 19). Arnold's pilot ratings were intended for comparison with the flight-measured ratings in order to examine possible effects on ratings due to motion or to task differences. His subjects were free to select control stick gearing (i.e. controlled element gain) over a range of one to ten lb/deg. For purposes of establishing a calibration between the proposed pilot rating metric $\sigma_{\beta x}$ and pilot rating this procedure is probably ade-

quate for ensuring that the experimental rating data are not contaminated with effects due to nonoptimum controlled element gain. A force stick was used.

Arnold's subjects selected a random w-gust intensity of 10 ft/sec rms value. The spectral shape used was a first-order approximation to the Dryden gust model of reference [2]. This rather high intensity turbulence level was selected on the basis that it provided a realistic and natural pitch tracking task similar to actual flight conditions.

Table 2 is a listing of stability derivatives and various short-period parameters as tested in the Arnold experiment. These data had already been analyzed by Major James Dillow of the Air Force Institute of Technology. He used a modified version of the Kleinman model which allowed the incorporation of the display threshold and selected a cost functional and its weights to yield a close match between model-predicted and measured closed loop tracking performance (viz., mean square pitch attitude error). This work, recently published (reference 25), and the associated computer programs were made available to this author by Major Dillow.

The Kleinman-Dillow model (subsequently referred to as the K-D model) departs from the conventional Kleinman model (figure 2) in that display or physiological thresholds are incorporated into the rate and position feedback paths just prior to the Kalman filter. Each is included in the model as a gain term (which, for random inputs, is the describing function representation for a threshold nonlinearity) followed by an injection of remnant to simulate the nonlinear portion of the threshold's response. The threshold gain and the signal level of the threshold remnant are adjusted iteratively, during the solution of the optimal control problem, to ensure that the threshold's input and output signal levels are consistent with the choice of describing function. The cost functional used in the K-D model consists of the weighted sums of the variances of state variables as they are perceived by the human operator. This is a conceptual departure from the original Kleinman model (illustrated on figure 2).

Another unique feature of the K-D model is its incorporation of a calculation for the equivalent Kalman filter gain in each feedback channel. This is done in ad hoc fashion, following convergence of the routine for solving the matrix Riccati equation, by computing the ratio of root-mean-square signal levels for the estimated and actual variables. This, in essence, is a random input describing function representation for the Kalman filter.

The K-D model for the Arnold pitch attitude tracking experiment, following its convergence to the optimal control solution, can be approximated as shown in figure 23. The predictor gain is unity in both channels. The remnant due to rate and position thresholds and to motor

noise has been lumped into an equivalent observation noise injection process. Both the time delay and the predictor have been omitted from figure 23; their effects tend to be self-canceling. Further, delays will have no effect on the use of the K-D model for estimation of the pilot rating metric. The reader should compare the model of figure 23 with that of figure 10 (which is a specialization of figure 9). They are the same, except for their treatments of neuromuscular system dynamics, provided that the command input of figure 10 is transformed into the vehicle disturbance of figure 23 - - an easy matter. The cost functional weights of 70 and 7 for mean-squared pitch attitude and mean-squared pitch attitude rate, respectively, had been previously determined by Dillow to yield a global match of model-predicted and measured σ_θ and $\sigma_{\dot{\theta}}$. [It should also be noted that $\dot{\theta} = \ddot{\theta}$ was a feedback variable to the state predictor in the K-D model. However, it was not controlled in closed loop fashion.] The disturbance was identical to that used in the Arnold experiment - - i.e., with a first-order approximation to the Dryden spectra.

Table 3 is a summary of K-D model parameters for the Arnold configurations of Table 2. Both experimental and K-D model-predicted values for $\sigma_{\dot{\theta}}$ and σ_θ are shown for the reader's assessment of the quality of the model's match of closed loop performance. The average pilot opinion ratings (POR) obtained from Arnold's experiment are also listed; these are the familiar Cooper-Harper rating scale values. The pilot rating metric $\sigma_{\dot{\theta}}$ (from equation 19) is computed using the model-predicted gains (with $K_p \equiv 1$) and the experimental values for $\sigma_{\dot{\theta}}$; the results are shown for each of Arnold's cases in Table 3.

The calculation of the rate feedback activity parameter $\sigma_{\dot{\theta}}$ deserves further comment since it illustrates a problem that arises in the application of state-of-the-art pilot models for the calculation of signal levels internal to the pilot. It has already been indicated on these pages that an ambiguity exists in the determination, by the application of theory, of the pilot model gains; viz., variations in control effectiveness will produce counter-balancing variations in pilot gains. It is therefore necessary that the gain terms be normalized with respect to a selected value of control effectiveness. This value should be optimum with respect to POR for at least one controlled element configuration; otherwise it is arbitrary. If the predicted $\sigma_{\dot{\theta}}$ is not normalized with respect to control system gain, then systematic error will be introduced in attempts to correlate POR data from different sources or to predict POR using the present theory. The value $M_{de} = -14.54 \text{ rad/sec}^2$ was selected from Arnold's data as the normalizing control effectiveness for all data discussed in this report. This normalizing contrivance is necessary due to shortcomings in available models for pilot dynamics. It will no longer be required when $\sigma_{\dot{\theta}}$ can be directly estimated in a fashion that accounts for the effects on POR of controlled element gain and neuro-

muscular system dynamics. It should be understood that these remarks are not meant to imply that a universal optimum control effectiveness exists. This is definitely not true in actual flight due to the conflicting requirements posed by the joint control of pitch attitude and normal acceleration. The reader should also note the remark at the close of the introduction to this report about the nomenclature used here for defining control effectiveness.

The variation of measured, average pilot opinion rating (POR) with the predicted value of the proposed rating metric $\sigma_{\beta q}$ from Table 3 is shown on figure 24. The nominal curve is an eyeball fit which weights the better POR conditions more heavily than the poor ones. The rationale for this is provided by the McDonnell study (reference 17) which concludes that the number of experimental trials required to obtain accurate estimates of average pilot opinion ratings increases rapidly with increasing pilot ratings. Thus, many more trials are required to accurately determine the average POR for Arnold's worst-case configurations than were actually performed. The nominal curve of figure 24 is bounded by curves of plus and minus one-half rating unit. It can be seen that the fit between POR and $\sigma_{\beta q}$ is remarkably good. All fourteen data cases are nominally contained within the \pm one-half unit range. As a matter of interest, $\sigma_{\beta q}$ correlates POR better than Arnold's metric based on the minimum pilot rating concept (i.e., Anderson's Paper Pilot scheme). Based on a trial and error approach, Arnold selected the pilot rating functional

$$POR = 5.8 \sigma_{\theta} + 0.43 \sigma_q + 0.43 T_L + 1.0 \quad (21)$$

where T_L is the lead time constant in the servo model for pilot dynamics. The Paper Pilot computer program used by Arnold optimized the choice of pilot model parameters to minimize this functional. The pilot ratings predicted by this process are compared in figure 25 with the averaged ratings obtained from the simulation; figure 25 is a direct reproduction of Arnold's figure 16. The functional together with the Paper Pilot program is seen from figure 25 to correlate POR to \pm one rating unit, nominally.

The Arnold data as analyzed with the K-D model and plotted in figure 24 confirms the hypothesized variation of POR with the metric $\sigma_{\beta x}$ (figure 22). According to the hypotheses of this report the curve of figure 24 has a basic physical connotation; the existence of a unique relation between POR and $\sigma_{\beta q}$ should not be regarded as empirical but is, by hypothesis, a basic physical property of human subjective response. However, the quantitative calibration of POR vs. $\sigma_{\beta q}$ is based on the use of empirical data (i.e., Arnold's) and a control theoretic provided by the Kleinman model for pilot dynamics. Errors in either the data or the pilot model will affect the POR vs. $\sigma_{\beta q}$ calibration. It is plausible to suspect that the POR calibration will depend upon pilot background.

It is not within the state-of-the-art to predict pilot biases of this nature; it is this author's belief, however, that the use of σ_{pq} as a diagnostic tool will permit the identification of pilot bias to a degree that has not been possible heretofore. According to McDonnell's study we must also expect random variations in POR among a fixed pilot population; the degree of this randomness is related to task difficulty. For that reason, the σ_{pq} vs. POR relation of figure 24 must be regarded as an average correlation.

The POR- σ_{pq} curve of figure 24 is conceivably a suitable tool for the prediction of POR in any single loop tracking task. However, it is desirable that its validity be confirmed with additional data sources. Almost no usable data are available for this purpose.

The McDonnell experiment of reference 17 generated data that are of limited use. His experiment was similar to Arnold's, but not nearly as much data were collected. No measures were made of σ_q and McDonnell served as his own subject for all his published data runs that are of potential value here. His goal was to examine relative rating scale effects. His data cannot be used with the same degree of confidence as can Arnold's for validation of the handling qualities metric. Despite its inadequacies, the McDonnell data can be used to qualitatively confirm the relation of figure 24.

The K-D model was applied to the McDonnell configurations in a manner similar to that for the Arnold cases. A computer program made available by Dillow was adapted to this application. Small thresholds, representing limits of visual perception, were placed in the pilot model's rate and position channels. The computations of optimal control gains and system performance were made using the same cost functional and weights as were used for analysis of the Arnold data. Further details of the system model may be found in reference 25.

Controlled element gain was a parameter in the McDonnell experiment. However, insufficient data were collected to permit the identification of the optimum gain (with respect to POR) for each controlled element. Present theory requires that only those data runs conducted with optimum gain be used for the determination of average POR and signal statistics. In order to extract as much information as possible from McDonnell's data, all his POR data for a given controlled element and a given command input standard deviation were averaged without regard for controlled element gain. This will therefore constitute a source for systematic error in the present analytical comparisons.

According to present theory, POR will be affected by both the system input intensity and its spectral distribution. However, use of the Kleinman model - - which is linear - - will not permit the resolution of effects on σ_{pq} (and, therefore, on POR correlations) due to

input bandwidth - - another experimental parameter. McDonnell's POR data were averaged without regard for input bandwidth which constitutes another source for systematic error in the present attempt to confirm a correlation between POR and $\sigma_{\beta q}$. It is reasonable to expect that for the low-bandwidth inputs used by McDonnell this will be a small effect. It could be extremely important, however, if the input bandwidth were large relative to the closed loop cross-over frequency.

The K-D model parameters, input standard deviation, controlled element dynamics, measured and predicted σ_{θ} , predicted σ_q and $\sigma_{\beta q}$, measured servo model lead time constant T_L , number of data runs available for the estimation of average POR, average POR, POR estimated from the POR- $\sigma_{\beta q}$ calibration of figure 24, and POR estimated from a Paper Pilot based formula derived by Arnold (equation 21) are all shown in Table 4. McDonnell's units for pitch attitude were in centimeters of displayed error; this is immaterial for the calculation of $\sigma_{\beta q}$, however, since rescaling of the program variables would merely rescale the optimal controller gains from the K-D model by a compensating amount. We may assume, therefore, that $\sigma_{\beta q}$ is in units of degrees in Table 4 and is dimensionally consistent with the Arnold data.

It should be noted that the estimates for $\sigma_{\beta q}$ shown in Table 4 for the final three cases may not be reliable. In each case only one data run was conducted so that a reasonable average for POR cannot be determined. The final two controlled elements (cases 12 & 13) are unstable. The suitability of the Kleinman model for unstable plants has not been generally confirmed. Case 13 will be disregarded since the pilot lost control during the run (POR = 10), no further attempts were recorded, and the instability is not so severe as to preclude manual control with practice.

The variation of the predicted $\sigma_{\beta q}$ with average POR is shown on figure 26 for the data of Table 4. The agreement between the McDonnell and the Arnold data is surprisingly good considering the experimental and analytical uncertainties noted above. It is clear that $\sigma_{\beta q}$ is a useful metric for the correlation of McDonnell's rating data. These data appear to support the hypothesis that the variation of POR with $\sigma_{\beta q}$ shown in figure 24 can be used as a predictor for POR provided that a satisfactory model exists for the estimation of $\sigma_{\beta q}$.

Reference 20 examines the pitch attitude tracking data of Onstott, et al (reference 21) with the Paper Pilot method. The reference 21 experiment included a moving base simulation of pitch attitude tracking in turbulence. Measurements of σ_q were not recorded nor was control effectiveness optimized with respect to pilot opinion for each configuration tested. Thus, the reference 21 data base is too

incomplete to warrant detailed treatment here. Nevertheless, it can provide a limited sample for comparison with figure 24.

Johnson, in reference 20, estimated servo model parameters for the Onstott configurations using the Paper Pilot methodology and an empirical rating functional derived from Onstott's data. Of the 35 configurations examined by Johnson only 2 resulted in non-zero estimates for the pilot's lead time constant. This may have been partly due to the form used for the pilot rating functional. Once more, however, it should be recalled that servo model lead does not necessarily reflect rate feedback activity; that is, there can be quite a lot of rate control without this being manifested as a lead time constant in the pilot model

$$Y_p(j\omega) = \frac{\Phi_{y_i, \delta}(j\omega)}{\Phi_{y_i, y_e}(j\omega)}$$

This remark is based on the postulated validity of the nonlinear, multiple loop model as a representation for pilot dynamics. Thus, without more extensive analysis, only two of Johnson's 35 data sets can be used here for validation of the POR metric σ_{pq} . Johnson's Paper Pilot estimates and the POR for these two cases are shown in Table 5 together with the estimated metric σ_{pq} obtained from the application of equation 20. The two data points are compared in figure 26 with the proposed rating metric. The agreement is surprisingly good - especially when one considers the uncertainties involved in the Paper Pilot method, the lack of an experimental measurement for σ_q , and the possible contaminating effects on pilot ratings of a non-optimum control effectiveness.

No other data base is known to this author that would be immediately suitable for validation of σ_{pq} as a general metric for the correlation or prediction of pilot opinion ratings. Other data probably exists but a major effort would be required to seek it out, document it, and verify its suitability for present purposes. The roll tracking data of Onstott, et al (reference 21) is one such set that might be useful. These data were examined by Naylor (reference 22) using the Paper Pilot scheme to correlate POR. Unfortunately, neither source documents σ_p (p = roll rate), although this variable was probably recorded during the experiment and may have been available from the Paper Pilot printout. Onstott's roll tracking experiment was performed in a moving base simulator with artificial turbulence of various intensities. Control effectiveness however, was, not a parameter in these experiments and could be a source for systematic error in pilot opinion ratings.

Both McDonnell's and Onstott's limited data were shown to correlate fairly well with the data set derived from Arnold's experiment. For all these data σ_{pq} has been shown to be a very sensitive measure for handling qualities. These three data sets represent a wide range of controlled element dynamics and input intensities. The Onstott data were from a moving base simulation. McDonnell's data were for a command

input. The pilots used for the collection of rating data had a very wide range of experience. The control stick properties were widely different.

At the time of this writing there is no data available to this author to refute the validity of $\sigma_{\delta q}$ as a tool for the prediction of pilot opinion. Accordingly, it is postulated that figure 24 may be used to predict pilot opinion ratings for any single loop control task for which a reasonable estimate can be made of $\sigma_{\delta q}$ or, in general, $\sigma_{\delta x}$; it must be understood that the predicted POR is valid only to the extent that the feel system characteristics are optimized with respect to POR.

E. RATING DIFFERENCES: IN-FLIGHT VS. FIXED-BASE

Arnold compared his fixed base simulation measurements of POR with the Neal-Smith flight test measurements for the identical aircraft dynamic configurations. His final comparison is repeated for convenience in figure 27. The squares represent the average pilot ratings; the rating ranges are also shown. The configuration number is shown inside the square and corresponds to the data of Table 2.

The comparison is generally quite good. Three cases, however, differed enough to prompt comment by Arnold (reference 18). He noted that configurations 9, 10 and 11 were significantly down-rated in flight whereas each had been rated as good-to-excellent in the simulation. He attributed this discrepancy to task differences between the two experiments. The flight test rating was based on the aircraft's behavior during tracking tasks (IFR and VFR) and simulated air combat maneuvers of both a gross and precision type. The simulation rating was based only on precision tracking without motion cues.

These three configurations (i.e., 9, 10 and 11) are re-examined in this article to see whether another explanation might not exist for the flight vs. simulator POR differences.

The approach taken was to re-apply the Kleinman-Dillow model to each of the three errant configurations; the K-D model, however, was suitably parameterized to simulate the Neal-Smith flight test conditions, rather than the fixed-base simulation, insofar as this was possible. It was hypothesized that - - at least for the tracking experiments - - the major parametric change required of the K-D model to re-create the flight tests was to remove the large display threshold effect from the q and θ feedback paths that had been necessitated by Arnold's display. There were no known significant visual thresholds in the Neal-Smith tests (other than the unavoidable physiological limitations which are negligible for this analysis). The same gust spectrum and level were used as for

Arnold's experiment and for the previous analysis of his data with the K-D model - - i.e. a first-order approximation to the Dryden spectra with an rms value $\sigma_{w_g} \approx 10$ f/s. The K-D model was further modified to include feedback control of the motion variables $\dot{\theta}$, $\ddot{\theta}$ and a_{zp} - - the normal acceleration at the pilot's station. It was hoped that this would be sufficient to account for any handling quality effects due to aircraft motion during the actual flight tests. The weighting on the control of θ and q was the same as previously used for Arnold's data. By trial and error, it was determined that the results are insensitive to the weights on $\dot{\theta}$, $\ddot{\theta}$ and a_{zp} . Basically, these motion feedbacks only affect the quality of the state variable estimation via the Kalman filter and the predictor in the K-D model. This quality, however, is already high and leaves little room for improvement. The resulting parameters predicted by the K-D model for these three configurations are listed in Table 6. The predicted value for σ_{β_q} is also shown. This value was used to estimate the flight-test POR from the calibration curve of figure 24. This estimate is also shown in Table 6 together with the Neal-Smith and Arnold values.

Comparison of the POR values of Table 6 indicates that the model predicted values are in substantially better agreement with the flight-test values for cases 9, 10 and 11 than are the simulator results. It was determined by a separate investigation to be discussed in Section V that the motion feedbacks have no substantial effect on the POR prediction shown in Table 6. It is, in fact, obvious that the good correlation between predicted and flight-test measured POR for cases 9, 10 and 11 is entirely due to the removal of effects from the K-D model of Arnold's display threshold. Compare the parameters of Tables 3 and 6 for these cases. With Arnold's display the display gain is very small or zero; it is 1.0 for the flight-test parameterization of the K-D model. Without the threshold effect the Kalman filter gain is much larger. The net effect due to removal from the K-D model of the display threshold is to increase the estimated σ_{β_q} which, from figure 24, will increase the predicted rating for the flight test condition.

The above procedure is potentially a remarkable way to "adjust" simulator-derived POR to predict ratings in flight test. If POR from a simulation experiment can be correlated with σ_{β_q} (or, in general, σ_{β_x} for any tracking task), and if the pilot-vehicle system model used for the prediction of σ_{β_q} can be modified to account for differences known to exist in flight, then the predicted σ_{β_q} for flight will correlate the flight test POR in exactly the same way as the POR- σ_{β_q} correlation from the simulation. This procedure has the appearance of a "bootstrap" operation. It really isn't, however; its successful application depends only upon the validity of σ_{β_q} (or σ_{β_x}) as a physiological trigger for POR.

From the above analysis it is concluded that the major source of the differences between Arnold's fixed-base simulation and the Neal-

Smith flight tests was the display threshold in the simulation. This would be expected to have its major effect on the very best of Arnold's configurations; these are cases 1, 6, 9, 10 and 11 which are all Level 1 ($POR \leq 3.5$). For these, σ_q is small with q often buried in the threshold region. This can be seen from the K-D parameters of Table 3; for these cases the display describing function K_{Dq} is very small. Observe that, from figure 27, these cases are all rated more poorly in flight than in the simulation. In fact, these are the only cases falling to the right of the line of perfect agreement in figure 27. It should be completely obvious that there will be only a small threshold effect on the other cases; in other words, the removal of the display threshold from the K-D model and the calibration curve of figure 24 will permit the correlation of the Neal-Smith flight test data with σ_{sq} to within about ± 1 rating unit except for case 5. Case 5 was the most poorly rated case tested by Arnold. It is possible that the in-flight motion cues benefit the handling qualities of this configuration. It is perhaps noteworthy that all of Arnold's Level 2 and 3 cases were rated better in the flight tests.

Another interesting point to be noted is that the POR predictions were based only on tracking considerations, yet they are in remarkably good agreement with flight test values. The flight tests involved many open and closed loop flight control tasks related to air combat with fighter-type aircraft. The ratings obtained are overall ratings which, in some ill-defined manner, are supposed to rate the global qualities of the aircraft for use in air combat tasks. This comparison therefore suggests two interesting corollaries:

- (1) The pilot's overall impressions of an aircraft in an air combat environment are very much dependent upon considerations that are important to closed loop tracking.
- (2) Attitude-only control is the central problem to the determination of an aircraft's overall handling qualities.

The evaluation pilots in the CALSPAN flight tests were free to select optimum control stick gearing for tasks involving both attitude tracking and gross maneuvering. In general, the stick force - deflection sensitivity requirements differ for each; viz., lighter stick forces for tracking and heavier forces for maneuvering. The pilots tended to downrate the aircraft's handling qualities when the optimum stick sensitivity requirements for tracking and maneuvering greatly differed (reference 19). This is an excellent potential reason to explain the differences between the predicted in-flight POR, above, and the flight-test values.

There is, at this writing, no basis for believing that either task differences or motion cues are responsible for the differences shown in figure 27 between fixed-base and flight-test measured POR.

F. RATING PREDICTION IN MULTIPLE LOOP TRACKING

The original scope of this study was restricted to single loop tracking tasks representative of aircraft attitude control. The lack of suitable data has prevented definitive validation of σ_{p_x} as a metric for pilot opinion rating in single loop tracking, however. In an effort to extend the available data base the simulation data of Miller & Vinje (reference 23) were examined vis-a-vis present theory. They simulated precision hovering control (a multiple loop task) of a multitude of VTOL aircraft configurations. Only their longitudinal data are considered here. A high-fidelity contact analog simulation of VFR flight was used for the pilot's display. Their work is valuable mainly because it is one of the few experimental sources for which full documentation is available for pilot opinion ratings, aircraft dynamics, and suitable closed loop performance measures. This was the source used by Anderson in his development of the Paper Pilot methodology of reference 3.

The Miller-Vinje precision hover configurations had already been analyzed by Major James Dillow of the Air Force Institute of Technology, who used the Kleinman model to match the experimental performance measures. These unpublished results were made available to this author for use in this report. Table 7 summarizes the match achieved by Dillow of the measured rms performance values. The Kleinman model parameters determined by Dillow are used here to continue the search for a predictive metric for pilot opinion rating.

Miller and Vinje used the older Cooper scale for the collection of their pilot opinion rating data. The conversion of these ratings to the Cooper-Harper scale is shown in Table 8. The conversion equations are those suggested by McDonnell (reference 17) from his study of rating scales. These estimated Cooper-Harper ratings will be used in further discussions of the Miller-Vinje data.

Dillow's optimal control model for this experiment used feedback control of error in longitudinal position x , longitudinal velocity $\dot{x} = \dot{x}$, longitudinal acceleration \ddot{x} , pitch attitude θ , and pitch attitude rate $\dot{\theta} = \dot{\theta}$. The analysis was similar to that for the Arnold experiment -- previously discussed -- and will not be discussed here in detail. Only the principal results are relevant to the present discussion. Table 9 summarizes the Kleinman model's prediction of optimal controller gains and equivalent Kalman filter gains. Thresholds were included in Dillow's version of the Kleinman model to simulate physiological limits of the visual senses. These were too small to be of significance and their effects are ignored here (i.e. the threshold describing functions were all ≈ 1.0). Table 10 summarizes the cross-correlations of various signal products predicted by the Kleinman-Dillow model.

It should be noted that the Miller-Vinje units for control effectiveness $M_{\delta e}$ are rad/s^2 per inch of control stick deflection. The control stick's effective length is not given in reference 23 but can be expected to be about 24 inches for a floor-mounted cyclic control. Multiplication of the Miller-Vinje $M_{\delta e}$ by 24 will yield an $M_{\delta e}$ in units of rad/s^2 which is consistent with the Arnold units. In units of rad/s^2 the Miller-Vinje $M_{\delta e}$ magnitudes are typically about equal to the values used by Arnold. This isn't too surprising since the hover task is basically one of attitude control (as in Arnold's experiment) and the evaluation pilots were allowed to optimize the control sensitivity for each data run (also as in Arnold's experiment). The Miller-Vinje values for $M_{\delta e}$ were used for the exercise of the K-D program. The resulting optimal controller gains must therefore be normalized by the factor $M_{\delta e}/14.54$ to compare with previous estimates. The units of $M_{\delta e}$ are irrelevant to this normalization. The normalized pilot rating metric $\sigma_{\beta q}$, however, will have units of degrees.

Table 11 lists the estimated, normalized pitch attitude rate loop activity metric $\sigma_{\beta q}$ for the Miller-Vinje precision hover cases. The metric is calculated according to equation 19 with both $K_{\beta x}$ & $K_{F x}$ set to unity. The measured values σ_q (from Table 7) and predicted gains (from Table 9) are used for the calculation. Table 11 also shows the estimated u-loop activity metric $\sigma_{\beta u}$; this parameter is defined analogously to $\sigma_{\beta q}$ with u substituted for q. It is intended to represent the activity in the rate of position (i.e. speed) control feedback loop. Also shown is a metric $\sigma_{\beta x}$ defined as follows:

$$\sigma_{\beta x}^2 = \sigma_{\beta q}^2 + \sigma_{\beta u}^2 + 2 K_q^* K_{F q} K_u^* K_{F u} \left(\frac{M_{\delta e}}{14.54} \right)^2 E[uq] \quad (22)$$

This metric represents the value of a signal $\beta_x = \beta_q + \beta_u$; it is, in effect, a measure of total feedback activity for the control of system rates. In this context, the term "rate" is expanded to include the first derivative of all attitude and position variables that are controlled in closed loop fashion. The variations of $\sigma_{\beta q}$ and $\sigma_{\beta x}$ with POR are shown in figure 28 where they are also compared with the corresponding variation estimated from the Arnold data (figure 24).

It is interesting that the values $\sigma_{\beta q}$ estimated for the Miller-Vinje experiment are asymptotic to the Arnold values as POR approaches the Level 1 region. This suggests the following:

- (1) Within the Level 1 region, POR is primarily a function of attitude control behavior.
- (2) The variation of just $\sigma_{\beta q}$ with POR can be used as a sufficiency criterion for the specification of Level 1 flying qualities boundaries even though the pilot controlled several other variables.

It is tempting to accept the generality of these observations; both are intuitively acceptable and provide a rational basis for the widely-held opinion that good attitude control is sufficient for good flying qualities, regardless of mission or task specifics.

The Kleinman model for the Miller-Vinje simulation is structurally similar to the single loop model of figure 2. It has 5 feedback loops corresponding to $\dot{u}, u, x, q \in \Theta$. It was anticipated that the proposed single loop pilot rating metric $\sigma_{\beta x}$ could be extended to multiple loop tracking control by defining the appropriate "rate" signal x to be some function of the rates of position or attitude variables which, for the Miller-Vinje data, would be u and q [As an aside it should be noted that the K-D model indicated that the acceleration feedback \dot{u} was not of first-order importance in establishing closed loop system performance or dynamic properties. For that reason, its effects are ignored in this analysis]. The two most obvious functional relations between the feedback signal rates in the u and q channels and a potential POR metric are

1. $\sigma_{\beta x} = \sigma_{\beta q} + \sigma_{\beta u}$; POR effects due to attitude and positional control are additive, and
2. $\beta_x = \beta_q + \beta_u$ with $\sigma_{\beta x}$ given by equation 22.

For the Miller-Vinje data there is no significant difference between these two metrics; the cross-correlation between q and u is simply too small. Only the value $\sigma_{\beta x}$ from equation 22 is shown in figure 28.

If the proposed physical theory for the prediction of pilot opinion rating is correct then there is a point within the central nervous system at which some measure of nerve activity will correlate one-to-one with POR. Once the basic relationship between this metric and POR has been established for one tracking task, the relation should apply for all tracking tasks. Thus, if present theory is correct, the POR metric $\sigma_{\beta x}$ for the Miller-Vinje multiple loop tracking data for a hovering VTOL should be quantitatively related to POR according to the POR- $\sigma_{\beta q}$ relation derived from Arnold's data for attitude control of fighter-type aircraft.

From figure 28 it is apparent that $\sigma_{\beta q}$ and the two measures for $\sigma_{\beta x}$ above, do not generally match the Arnold curve except in the Level 1 region where $\sigma_{\beta q}$ is in excellent agreement between the two data sets. There are three possible explanations for failure to achieve the expected correlation:

1. The present theory for POR prediction is wrong.
2. Either the Arnold or the Miller-Vinje data bases, or both, are faulty.

3. The prediction of $\sigma_{\beta x}$ is incorrect due to:
 - a. use of the wrong definition for $\sigma_{\beta x}$, or
 - b. use of a faulty model for pilot dynamics.

The theory proposed in this report for the understanding and prediction of POR in tracking tasks is physical, not empirical. This, together with its striking success in correlating available single loop POR data, indicates that the first possibility above should be dismissed - - at least until it receives a fair test. It is the author's opinion that the Arnold data are of high quality. The Miller-Vinje data suffer from two points: Miller & Vinje were their own evaluation pilots, which is a questionable procedure; their pilot ratings were obtained with the use of the Cooper scale. Nevertheless, both data sets seem credible; the second possible explanation for the POR metric failure is also discounted. Possibility 3a can't be evaluated. Possibility 3b remains a very plausible explanation, however.

The search for a unified model for pilot dynamics, described in Sections II and III, led to the proposition that a mode-switching model might be consistent with the available data base for pilot dynamics and be physically acceptable. A mode-switching model such as that shown generically in figure 9 could conceivably yield a candidate "rate" signal $\beta_x(t)$ equal to either $K_{eq} q(t)$ or $K_{eu} u(t)$, depending on which (if either) variable was being controlled at the measurement time [K_{eq} and K_{eu} are the equivalent pilot gains in a mode-switching model between q , u and β]. This situation is depicted on figure 29. If a switching model is physically appropriate then it is clear that use of the Kleinman model or the servo model (both of which are continuous in all feedback paths) could lead to gross errors in the estimation of K_{eq} and K_{eu} and, hence, $\sigma_{\beta x}$. Specifically, the values K_{eq} and K_{eu} from an intermittent control model could be considerably larger than the corresponding Kleinman model gains. It is intuitively reasonable to suspect that the effects of mode switching would be least apparent for Level 1 aircraft dynamics. For these, attitude control would be expected to dominate the calculation of $\sigma_{\beta x}$ via a switching model for pilot dynamics, and $\sigma_{\beta x} = \sigma_{\beta q}$ might be a reasonable approximation. Conversely, switching should have a very significant effect on the rate gain calculations for the poorer configurations.

It is tentatively hypothesized that the Miller-Vinje POR data could be shown to satisfy the POR- $\sigma_{\beta q}$ variation derived from Arnold's single loop data if a mode-switching model for the human pilot were available for the estimation of $\sigma_{\beta x}$. There is no reason to believe this is not true. In any event $\sigma_{\beta x}$ as calculated from $\sigma_{\beta q}$ and $\sigma_{\beta u}$ above is seen to be a reasonably consistent and sensitive metric for the pilot opinion rating data of Miller and Vinje. It is quantitatively consistent with the Arnold single loop data base within the Level 1 region.

There is always the possibility that pilot ratings in multiple loop tracking tasks are not truly predictable. In a sense, one might classify $\sigma_{\beta q}$ as a "reflex parameter" for human performance and workload measurement and attribute its (apparent) success as a predictive tool for POR to the basic "athletic" nature of the attitude control task. Multiple loop control of path variables, by comparison, casts the pilot in a role that is conceivably more contemplative. His ratings may represent a complex synthesis of component ratings for the control of some or all feedback quantities that can be "modeled" only after-the-fact, somewhat in the nature of the Paper Pilot approach to ratings prediction. The author's position, however, is that such a dismal portent for the future of analytical flying qualities need not be accepted until a thorough evaluation has been made of switching logic models for pilot dynamics in the manner suggested above.

There are other data sets for multiple loop tracking that could conceivably be examined in the same manner as the Miller-Vinje data to corroborate the POR metric. Notably, these include the data of Teper (reference 12) and Taylor (reference 24). Unfortunately, neither data set is suitable for present purposes without a great deal of additional analysis after which serious questions would still remain unresolved. Some limited remarks on these sources follow.

The Teper data are from an experiment intended to replicate the Miller-Vinje VTOL precision hover simulation. Teper obtained describing function measures for pilot dynamics and used these in an evaluation of the Paper Pilot methodology. His task definition differed from that of Miller & Vinje in that the evaluation pilots were instructed to hover over a spot with an allowable error tolerance of ± 2 feet. The display was an IFR presentation on a CRT that, to this author, seemed rather non-physical and may have placed unnecessary intellectual demands on the pilots. Teper's measurements did include $\sigma_{\dot{q}}$ and σ_u . The subjects were permitted to optimize their choice for control effectiveness as was done in the Miller-Vinje simulation; unfortunately, the values selected are not among Teper's published data. Undoubtedly, these are available and could be obtained. However, time did not permit the matter to be further pursued. The principal objection to the use of Teper's data, as published, is the concern that his describing function measurements and corresponding servo model parameters will give severely biased estimates for the u-and q-loop feedback gains required in the calculation of $\sigma_{\beta q}$ and $\sigma_{\beta u}$ in the manner previously discussed in this report. There is every reason to believe, however, that the Teper data are valid. It would be interesting to re-analyze this data with the Kleinman model. If this were done the problem of validity of a model for pilot dynamics, continuous in all feedback paths, would still remain.

Despite these objections, Teper's data were used to investigate $\sigma_{\beta x}$ as a potential metric for the correlation and prediction of pilot

opinion rating. This was done as follows:

$$\sigma_{\beta x} = \sigma_{\beta q} + \sigma_{\beta u}$$

$$\sigma_{\beta q} = K_{p\phi} T_{L\phi} \sigma_q$$

$$\sigma_{\beta u} = K_{p\psi} T_{L\psi} \sigma_u$$

The results, without normalization (which wasn't possible without knowing the control effectiveness values used), are shown in figure 30. There is an apparent trend of POR vs. $\sigma_{\beta x}$ but the data quality and the lack of substantial data at the poorer POR configurations makes it difficult to reach a positive conclusion about its merits. It is, perhaps, more illuminating to examine the variation of $\sigma_{\beta q}$ with POR for these data. This is shown in figure 31. It seems evident that there is no apparent correlation. This could be a result of Teper's display and its possible effects on piloting strategies. That is, the pilot really "flies" the display - - not the aircraft dynamics. We can't be sure (even a posteriori) that pitch attitude control was of comparable importance to system performance with the Teper display as it apparently was in the Arnold and Miller-Vinje experiments. This lack of expected correlation could also result from the indicated weaknesses of the servo model for this application and from our inability to normalize $\sigma_{\beta q}$ for Teper's data.

Taylor (reference 24) used the data of reference 21 for correlation with Paper Pilot methodology. The reference 21 experiment, in part, consisted of a moving base simulation of aircraft heading control in turbulence. The task was (apparently) one in which roll control with aileron was central to system performance. However, experimental measurements of σ_p , the standard deviation of roll rate, were not published in either of references 21 or 24; values estimated by Taylor from his Paper Pilot analysis are used here. There is justifiable reservation about how clear any further computations involving σ_p can be. As a check, however, Taylor's Paper Pilot estimates of other system signal values are in good agreement with his experimental values given in reference 21. The Taylor estimates of $K_{p\phi}$, $T_{L\phi}$, $K_{p\psi}$, $T_{L\psi}$, σ_p and σ_r were used by this author to estimate

$$\sigma_{\beta x} = \sigma_{\beta p} + \sigma_{\beta r}$$

$$\sigma_{\beta p} = K_{p\phi} T_{L\phi} \sigma_p$$

$$\sigma_{\beta r} = K_{p\psi} T_{L\psi} \sigma_r$$

The results will not be presented. The data quality permitted by the Paper Pilot estimates of servo model parameters, their use in estimating $\sigma_{\beta p}$ and $\sigma_{\beta r}$, and the lack of experimental measurements for σ_p is simply too poor to permit useful resolution of $\sigma_{\beta x}$ as a POR metric. Briefly, it was found that $\sigma_{\beta x}$ does not correlate the reference 21 POR

data. However, $\sigma_{\rho p}$ is correlated with POR over the entire data base. It is conceivable that the lack of correlation between POR and $\sigma_{\rho x}$ was the result of the lack of closed loop control of heading ψ . Heading may, in fact, have been controlled in an intermittent fashion.

As an aside, it is plausible to imagine that in future experiments of multiple loop or multiple axis tracking, given a physically accurate dynamic model for pilot dynamics, $\sigma_{\rho x}$ could be used to ascertain which vehicle response quantities are tracked in closed loop fashion.

The reference 21 data indicate a dramatic difference in POR vs. gust intensity levels for two of the evaluation pilots. Pilot JBJ was very sensitive to increased turbulence intensity (i.e. to σ_{v_g}) and gave greatly increased ratings for increases in σ_{v_g} . Pilot WWK showed almost no effect on POR of σ_{v_g} . For two identical configurations (A-7 aircraft dynamics with no SAS) and near-identical σ_{v_g} , pilot JBJ gave a POR of 10, whereas pilot WWK rated the configuration a 5. This may have resulted from WWK's considerable experience with helicopters and VTOL (i.e. "bad" aircraft); JBJ had no similar experience. It may also reflect a weakness in the experimental design through failure to provide satisfactory guidelines to the pilots to establish what, specifically, and in an operational context, they were being asked to evaluate. It is, for example, entirely possible that WWK rated the aircraft response to control in open loop fashion while, in effect, ignoring motions associated with σ_{v_g} . [This would be possible, for instance, if he could hear or feel the workings of the motion system actuators]. Similarly, it is reasonable to suspect that JBJ rated task performance as assumed by the theory on which the metric $\sigma_{\rho x}$ was based. If that is true, then only JBJ's data at larger σ_{v_g} would correlate with the metric $\sigma_{\rho x}$ (or just $\sigma_{\rho p}$). Unfortunately Taylor averaged all these pilot ratings, thereby making it impossible to test this possibility with his data.

Given all these criticisms of the reference 21 data base and Taylor's Paper Pilot analysis, it is indeed remarkable that any correlation of the metric $\sigma_{\rho p}$ and POR is evident as, in fact, it is.

These three sources (i.e., references 12, 23 & 24) exhaust the available data, known to this author, that might be suitable for rapid assessment of the proposed POR theory for flying qualities. The tentative conclusions that have been reached are summarized as follows:

1. The variation of POR with $\sigma_{\rho q}$ derived from Arnold's data and shown in figure 24 is generally applicable to single and multiple loop tracking tasks with a single controller provided that $\sigma_{\rho q}$ is replaced by $\sigma_{\rho x}$. The signal x is intended to represent a synthesis of all feedback signals that represent the first derivatives of path or attitude feedback cues.

2. State-of-the-art models for pilot-vehicle systems analysis are inadequate for the quantitative prediction of $\sigma_{\beta x}$. They can, at best, be used for the relative estimation of $\sigma_{\beta x}$ (and, therefore, POR) over a range of candidate airframe-controller configurations.

3. A physically attractive model for pilot dynamics that may permit accurate predictions of $\sigma_{\beta x}$ will incorporate mode-switching to control each feedback cue in intermittent fashion.

4. A sufficient condition for the specification of Level 1 flying qualities, almost without regard for multiple loop aspects of control, is that the aircraft's attitude control dynamics be in the Level 1 region. In general, and with an eye cast on CCV concepts, "attitude" can be replaced by the dominant, innermost, single loop variable that might arise as the result of modern display-controller design for the execution of a specific task (e.g. pipper control during weapons delivery).

G. COMMENTS ON MULTIPLE AXIS RATING PREDICTION

If the remarks in the last article on the necessity for an intermittent control model for human pilot dynamics are accepted, then it is reasonable to assume that the classical distinctions between multiple loop and multiple axis tracking will no longer apply. That is, within the context of such a model, the pilot only does one thing at a time. It therefore makes little difference in the theoretical sense whether he controls one or several axes in single or multiple loop fashion. Practically, of course, the switching logic required to construct a successful pilot model may become very complicated with increased task complexity. If the correct signal x within the central nervous system can be deduced, however, then the calculation of $\sigma_{\beta x}$ should permit the prediction of pilot ratings. For example, a suitable "rate" signal for multiple loop or multiple axis control might be

$$x = \sum_{i=a}^b K_{E_{x(i)}} x(i)$$

where the $K_{E_{x(i)}}$ are pilot model gains in each of the feedback channels $x(i)$. The variables $x(i)$ represent system rates, i.e. they are first derivatives of path or attitude feedback cues. The $K_{E_{x(i)}}$ are zero except when the mode switch is set to the control of $x(i)$; thus, $x(t)$ is a piecewise continuous signal such as depicted by β_x in figure 29.

Clearly, these remarks are conjectural. They do follow from present theory, however. Considerable research will be required to evaluate this proposal for the prediction of multiple axis POR.

Before leaving this article it should be noted that if this theory could be validated then it follows immediately that a rule could

be devised for the "addition" of longitudinal and lateral-directional flying quality requirements. At the present time, for example, we cannot be certain that the specification of borderline Level 1 flying qualities in both modes - - separately considered - - will result in Level 1 evaluations of these same modes in flight, where both must be controlled.

H. RE-EXAMINATION OF THE PAPER PILOT CONCEPT

It was previously indicated in this report that the Paper Pilot approach to pilot rating prediction, as introduced in reference 3, is a tremendously novel idea. It relies upon the use of a servo description of the human pilot and an optimal control formalism. The optimal control cost functional (defined as the pilot rating functional), when minimized through selection of the servo model parameters, yields a numerical prediction of the pilot's opinion rating for the task.

The Achilles' heel of the Paper Pilot theory is the a priori requirement for a detailed rating functional description. There has been no physical theory proposed to assist in the derivation of these functionals. They have been derived in all past work in a contrived fashion that relies on the availability of large quantities of POR data and on the employment of statistical measures to, in effect, curve-fit these data. This is not an approach that is generally acceptable for the prediction or specification of flying quality requirements. It could be acceptable, however, if a physical theory became available to justify a "universal" rating functional and if this functional were not restricted by the nonavailability of handling qualities data (which is, in general, the situation for those conditions for which the current MIL-F-8785B is most seriously deficient).

The thought seems to prevail in all the published applications of Paper Pilot methodology that such a universal rating functional may exist and, if found, would produce a genuinely predictive model for POR evaluation in any conceivable tracking task with any airframe - controller dynamic configuration. None has been found. In fact, each new data base examined seems to require a new rating functional that differs significantly from past ones. Also, it has been observed that relatively small changes in rating functionals can produce significant changes in predicted POR. Thus, the Paper Pilot method, in its present form, is most accurately described as an empirical tool suitable for the correlation and interpolation of existing handling qualities data. The successful application of the scheme to control tasks that involve performance requirements or airframe - controller dynamics that differ significantly from those for which a rating functional has already been developed and validated will be highly problematical.

From the viewpoint of the theory proposed in this report, it is tempting to propose that a suitable rating functional for use with Paper Pilot might be

$$R = K_p T_L \sigma_x$$

where σ_x is the rms value of the rate feedback signal. The minimization of R would, according to present theory, automatically minimize POR. The value R predicted by Paper Pilot could be directly used to determine POR from figure 24. This functional would strictly apply to single-loop tracking tasks. It could be used for relative handling quality evaluations of multiple loop tasks or it could be generalized in the manner suggested in article F of this section for multiple loop predictions. The functional R is universal in the sense that it is independent of task specifics, dynamics, display, or input. Unfortunately, as has been previously indicated, the use of the servo description of the human pilot will simply not permit accurate prediction of the rating metric $\sigma_{\beta x} = K_p T_L \sigma_x$ in the most general case. Also, the minimization of R will not obviously produce a pilot-vehicle system model that is physically acceptable or that correctly estimates other measures of system performance or dynamics.

A GENERALIZED PAPER PILOT MODEL (TENTATIVE):

It is conceivable that a blend of the Paper Pilot concept and the Kleinman model could produce a method for pilot rating prediction that is consistent with present theory.

Recall the manner in which the baseline variation of POR with $\sigma_{\beta q}$ was derived from the Arnold data set. The Kleinman-Dillow model was used to minimize the cost functional

$$J = 70 \sigma_{\theta_p}^2 + 7 \sigma_{\dot{q}_p}^2 + R \sigma_{\delta}^2 \quad (23)$$

where θ_p and \dot{q}_p are the perceived attitude and rate accounting for the effects of display or physiological thresholds, and for the Kalman filter model for signal identification. The resulting optimal controller gain $K_{\dot{q}}^*$ and the experimental value of $\sigma_{\dot{q}}$ were used to estimate the POR metric $\sigma_{\beta q} = K_{\beta q} K_{Fq} K_{\dot{q}}^* \sigma_{\dot{q}}$ (following equation 19). This metric was then correlated with measured POR to obtain the result shown on figure 24.

This process could be modified to incorporate the Paper Pilot concept (viz., that the pilot is a self-adaptive controller who minimizes his own ratings) by including the POR metric in the cost functional.

This is illustrated below for a generalized pitch tracking task:

$$J = W_{\theta} \sigma_{\theta p}^2 + W_q \sigma_{q p}^2 + R \sigma_{\delta}^2 + r \sigma_{\beta q}^2 \quad (24)$$

$$\sigma_{\beta q} = K_q^* \sigma_{q p}$$

$$J = W_{\theta} \sigma_{\theta p}^2 + [W_q + r K_q^2] \sigma_{q p}^2 + R \sigma_{\delta}^2 \quad (25)$$

[Observe that the * superscript indicates an optimum value; it is therefore omitted from the general expression for J]. However, J is now explicitly dependent on the feedback gain K_q . It is not clear what theoretical or practical difficulties might be encountered in solving an optimal control problem of this form. This generalized Paper Pilot model would predict ratings by using only the component term $K_q \sigma_{q p}$ from J^* , together with figure 24, used as a POR calibration.

DILLOW-PICHA MODEL FOR RATING PREDICTION:

In an interesting, recent study (reference 25), Dillow and Picha attempted to unify the Paper Pilot concept in a manner similar to that above. They replaced the servo model for pilot dynamics with the Kleinman model and defined the cost functional given in equation 23 to be the rating functional required by the Paper Pilot theory; i.e., for the pitch tracking task

$$J = W_{\theta} \sigma_{\theta p}^2 + W_q \sigma_{q p}^2 + R \sigma_{\delta}^2 \quad (26)$$

They arbitrarily defined the predicted pilot rating to be the square root of the minimized rating functional (for $1 \leq \text{POR} \leq 9$); i.e. $\text{POR} = \sqrt{J^*}$. These authors selected the rating functional weights to ensure a satisfactory match between model-predicted and experimental rating and performance data. The weighting of the cost functional to fit pilot rating data and its definition in terms of perceived state variables represent the principal points of departure of the Dillow-Picha approach from the usual Kleinman Model or Paper Pilot application.

Dillow's and Picha's attempts to generalize Paper Pilot methodology appear to have been motivated by two considerations:

1. Considerable artistry is required to parameterize the servo model for pilot dynamics given a description of the control task and system dynamics; the optimal control model, by contrast, is considered by many to be much more mechanistic to apply - especially for multiple loop or multiple axis tasks.

2. A universal rating functional, if one exists, has eluded description when conventional Paper Pilot methodology is employed.

Their ad hoc prediction scheme was only partly successful, although it is possibly superior to past versions of Paper Pilot in its ability to unify the prediction of pilot ratings. Their approach suffers from lack of a unifying physical theory. They note, for example, that"The weakness of the scheme described in this report is that the term $R\sigma_\delta^2$ in the quadratic cost function was considered to be the workload. Yet the exact interpretation of the product R, which is adjusted to yield a .1 sec lag in the pilot model, and the variance of the control rate σ_δ^2 , is not known".... (reference 25, p. 113).

A potential tie exists between the Dillow-Picha work and the theory of this report. Again, the pitch tracking task is used as an example. From figure 23, in terms of perceived variables,

$$\delta = K_q^* \dot{q}_p + K_\theta^* \theta_p$$

$$\dot{\delta} = K_q^* \ddot{q}_p + K_\theta^* \dot{\theta}_p$$

Assume that the inequality $|K_\theta^* \dot{q}_p| \gg |K_q^* \ddot{q}_p|$ is generally valid. Then

$$\sigma_\delta \cong K_\theta^* \sigma_{\dot{q}_p}$$

$$\sigma_{\dot{q}_p} \cong \frac{1}{K_\theta^*} \sigma_\delta$$

The pilot rating (or workload) metric proposed in this report is

$$\sigma_{\beta q} = K_q^* \sigma_{\dot{q}_p}$$

Then

$$\sigma_{\dot{q}_p} = \frac{1}{K_q^*} \sigma_{\beta q}$$

Finally, the "workload" term in the Dillow-Picha rating functional is seen to be

$$R\sigma_\delta^2 \cong R \left(\frac{K_\theta^*}{K_q^*} \right)^2 \sigma_{\beta q}^2 = f(PDR)$$

It is therefore verified by present theory that $R\sigma_\delta^2$ is a workload measure as suggested by Dillow and Picha. However, present theory suggests that this peculiar term, rather than $\sqrt{J^*}$, should, when properly scaled, entirely predict pilot rating! The weight R, however, cannot be arbitrarily selected to simulate neuromuscular system dynamics as was done. To see why this is so, consider that by the above approximations

$$r K_q^2 \sigma_{\dot{q}_p}^2 \cong r \left(\frac{K_q^*}{K_\theta^*} \right)^2 \sigma_\delta^2$$

The cost functional postulated for the generalized Paper Pilot theory (equation 25) can be written as

$$J = W_{\theta} \sigma_{\theta_P}^2 + W_q \sigma_{q_P}^2 + R \sigma_{\delta}^2 + r \left(\frac{K_q}{K_{\theta}} \right)^2 \sigma_{\delta}^2$$

$$J = W_{\theta} \sigma_{\theta_P}^2 + W_q \sigma_{q_P}^2 + \left[R + r \left(\frac{K_q}{K_{\theta}} \right)^2 \right] \sigma_{\delta}^2 \quad (27)$$

Comparison of equation 26, from Dillow and Picha, and equation 27, from the theory of this report, indicates that the Dillow-Picha cost functional is correct only if

$$R \gg r \left(\frac{K_q}{K_{\theta}} \right)^2$$

Reference 25 contains insufficient data to ascertain whether this inequality was generally satisfied.

DILLOW-PICHA VS. PRESENT THEORY:

The weightings used in this report for the Arnold pitch attitude control data (and, in fact, for all applications of the Kleinman-Dillow model in this report) are shown in figure 23 to be

$$W_{\theta} = 70$$

$$W_q = 7$$

These were graciously supplied to this author by Dillow as representative weights for obtaining reasonable correlation between model-predicted and measured system performance. At the time these computations were made, however, this author was unaware that these weights had been selected by Dillow and Picha to also yield a good correlation between their predicted $POR = \sqrt{J^*}$ and Arnold's measured values (see reference 25, p. 53)! What this means is that, more by accident than by design, the Paper Pilot modifications proposed by Dillow and Picha may be directly compared with the results shown previously in this report for the Arnold experimental data. That is, it is claimed in this report that Arnold's POR data should be correlated with the metric σ_{θ_q} ; this correlation was established by the application of Kleinman's model with the Dillow-Picha cost functional. The resulting correlation is shown on figure 24. Dillow's and Picha's model for POR prediction says that $POR = \sqrt{J^*}$; a comparison of their predicted POR versus the actual pilot rating is shown in figure 35 (this is figure 19, page 56, of reference 25). The POR correlation

AD-A040 940

VANTAGE ENGINEERING FRENCHTOWN N J
A THEORY FOR HANDLING QUALITIES WITH APPLICATIONS TO MIL-F-8785--ETC(U)
OCT 75 R H SMITH

F/G 1/3

F33615-74-C-0035

UNCLASSIFIED

2 OF 2

AD
A040 940

AFFDL-TR-75-119

NL



with $\sigma_{\beta q}$ is clearly superior to that between actual and predicted POR from Dillow and Picha. This, however, is not a fair comparison. Figure 24 is merely a calibration of the proposed POR metric and is not a POR prediction. A fair comparison would require that the $\sigma_{\beta q}$ -POR calibration curve of figure 24 and the proposed Paper Pilot model from Dillow and Picha both be used to predict POR for an independent data source.

This is fortunately possible. A direct, valid comparison can be made for the McDonnell pitch tracking data of reference 17.

Dillow and Picha used the same weighted cost functional for predicting POR for the McDonnell experiment as they used for their analyses of Arnold's data. They did not alter the performance weights to optimize the fit between predicted and actual pilot ratings. Thus, their results are a clear indication of the predictive capability of their Paper Pilot model; these are shown in figure 36 (this is figure 31, p. 88, of reference 25). It is evident that the predicted ratings are in very poor quantitative agreement with the actual POR. In fact, Dillow and Picha note that the metric $1/2\sqrt{J^*}$ is a superior predictor for these data. They note that better agreement might have been obtained if the cost functional weights had been selected to optimize the POR prediction for McDonnell's data; this, however, would destroy the potential value of their method as a predictive tool for handling qualities.

All applications of the Kleinman-Dillow model in this report were made with the same cost functional (viz. equation 26) and with the same weights as used for the Arnold data. Thus, the metric $\sigma_{\beta q}$ predicted for the McDonnell data and shown on figure 26 represents an independent prediction of POR according to the theory proposed in this report. The calibration curve of POR vs. $\sigma_{\beta q}$, derived for Arnold's data set, represents the POR predicted by this theory, given the estimated value of $\sigma_{\beta q}$. It is clear that $\sigma_{\beta q}$ accurately correlates McDonnell's rating data and yields a reasonable quantitative prediction of POR.

The above comparison indicates that the metric $\sigma_{\beta q}$ proposed in this report is superior as a predictive tool to the modified Paper Pilot model proposed by Dillow and Picha. The real power of the metric $\sigma_{\beta q}$ (or, in general, of $\sigma_{\beta x}$) is that it results from a physical theory for pilot dynamics and subjective response. Thus, a basis has been created for modifying the metric to accommodate new data on human dynamics or refined models for human dynamic behavior. This is not generally possible with an empirically-oriented theory.

SUMMARY:

The metric $\sigma_{\beta q}$ (or, in general $\sigma_{\beta x}$), when used with the POR calibration curve (figure 24), appears to be superior to the Paper Pilot method as a tool for understanding, correlating, or predicting POR. The best available state-of-the-art model for the estimation of $\sigma_{\beta q}$ appears to be the Kleinman optimal control model.

The effort by Dillow and Picha (reference 25) appears to address the principal weaknesses of the Paper Pilot method in its current form. However, the correlations established between actual POR and their predictions for two pitch tracking data sets are much less convincing than those obtained by using the proposed metric $\sigma_{\beta q}$.

It is suggested that the Paper Pilot method can be generalized and unified with present theory and with Dillow's and Picha's proposal in exactly the manner suggested above. This will require:

1. use of the Kleinman model,
2. definition of the cost functional as in equation 25, and
3. use of figure 24 to estimate POR given a predicted value for the metric $\sigma_{\beta q}$ (or, in general, $\sigma_{\beta x}$).

The relative weighting factor r in equation 25 should be determined to ensure an acceptable match between predicted and measured system performance and POR for a baseline data set (e.g. Arnold's, reference 18). It may be task-dependent. This should be investigated in future research.

It is anticipated that this generalized Paper Pilot should largely eliminate past difficulties in making a priori assessments of how the cost functional weights might vary with task specifics. Future research may establish that these are not highly variable among single degree-of-freedom tracking task data sets (such as attitude control or "pipper" tracking).

The Kleinman model and the conventional Paper Pilot can be applied to the analysis of multiple loop or multiple axis tracking. The generalized Paper Pilot model proposed here can also be used for such tasks. Unfortunately, as was previously discussed in this section, neither the Kleinman model nor the servo model for pilot dynamics appears to be suitable for quantitative prediction of the generalized POR metric $\sigma_{\beta x}$; in fact, the proper definition of $\sigma_{\beta x}$ for higher-order control tasks is not entirely clear. Nevertheless, from earlier discussion, if the proposed, general Paper Pilot model is used for the study of such tasks, then $\sigma_{\beta x}$ - - however it is defined - - should

correctly rank vehicle configurations according to their handling qualities acceptability. Also, from previous arguments regarding the Miller-Vinje data, it is postulated that the method will yield a satisfactory, quantitative prediction of POR for actual Level 1 configurations.

SECTION V

IMPLICATIONS TO MIL-F-8785B

A. GENERAL COMMENTS

The theory for the prediction of pilot opinion rating, presented in Section IV, is directly applicable to the single loop control of aircraft attitude with command or disturbance inputs and with any airframe or automatic controller dynamics. The purpose of this section is to compare the predictions of this theory with the current requirements of MIL-F-8785B. Only the longitudinal short-period, Category A requirements for up-and-away flight will be considered. It is anticipated that this application will accomplish three goals:

1. It will establish general confidence in the theory for POR prediction by showing that, over large regions, it substantially agrees with the flying qualities specification; this, after all, is based on an amalgamation of experimental data collected over a span of many years.
2. It will suggest areas in which the specification is deficient and offer guidelines for its improvement.
3. It will suggest an analytical approach to the general task of updating and extending the specification to encompass nonclassical airframe dynamic configurations as might result from changing operational or performance requirements or from the use of highly augmented automatic flight control systems.

The short-period requirements are selected for study since these are important, fall within the current practical limitations of the rating prediction theory, and have long been a major source of controversy among the flying qualities community. It is therefore anticipated that the analyses of this section will contribute to a more unified understanding of this important problem area.

B. SELECTED AIRFRAME DYNAMIC CONFIGURATIONS

In order to test the proposed theory for pilot opinion prediction against MIL-F-8785B it is necessary that a number of airframe dynamic configurations be selected for analysis. Their dynamics should be tailored to emphasize particular attributes of the specification. MIL-F-8785B codifies aircraft handling qualities according to various parameters. These represent specialized groupings of aircraft stability derivatives and are intended to correlate specific features of aircraft dynamic response with the available POR data base. For the specification of classical, short-period dynamics the principal parameters are n/α ,

T_{θ_2} , ω_{sp} , ζ_{sp} and CAP. The Category A short-period frequency and damping requirements from reference 1 are shown on figure 32. The current version of MIL-F-8785B does not specify limits on T_{θ_2} , the numerator lead time constant of the θ/δ_e transfer function.

Three principal categories of parametric variations were selected for analysis as follows:

Case 1; vary n/α with constant T_{θ_2} , CAP and ζ_{sp} .

Case 2; vary n/α with constant T_{θ_2} , ω_{sp} and ζ_{sp} .

Case 3; vary T_{θ_2} with constant n/α , ω_{sp} and ζ_{sp} .

Values for n/α , CAP, ω_{sp} and ζ_{sp} corresponding to specification boundaries, wherever applicable, were selected from figure 32. Longitudinal mode stability derivatives compatible with each combination of specification parameters were derived by arbitrarily selecting $M_{\delta_e} = -14.54 \text{ } 1/s^2$ for all configurations, choosing Z_{δ_e} and M_w to yield reasonable Z_w for the prescribed T_{θ_2} , and calculating compatible M_q and $M_{\dot{\alpha}}$. The necessary equations for this are as follows:

$$\omega_{sp}^2 = CAP \times n/\alpha$$

$$U_o = \frac{32.2}{1/T_{\theta_2}} \left(\frac{n}{\alpha} \right)$$

$$Z_w = -\frac{1}{T_{\theta_2}} + \frac{Z_{\delta_e}}{M_{\delta_e}} M_w$$

$$M_q = \frac{1}{Z_w} (\omega_{sp}^2 + U_o M_w)$$

$$M_{\dot{\alpha}} = -2\zeta_{sp}\omega_{sp} - M_q - Z_w$$

The control effectiveness M_{δ_e} was selected to normalize the resulting calculations of the pilot rating metric $\sigma_{\theta q}$ with respect to the calibration curve (figure 24) derived from Arnold's data base. All derivatives are defined according to conventional usage (e.g. WADC TR-58-82). The resulting data sets are tabulated in Tables 12, 13 and 14.

It should be noted that the rotary derivatives are unusual by current standards and the speed U_o (which is fixed by the choice of n/α and T_{θ_2}) varies from one non-physical extreme to the other. Our interest here, however, is only that the short-period dynamics are chosen to be compatible with the parameters of MIL-F-8785B and T_{θ_2} . This will be assured by the satisfaction of the above 5 equations. [The reader should note that the a_2 and w responses to control will be reasonable by comparison with current state-of-the-art aircraft so long as M_{δ_e} , Z_w & M_w

are reasonable]. The unusual speed and rotary derivatives may be more acceptable to the reader if it is recognized that these could result from motion variable feedbacks through a stability augmentation system. In other words, M_q , $M_{\dot{\alpha}}$ and U_0 shown in the data sets could each consist of an aerodynamic component plus a component due to feedback augmentation.

C. INVESTIGATION OF SHORT-PERIOD REQUIREMENTS

The handling qualities boundaries of figure 32 are derived from an empirical data base documented in reference 2. The purpose of this article is to assess the validity of these boundaries by predicting the pilot opinion rating for short-period dynamic configurations complying with them. The predictions of POR will be made by using the theory of the last section to estimate the pitch attitude control metric $\sigma_{\beta q}$ and, from this, determine POR from the calibration curve of figure 24. The estimate for $\sigma_{\beta q}$ will be made using the Kleinman-Dillow model for the human pilot in exactly the same manner as done for the Arnold experimental data, described in the last section. The important points about this application are that the same cost functional and cost functional weights are used as were used for the Arnold data, the basic control problem is assumed to be pitch attitude control with elevator, and the system disturbance is a w-gust with the same spectral properties as used for the Arnold experiment. The same gust intensity $\sigma_{wq} = 10$ as used for the Arnold experiment was used in the present analysis for baseline comparisons with MIL-F-8785B. The pilot-vehicle system model in block diagram form is shown in figure 23. The cost functional weights and gust intensity selected for the Arnold data are used here since it has already been established that they are self-consistent with both fixed-base simulator and flight-test results; thus, the POR predictions should correspond as closely as the state-of-the-art will permit with expected results in flight test. Physiological thresholds for human perception of visual position and rate were included in the K-D model but these had no significant effect on the estimate of $\sigma_{\beta q}$. They are ignored in further discussion.

The resulting K-D model parameters and predicted POR are shown in Tables 15, 16 and 17 for the 45 dynamic configurations tabulated in Tables 12, 13 and 14. The configuration numbers shown in Tables 15, 16 and 17 match those of Tables 12, 13 and 14. Comparisons of these results with MIL-F-8785B follow.

The case 1 data, showing the variation of POR with n/α at constant CAP, are plotted in figure 33. The predicted POR for each configuration is noted beside each data point. The following points are noted:

1. For CAP = .16 the agreement between the model-predicted POR and the Level 2 Specification boundary is remarkably good. This result, however, is probably dependent on the existence of favorable S_{SP} and T_{θ_2} .

2. For CAP = .28 the present specification requirement on ω_{SP} v. n/α is seen to be in reasonable agreement with POR predictions only for n/α greater than about 20 (with $1/T_{\theta_2} = 2.0$). In fact, there is nothing in the theory of POR prediction to indicate that n/α is of any significance, per se, to POR; the variation of POR with n/α at constant CAP, as shown in figure 33, could only result from variations in ω_{SP} . The data point corresponding to configuration 8 might be considered suspect. For it, the predicted POR is 7.9 which seems inconsistently high compared with the overall trend. If this were a flight test rating, the point might be discounted due to pilot "variability" or "bias." Since it is analytically derived it is tempting to attribute it to a localized failure of the Kleinman-Dillow model due, possibly, to non-optimum choices for cost functional weights (which, recall, are held constant and equal to those derived for the Arnold data set for present analysis). However, there is an alternative explanation which may benefit the interpretation of flight test data; this will be discussed later when turbulence effects are examined.

3. For CAP = 3.6 the model's predictions and the Level 1 boundary are in excellent agreement for $1/T_{\theta_2} = 2.0$ and $S_{SP} = 0.5$. The choices $1/T_{\theta_2} = 0.2$ and $S_{SP} = 0.35$ will, however, lead to predicted POR more indicative of a Level 2 boundary.

4. For CAP = 10.0 with $1/T_{\theta_2} = 2.0$ and $S_{SP} = 0.35$ the model-predicted POR is much better than the present specification would indicate. [In fact, for $1/T_{\theta_2} = 2.0$ the model's predictions of POR are nearly independent of CAP in this region.] Possibly the model and the specification would be in better agreement if the Level 2 lower limit on S_{SP} ($S_{SP} = 0.25$) were used in the calculation of the POR metric. The specification is known to be weak in this area; considerable artistry was used in the definition of the Level 2 boundary (CAP = 10) as may be seen from reference 2.

The case 2 data are plotted in figure 34. It is clear that for $1/T_{\theta_2} = 0.2$ the predicted POR are in almost total disagreement with requirements. These data also indicate that neither CAP nor n/α correlates with predicted POR. Short-period natural frequency, however, has a strong effect.

The case 3 data are not plotted. The configurations examined should all be Level 1 if one can believe MIL-F-8785B. It is seen (Table 17) that the predicted PORs vary from the Level 2 boundary to unflyable.

In general, it is apparent that $1/\tau_{\theta_2}$ can have a powerful effect on POR. Variations in this parameter from optimum can completely destroy the validity of MIL-F-8785B as a useful specification of flying qualities to be expected from a new aircraft design. It is also obvious that, by present theory, neither CAP nor n/α are directly relevant to the prediction of closed loop flying qualities of the sort encompassed by the Category A definition. The involvement of both CAP and n/α is confused by the fact that both have intuitive and possible practical merit for the evaluation of flying qualities of tasks involving rapid and precise maneuvering from one trajectory to another. Such tasks are included within the Category A definition of the current specification. Furthermore, both CAP and n/α are related to each other and to the closed loop parameters of interest to the present flying qualities theory through the parameter U_0 . Speed is not usually variable over a wide range for the flight test determination of POR vs. some prescribed parameter. As a consequence either CAP or n/α will, to some extent, correlate with POR trends observable from existing data bases. Their use in the current version of MIL-F-8785B for the specification of short period flying quality requirements is akin to treating the symptoms of the problem and not the disease. There is a further confusion factor involving these two parameters; a discussion of this will be deferred until the next Article.

The opinion of this author is that the predictions of POR using the theory proposed in this report are in good agreement with the short-period requirements of MIL-F-8785B in those areas where the specification is a reasonable empirical correlation of the available data, and for satisfactory choices of $1/\tau_{\theta_2}$. In other areas, it is this author's opinion that the theory is more versatile and reliable than the specification.

D. TURBULENCE EFFECTS

The theory of this report for the prediction of POR indicates that turbulence intensity will affect the prediction of σ_{θ_g} and, therefore, POR. MIL-F-8785B does not address this potential problem area. We wish to examine the effects on predicted POR of varying σ_{w_g} and, from this, draw inference as to whether or not gust effects should be incorporated into the attitude control requirements of the specification. This will be done only for a few configurations. Tables 18, 19 and 20 summarize the Kleinman-Dillow model parameters and predicted POR for certain case 1, 2 and 3 configurations, all with $\sigma_{w_g} = 16$ f/s. Table 21 shows the results for other case 1 configurations with $\sigma_{w_g} = 5.0$ f/s. Comparison of these predicted POR values with those for $\sigma_{w_g} = 10$ f/s (Tables 15-17) indicates:

1. The Levels 2 and 3 specification boundary for CAP = 0.16 is somewhat degraded at the higher gust intensity condition but is still reasonable

with respect to the theoretical POR. This, of course, is strictly true only for the values of T_{θ_2} and ξ_{sp} used.

2. The Level 1 specification boundary for CAP = 3.6 with $1/T_{\theta_2} = 0.2$ and $\xi_{sp} = 0.35$ is even more inadequate for the higher gust level than it was for $\sigma_{wg} = 10$ f/s.

3. The Case 2 configurations for constant ω_{sp} (= 0.5 and 3.0) are not substantially affected by the higher turbulence level. The largest POR degradation is for the poorer POR cases (for $\omega_{sp} = 3.0$); this is only about 0.8 units, however.

4. The case 3 configurations that are predicted to be flyable with $\sigma_{wg} = 10$ (configurations 37, 38, 39 and 40) are predicted to remain flyable with $\sigma_{wg} = 16$. The POR is predicted to increase, however, by about 0.8 units. The unflyable configurations are predicted to remain unflyable at the higher turbulence level, as expected.

5. The Level 1 specification boundary for CAP = 0.28 is a very good match for the predicted POR with $\xi_{sp} = 0.5$, $1/T_{\theta_2} = 2.0$ and $\sigma_{wg} = 5$. An isolated exception is configuration 8 which appears to have a predicted POR out of line with the indicated trend for increasing n/α . This also was observed with $\sigma_{wg} = 10$. More on this later. The decrease in turbulence intensity from 10 to 5 f/s is predicted to give a substantial improvement on POR for the more poorly rated configurations with CAP = 0.28; the corresponding improvement for the better configurations is much smaller. Decreasing σ_{wg} from 10 to 5 f/s is predicted to give a slight improvement of the CAP = 3.6 and 10 configurations. These, however, were nearly all Level 1 configurations at $\sigma_{wg} = 10$ and would be expected to remain so with smaller σ_{wg} . Given the nonlinear nature of $\sigma_{\beta g}$ vs. POR (figure 24), very large percentage decreases in σ_{wg} are required to produce a significant improvement in predicted POR for Level 1 configurations.

In general it appears that there is a significant effect of turbulence intensity on predicted POR only for those configurations that are Level 2 or worse for nominal turbulence levels. There appears to be a short-period frequency effect, however, which produces an aggravated POR sensitivity to turbulence level primarily at higher ω_{sp} . The value $\sigma_{wg} = 10$ was selected by Arnold for reasons of task realism in fixed base tracking. The resulting POR predictions based on Arnold's data and the proposed theory are in good agreement with the Neal-Smith flight test results with the USAF variable stability T-33. It is hereby assumed that $\sigma_{wg} = 10$ is a useful baseline value for the comparison of predicted POR with MIL-F-8785B requirements which, in large part, reflect flight test experience. Then $\sigma_{wg} = 16$ f/s should be assumed to constitute a very severe input condition. It therefore follows that the intensity for random, gaussian turbulence should have only small

effect on the specification of Level 1 short-period flying quality requirements. The effect on Levels 2 and 3 will be stronger for the higher CAP (actually, higher ω_{sp}) regions. It should therefore be expected that flight test measurements of POR for CAP greater than about 4.0 will likely contain spurious errors due to effects of natural (and probably un-measured) turbulence.

Table 22 summarizes the variation of predicted POR with ω_{sp} ; $1/T_{\theta_2}$ and ζ_{sp} are parameters. These data are tabulated in this fashion to illustrate the point that preconceived notions about how to parameterize POR data can lead to possible misconceptions about POR. For the three data sets shown it might appear that monotonic variations in ω_{sp} should result in a predicted monotonic variation in POR. This is generally true. Configurations 43, 21, 45 and 8 are notable exceptions. For each of these the predicted POR is either significantly lower or higher than those for neighboring configurations in the sequence. The irregular POR for these four cases could be attributed to eccentricities in the Kleinman-Dillow model when used in present fashion. This possibility was previously indicated for configuration 8. If these were flight test or simulator derived POR with actual pilots, however, these "irregular" data would likely be attributed to pilot variability. In fact, both explanations are probably incorrect.

The real culprit in the Table 22 data is probably the airframe gust model. The airframe response to a gust-induced angle of attack $\alpha_g = w_g / u_o$ is, for the short-period approximation,

$$\begin{aligned}\frac{\theta}{\alpha_g}(s) &= \frac{-(M_{\alpha} + Z_w M_{\dot{\alpha}})}{s^2 + 2\zeta_{sp}\omega_{sp}s + \omega_{sp}^2} \\ \frac{\dot{w}}{\alpha_g}(s) &= \frac{-U_o Z_w (s - M_{\dot{g}} + U_o M_{w/Z_w})}{s^2 + 2\zeta_{sp}\omega_{sp}s + \omega_{sp}^2} \\ \frac{\dot{w}}{\alpha_g}(s) &= \frac{-U_o Z_w (s + 1/T_w)}{s^2 + 2\zeta_{sp}\omega_{sp}s + \omega_{sp}^2}\end{aligned}$$

The θ/α_g numerator is approximately equal to $-M_{\alpha}$ for most of the configurations examined in this study. The values of M_{α} for each of the four suspect configurations and one on each side are listed in Table 23. It is clear that for configurations 43, 21, 45 and 8 M_{α} is either much smaller or much larger than for neighboring configurations. The effect on gust-induced pitch attitude rate amplitude is directly reflected in the POR prediction. It is therefore concluded that the apparent POR discrepancies in the data of Table 22 are due to two effects:

1. The (unwarranted) assumption that monotonic variations in ω_{sp} should yield monotonic variations in POR with all other dynamic parameters held constant.

2. The effects of airframe gust response on the level of pitch attitude rate feedback.

In a flight test program designed for the collection of POR for various airframe dynamics one does not usually have full control over the airframe's dynamic response to natural atmospheric turbulence. The disturbance due to natural causes is not usually determined and, therefore, may be a source of "variability" in pilot rating data that is impossible to sort out without a measure of the POR metric $\sigma_{\beta q}$. From earlier conclusions in this Article it is probable that spurious errors of this sort would be most likely to occur for Levels 2 and 3 configurations in the region of higher ω_{sp} .

The airframe's response to an α -gust is parameterized by:

1. The $\frac{\partial}{\partial \alpha_g}(s)$ numerator; $-(M_\alpha + Z_w M_{\dot{\alpha}})$

2. The $\frac{W}{\alpha_g}(s)$ numerator time constant;

$$\frac{1}{T_w} = -M_q + u_o \frac{M_w}{Z_w}$$

3. Z_w

Observe that $1/T_w$ and Z_w are directly related to the MIL-F-8785B parameters CAP and n/α in the following way (the usual approximations are employed):

$$\frac{1}{T_w} = \frac{\omega_{sp}^2}{-Z_w}$$

$$\frac{n}{\alpha} = -\frac{u_o Z_w}{g}$$

$$Z_w = -\frac{g}{u_o} \left(\frac{n}{\alpha} \right)$$

$$\frac{1}{T_w} = \frac{u_o}{g} (CAP)$$

It therefore follows that CAP and n/α can affect POR, even for non-maneuvering tracking, by shaping the turbulence spectrum to determine the level of airframe excitation. Thus they may in effect become closed loop parameters of significance. It has already been indicated that their effects on closed loop tracking POR will probably be isolated at the higher ω_{sp} , Levels 2 and 3 dynamic configurations. In general, it is suspected that CAP and n/α are parameters of second-order importance to the determination of closed loop POR. There may be unusual combinations of airframe aerodynamic response and response to control for which their effects are very important. This may arise in applications of the control-configured vehicle concept, with various possible gust alleviation systems, or with path control systems using direct force generation.

E. MOTION CUE EFFECTS

Certain of the case 1 and all the cases 2 and 3 airframe configurations were re-analyzed. The Kleinman-Dillow model was modified from that previously applied to these data by the feedback of a_{zp} , the normal acceleration at the pilot's station, and the angular motions θ and $\dot{\theta}$. Two pilot locations, 20 and 60 feet ahead of the aircraft's center of gravity, were evaluated. The detailed results will not be shown here.

The purpose of this study was to make an exploratory assessment of motion feedback effects on the calculation of $\sigma_{\beta q}$. No readily usable data were available to permit the construction of a reliable cost function, with weights, which incorporated the motion cues. Instead, the author elected to use zero weightings on θ , $\dot{\theta}$ and a_{zp} with the same weights on θ and $\dot{\theta}$ as used in the analysis of Arnold's data. It was expected that this would ensure that differences in predicted POR with and without motion would reflect only motion effects and not effects due to the choice of cost functional.

It was found that in nearly every case the equivalent Kalman filter gain was larger with motion cues than without. This is the result of higher quality predictions of state due to the availability of the higher derivatives to the predictor. Also, in nearly all cases the value σ_q decreased with the addition of motion. The feedback control gains K_θ^* and $K_{\dot{\theta}}^*$ were not affected. The percentage increase in the Kalman filter gain was greater than the percentage decrease in σ_q . The result of motion addition was, therefore, to increase the POR metric $\sigma_{\beta q}$. The predicted increase in POR was between 0 and 0.8 units in all cases. The good configurations were not significantly affected by motion; the poor configurations suffered the largest increase in POR. There was no significant effect of pilot location relative to the center of gravity on the predicted POR.

The physical significance of these results is difficult to assess. They are too preliminary to permit any resolution of questions pertaining to motion cues and their significance to flight test measurement of POR. It is suspected, however, that an appropriate cost functional for the Kleinman model (i.e. one which properly weights the motion cues) will enable the quantitative assessment of motion effects on POR through application of the theory proposed in this report. The present study results of motion effects are probably biased by failure to weight a_{z_p} in the cost functional. For certain of the poorly rated configurations it seems reasonable to expect improvements in POR due to motion. The data of figure 27, for example, indicate that this may be true.

F. OBSERVATIONS, CONCLUSIONS AND RECOMMENDATIONS

The shortcomings of MIL-F-8785B are well-known. The specification requirements are empirical and are not well-founded in theory. The handling quality data base for the specification is limited and expensive to extend. Combinations of classical vehicle dynamic parameters can often be found to yield configurations with handling qualities contradictory to what MIL-F-8785B would indicate. The document is not directly and obviously suitable for the design specification of highly augmented aircraft. It gives no guidance for estimating the effects of turbulence on handling qualities and the possible consequence to design. The significance of piloting task details can be assessed only in the most convoluted manner, if at all.

The motivation behind the present work was the desire to develop analytical methods for handling quality prediction that are not subject to these practical limitations. This goal has been partially accomplished. The resulting theory for pilot rating prediction is directly applicable to those flying qualities tasks that can be characterized as fundamentally single-axis in nature; these include a broad and important spectrum of flight control problems. It has been noted that, although the theory for rating prediction is general in scope, it is practically limited to single-axis tasks by the current state-of-the-art of pilot model development. The development of pilot models suitable for rating prediction in multiple axis or multiple loop tasks is a goal for future research. Still, it is not entirely clear how a general and valid theory for rating prediction should be implemented to overcome the present shortcomings of MIL-F-8785B. That too is a subject for research.

Certain features of MIL-F-8785B are objectionable from the viewpoint provided by present theory. The short-period dynamic requirements, for example, emphasize the importance to handling qualities of n/α and the CAP parameter - - neither of which directly influences

pilot rating, according to present theory, for closed loop precision control tasks. This situation is further confused by two complications:

1. Both n/α and CAP partly parameterize the airframe's gust response and will therefore correlate pilot rating data to some extent.
2. The Category definitions in MIL-F-8785B include both open loop and closed loop piloting tasks in each of Categories A and C. It is probably true that normal acceleration response is important to open loop short-period flying qualities; n/α and CAP could conceivably be suitable for the parameterization of normal acceleration control (although this has not really been established from theory or from flight test) and would therefore correlate pilot rating data from flight tests involving open loop maneuvering tasks. Since much of the current handling qualities data base is derived from such flight tests, we can expect that n/α and CAP will correlate with pilot ratings; unfortunately, it is conceivable that this correlation may confuse the proper interpretation of these data - - at least for precision, closed loop control tasks.

It appears to be generally true that the art of pilot-vehicle systems analysis has had very little impact on MIL-F-8785B. This is, partly due to the essential weakness of the state-of-the-art of analytical flying qualities. Nevertheless the theory of pilot-vehicle system dynamics has permitted the identification of several important handling quality parameters. The importance of the pitch attitude transfer function zero $1/\tau_{\theta_2}$, for example, was originally identified through use of pilot-vehicle systems analysis and has been confirmed by experiment; it still does not directly appear in the short period flying quality requirements of MIL-F-8785B.

The parameterization of flying qualities in terms of modal parameters is difficult in part because no one parameter is completely independent from the rest - - at least not in the practical sense. The theory presented in this report for the assessment and prediction of pilot opinion ratings directs that POR be correlated only with the metric σ_{β_x} ; this, however, is a result of closed loop control activity by the pilot. The metric σ_{β_x} is not obviously suited for use in specifying aircraft design.

Or is it? A future version of MIL-F-8785B might require that the short-period dynamics be such as to yield $\sigma_{\beta_q} \leq 0.4$ degrees for Level 1 handling qualities. This would be the only necessary short-period requirement for closed loop flying qualities. However, such a specification statement would require that an adequate model exist for predicting σ_{β_q} , that methods be available for the direct measurement of σ_{β_q} from flight test (in order to certify the satisfaction

of the design requirement), and that the test pilot perform to the limits of his capabilities during the certification flight tests.

Even with all these factors given, the real proof of the design will rest with the pilot's opinion rating. The validity of present theory would require, however, that the actual rating be consistent with the measured $\sigma_{\Delta q}$. In this sense, the actual rating would be redundant except as a final cross-check. This analytical approach to the specification of flying qualities seems impractical in view of the present state-of-the-art; the philosophy may be sound, however, and should be fairly and objectively evaluated.

On the other hand, there is no obvious reason to preclude the use of present theory as a design guide for flying qualities - - especially for those vehicle configurations that cannot be directly assessed through the use of MIL-F-8785B. This might be more realistic than the alternative approach of using MIL-F-8785B and its back-up documentation as a speculative basis for the assessment of probable flying qualities. Accordingly, it is recommended that MIL-F-8785B be revised to cite the theory for pilot opinion rating contained in this report as an optional method for flying qualities assessment of those vehicles for which the detailed specification is inapplicable by reason, for example, of augmentation or configuration design. The method should be standardized to include the pilot model, the control effectiveness, the turbulence model, and an algorithm for selection of the pilot model parameters and for the prediction of pilot ratings. The use of the Kleinman model with the empirical calibration of figure 24 is recommended until a more universal model for pilot dynamics becomes available.

At various places throughout this report it has been hinted that the theory should be applicable for non-tracking or non-continuous tracking tasks. It was also noted in the introduction that we define aircraft flying qualities in terms of pilot opinion rating primarily because we don't know how else to define flying qualities and because the pilot has been the traditional final judge of an aircraft's suitability. Pilot opinion rating requires a quantitative scale, however; the scale and the manner in which it is used may permit too much arbitrary choice to creep into the experimental assessment of flying qualities. This is (or should be) a particular concern with regard to the future design of aircraft, displays, or weapons that are novel in their piloting requirements or that place considerable emphasis on system accuracy requirements during short time intervals. It is beyond the state-of-the-art at this time to assess the significance of pilot opinion rating data obtained from such tasks. For such tasks, pilot opinion ratings may not be the best measure for handling qualities. This, too, is a subject for future research.

APPENDIX A

A COMPUTER MODEL FOR A NONLINEAR TIME DELAY

A. GENERAL DESCRIPTION

The subroutine XDELAY described in this appendix is a digital computer model intended for the simulation of a nonlinear time delay

$$\tau = K/|x|$$

The signal $x(t_i)$ is the input signal to the delay at time $t = t_i$. The corresponding time delay is τ_i . If on the interval $t_i < t_k < t_i + \tau_i$, a value $x(t_k)$ occurs for which $t_k + \tau_k \leq t_i + \tau_i$, then it is assumed that the output of XDELAY at $t \geq t_k + \tau_k$ will not be determined by $x(t)$ where $t_i \leq t \leq t_k$. That is, $x(t)$ on the interval $t_i \leq t \leq t_k$ will have no effect on the response of the nonlinear delay model XDELAY. In this way, the nonlinear delay acts like a peculiar filter. The major difficulty in programming XDELAY is due to this property that creates "null-subsets" of $x(t)$.

The nonlinear delay response and response time are programmed as subscripted files XOUT(I) and TIMEOUT(I) such that

$$\begin{aligned} \text{XOUT}(I) &= x(t) \\ \text{TIMEOUT}(I) &= t + \tau \end{aligned}$$

These are created on-line during a simulation exercise. The indexing variable I is re-set in XDELAY whenever a null-subset of $x(t)$ has been identified in order to over-write the stored output files XOUT and TIMEOUT.

When a system simulation involving XDELAY is conducted, it is assumed that the XDELAY output files are initially null; the first non-zero input $x(t)$ will begin to fill these. When the current value of simulation time T becomes equal to or greater than TIMEOUT, then a non-zero response from XDELAY is required. If $T = \text{TIMEOUT}(I)$ then the response of the nonlinear delay will be $\text{XDLAY} = \text{XOUT}(I)$ where $\text{XOUT}(I) = X(T - \tau)$ where $\tau = AK / \text{XOUT}(I)$. This is an unlikely occurrence, however. In general, XDLAY must be determined by interpolation within the output files. This is accomplished in XDELAY by a fourth-order Lagrange interpolation algorithm. Its use requires that four values of I be determined for which $\text{TIMEOUT}(I_1) < T < \text{TIMEOUT}(I_4)$ where

$$\begin{aligned} I_2 &= I_1 + 1 \\ I_3 &= I_1 + 2 \\ I_4 &= I_1 + 3 \end{aligned}$$

The program is mechanized to choose I such that

$$\text{TIMEOUT}(I_2) < T < \text{TIMEOUT}(I_3)$$

to maximize the accuracy of the interpolation. There are two cases when this is not possible. The first case occurs when

$$\text{TIMEOUT}(1) < T < \text{TIMEOUT}(2), I_{\max} \geq 4$$

In that case the output file points for $I = 1, 2, 3$, and 4 are selected and the interpolation is made over these with no further modifications required. The second case is more troublesome. If a very large, sudden increase occurs in $|x(t)|$ at $t = t_c$ near the start of a simulation then all of the output file storage for $\text{TIMEOUT} > T$ can be over-written and only that due to the current input remains; in that case, insufficient storage exists for the exercise of the interpolation algorithm. This problem is an inherent property of the simulation and cannot be avoided by, for example, choosing a smaller program step size ΔT . The solution to this problem, as programmed, is to use the last three values of the subroutine output XDELAY and the output times T plus the remaining point in the output file to provide the necessary four data points for the interpolation algorithm. Therefore, it is necessary that the output of subroutine XDELAY be subscripted for identification and recall, if necessary. The files for storage of XDELAY response and response time are called XHOLD and TSTORE, respectively.

Occasionally, the over-writing of the output files such as described above will occur before three responses have been obtained from XDELAY. In that case, the combination of XOUT(1) and the output storage XHOLD will not yield four points for use by the interpolator. This usually indicates that the program step size ΔT is too large. The program XDELAY detects this condition, prints an error message and aborts the program execution.

The subroutine XDELAY is designed to operate in conjunction with a subroutine INTEG for the numerical integration for a system of differential equations. INTEG may use either a forward integration or a predictor-corrector algorithm and be compatible with XDELAY. Either method, in general, will occasionally result in the back-spacing of time for the control of integration step size and accuracy. A test for this condition is made in XDELAY. When it occurs, the subscripting indices for all output and storage files are re-set to reflect the back-spacing of $x(t)$. Continued system operation then results in the over-writing of these files. It is not, in general, known in advance how much storage will be required to allow for the back-spacing of time. The programming solution adopted was to retain only the most recent 32 values for XHOLD and TSTORE, and 300 values for XOUT and TIMEOUT. This re-sequencing operation is performed every 20 program steps for XHOLD and TSTORE and every 200 steps for XOUT and TIMEOUT.

Compatibility of XDELAY and INTEG, in general, requires that the response XDLAY not be changed until a valid integration step has been completed in INTEG. The logical variable GOOD is available in XDELAY for this purpose. It is assumed that GOOD is set to FALSE by INTEG at intermediate integration points with GOOD set to TRUE for valid points corresponding to valid solutions of the system differential equations. If GOOD is FALSE upon entry to XDELAY, an automatic return to the calling program (usually a derivative subroutine for INTEG) is made.

The program defined in this appendix is known to be deficient in one respect; it will produce a step response for a pulse input. The computer model was designed to simulate a human pilot's time delay in the perception of visual rate stimuli in a closed loop feedback control system. Physiological data, known to this author at the time XDELAY was prepared, were insufficient to permit the determination of precisely when the rate $\dot{x}(t)$ should be used for the determination of τ or when the change in rate $\Delta \dot{x}(t)$ should be used. The author elected to ignore $\Delta \dot{x}(t)$ for the calculation of τ and use only the current value $\dot{x}(t)$. At the conclusion of an input pulse $\dot{x}(t) \equiv 0$ and $\tau = \infty$; thus, a pulse input becomes a step response in the present mechanization of XDELAY. This is not regarded as a serious deficiency in a closed loop system simulation since pulses don't generally occur in system rate. In the simulations for which XDELAY was used in the program described in this report $\dot{x}(t)$ tended to be periodic in nature. For periodic or near-periodic $\dot{x}(t)$, XDELAY is probably satisfactory as programmed. A better physical model for human visual sensation of rate would be required for the remedy of this defect. Such a model might incorporate a comparator and a refractory delay mechanism of some sort which would generate a time delay dependent upon changes in rate over a refraction interval.

B. DEFINITIONS OF VARIABLES USED IN SUBROUTINE XDELAY

1. A = coefficients computed for use in the Lagrange interpolation.
2. AK = the constant of proportionality in the expression for the nonlinear time delay:

$$\text{TAU} = \text{AK} / |\dot{x}|$$

3. DK = AK/4; this is, in effect, used as a threshold value for TAU. When $|\dot{x}| \leq \text{DK}$ at an entry time T, no time delay computation is performed and XDLAY is set to the last value computed. This is done to avoid needless computation and storage associated with small \dot{x} which will become a null-set member.

4. DLTX = $|\dot{x}|$

5. GOOD is a logical variable that must be set to TRUE by an integration subroutine at points for which the values X and T correspond to a valid solution to the system of differential equations. GOOD must be set to FALSE at points of intermediate calculation within the integration subroutine. It is available to XDELAY from the labeled common block INCTRL.

6. I = an indexing subscript used for the sequencing of XOUT and TIMEOUT.

7. IKY = 1 or 2; it is a counter used to by-pass the interpolation mode at to set the output XDLAY to zero at the time of first entry.

8. INTRP = a variable supplied by the integration subroutine and available, as an external control, to XDELAY through the labeled common block INCTRL. It is not used in XDELAY as programmed.

9. ISCORE = 1 or 2; it is set to 1 in the MAIN program at the program start time and re-set to 2 by XDELAY. It is an argument list variable used only for establishing the initial conditions in XDELAY.

10. J = an indexing subscript used for the sequencing of XHOLD and TSTORE.

11. JILLY = a do-loop variable used only to check for monotonic sequencing of TIMEOUT and possible re-sequencing of TIMEOUT and XOUT.

12. T = the current (entry) time; an argument list variable.

13. TAU = τ , the nonlinear delay time.

14. TIMEOUT = T + TAU, the time at which the current input X to XDELAY is to become equal to the response XDLAY; i.e. XDLAY (T + TAU) = X(T).

15. TOLD = the list value of T for which an entry to XDELAY was made.

16. TSTORE = the time for which the delay response XDLAY was produced; TSTORE is used to determine whether back-spacing of T has occurred due to the integration subroutine and for interpolation when the output files are sufficiently over-written by encounter with a null-subset of X.

17. TT = interim storage location for TIMEOUT for use in the Lagrange interpolation - - a dummy variable.

18. X = the current (entry) value of the signal to be delayed;
an argument list variable.

19. XDLAY = the desired response from XDELAY at the current
time T.

20. XHOLD = the subscripted equivalent of XDLAY used for temporary storage of the delay's response; XHOLD is used for interpolation whenever the output files XOUT is sufficiently over-written by encounter with a null-subset of X or due to the back-spacing of time T.

21. XOLD = X

22. XOUT = the computed output required at the time T = TIMEOUT.

23. XX = values of XOUT corresponding to TT for use in the Lagrange interpolation - - a dummy variable.

C. PROGRAM LISTING

A listing for XDELAY is given on the following pages. The program is prepared in Fortran IV.

```

SUBROUTINE XDELAY(T,X,XDLAY,AK,ISCORE)
DIMENSION A(4), TIMEOUT(500), XOUT(500), TSTORE(52), XHOLD(52)
LOGICAL GOOD
DIMENSION TI(4), XX(4)
COMMON /INCTRL/ INTRP,GOOD
C
C GOOD IS SUPPLIED BY INTEG. GOOD=TRUE INDICATES THAT THE ENTRY
C TO XDELAY CORRESPONDS TO A VALID POINT OF SOLUTION TO THE DEQS
C AND IS NOT DERIVED FROM AN INTERMEDIATE CALCULATION PRODUCED
C BY INTEG NUMERICAL INTEGRATION ALGORITHMS.
GO TO (10,20), ISCORE
10 CONTINUE
TOLD=-1.
XOLD=1.0E5
DK=AK/4.
I=1
J=1
IKY=1
ISCORE=2
XDLAY=0.
20 CONTINUE
IF (.NOT. GOOD) RETURN
IF (IKY-1) 30,90,95
90 IF (ABS(X)-DK) 91,92,92
91 XDLAY=0.
RETURN
92 TSTORE(1)=T
DLTX=ABS(X)
IKY=2
TAU=AK/DLTX
XOUT(1)=X
TIMEOUT(1)= T + TAU
XDLAY=0.
XHOLD(1)=0.
TOLD=T
XOLD=X
RETURN
95 IF (T-TOLD) 50,50,100
50 IF (T-TSTORE(J)) 55,55,100
55 J=J+1
GO TO 50
100 I=I+1
J=J+1
TSTORE(J)=T
DLTX=ABS(X)
TOLD=T
XOLD=X
IF (DLTX-DK) 102,102,101
102 XOUT(I)=X
TIMEOUT(I)=T+TAU
GO TO 150
101 TAU= AK/DLTX
XOUT(I)=X
TIMEOUT(I)=T+TAU
JILLY=I-1
DO 120 JJJ=1,JILLY
IF (TIMEOUT(I)-TIMEOUT(I-JJJ)-1.56E-3) 120,120,130

```

```

130 IF(JJJ-1) 150,150, 140
140 TIMEOUT(I+1-JJJ)= TIMEOUT(I)
    XOUT(I+1-JJJ)=XOUT(I)
    I=I+1-JJJ
    GO TO 150
120 CONTINUE
    TIMEOUT(1)=TIMEOUT(I)
    XOUT(1)= XOUT(I)
    I=1
    XDLAY=0.
    XHOLD(J)=0.
    GO TO 750
150 IF(T-TIMEOUT(1)) 160,170,170
160 XDLAY=0.
    XHOLD(J)=0.
    GO TO 700
170 IF(I-4) 171,190,190
171 IF(J-3) 173,175,175
173 WRITE (6,300)
300 FORMAT(1X,19HCHOOSE SMALLER STEP)
    STOP
175 DO 180 IBD=1,3
    TT(IBD) = TSTORE(J-4+IBD)
    XX(IBD)= XHOLD(J-4+IBD)
180 CONTINUE
    TT(4)=TIMEOUT(I)
    XX(4)=XOUT(I)
    GO TO 270
190 DO 210 IJK=2,I
    IF(T-TIMEOUT(IJK)) 220,210,210
210 CONTINUE
220 IF(IJK-2) 230,230,240
230 DO 250 II=1,4
    TT(II)= TIMEOUT (II)
    XX(II)=XOUT(II)
250 CONTINUE
    GO TO 270
240 DO 260 II=1,4
    TT(II)=TIMEOUT(IJK-4+II)
    XX(II)=XOUT(IJK-4+II)
260 CONTINUE
270 ZA=T-TT(1)
    ZB=T-TT(2)
    ZC=T-TT(3)
    ZD=T-TT(4)
    ZE=ZC * ZD
    ZF=ZA * ZB
    WA = TT(1) - TT(2)
    WB = TT(1) - TT(3)
    WC=TT(1)-TT(4)
    WD = TT(2) - TT(3)
    WE = TT(2) - TT(4)
    WF = TT(3) -TT(4)
    A(1) = ZB * ZE / (WA * WB * WC)
    A(2) = ZA * ZE / (-WA * WD * WE)
    A(3) = ZF * ZD / ( WB * WD * WF)
    A(4) = ZF * ZC / (-WC * WE * WF)

```

	XOLAY = 0.
	DO 290 N=1,4
290	XOLAY = XOLAY + (A(N) * XX(N))
	XHOLD(J)=XOLAY
700	IF(I.LT.500) GO TO 750
	DO 720 I=1,300
	TIMEOUT(I)= TIMEOUT(200+I)
	XOUT(I)=XOUT(200+I)
720	CONTINUE
	I=300
750	IF(J.LT.52) GO TO 810
	DO 800 J=1,32
	TSTORE(J)= TSTORE(20+J)
	XHOLD(J)= XHOLD(20+J)
800	CONTINUE
	J=32
810	RETURN
	END

APPENDIX B

A SUBROUTINE FOR THE ESTIMATION OF DESCRIBING FUNCTIONS

A. THE CLOSED LOOP SYSTEM

It is assumed that the describing function for the human pilot dynamics model $Y_p(j\omega)$ in the closed loop system described in figure 1 is desired. The system input is assumed to consist of a summation of randomly-phased sine wave components - each with an amplitude scaled to match a desired input spectra. The input therefore has power content only at n -discrete frequencies ω_k . The time interval for which the system response is to be measured and used for the estimation of $Y_p(j\omega_k)$ is assumed to be an integer multiple of all the input sine wave component periods; in particular, it is assumed to be several times larger than the period of the lowest frequency input sine wave. In practice, this is not always practical; it is therefore necessary that test cases be run to determine the minimum acceptable run times to ensure tolerable measurement accuracy.

Provisions are contained in the program described in this appendix for the estimation of the total open loop system describing function $Y_{OL}(j\omega_k) = Y_p(j\omega_k) Y_c(j\omega_k)$ where $Y_c(s)$ is one of five pre-scribed controlled elements corresponding to

$$K_c, \quad \frac{K_c}{s}, \quad \frac{K_c}{s^2}, \quad \frac{K_c}{s-2}, \quad \frac{K_c}{s(s-2)}$$

according to the value of the integer variable $OPTION = 1, 2, 3, 4, 5$, respectively.

The subroutine YPILOT described for describing function estimation, under the prescribed restrictions, may be used for the estimation of the describing function for any dynamic element (e.g. the neuromuscular system) provided that the input and response of this element are supplied via the argument list to YPILOT. For such applications, however, it is understood that the open loop describing function calculation $Y_{OL}(j\omega_k)$ may be meaningless.

B. THE ANALYTICAL METHOD

In general the describing function for the human pilot dynamic response (or any element of the closed loop system) is given as the ratio of the cross-spectral densities

$$Y_p(j\omega) = \frac{\Phi_{is}(j\omega)}{\Phi_{ie}(j\omega)}$$

For the special case where $i(t)$ is equal to the sum of a number of sine wave components at the frequencies ω_k , this ratio becomes

$$Y_p(j\omega_k) = \frac{\bar{i}(j\omega_k) \delta(j\omega_k)}{\bar{i}(j\omega_k) e(j\omega_k)} = \frac{\delta(j\omega_k)}{e(j\omega_k)}$$

It is understood that this ratio is defined only at the input frequencies ω_k . The quantities $i(j\omega_k)$, $\delta(j\omega_k)$ and $e(j\omega_k)$ are the Fourier coefficients of the time signals $i(t)$, $\delta(t)$ and $e(t)$.

For any signal $x(t)$, its Fourier transform is, in the subroutine YPILOT, computed in the following way:

$$\begin{aligned} X(j\omega_k) &= 2 \int_0^{TF} x(t) e^{-j\omega_k t} dt \\ &= 2 \int_0^{TF} x(t) \cos \omega_k t dt - 2j \int_0^{TF} x(t) \sin \omega_k t dt \\ &= \operatorname{Re}[X(j\omega_k)] + j \operatorname{Im}[X(j\omega_k)] \end{aligned}$$

$$\begin{aligned} \operatorname{Re}[X(j\omega_k)] &= 2 \int_0^{TF} x(t) \cos \omega_k t dt \\ \operatorname{Im}[X(j\omega_k)] &= -2 \int_0^{TF} x(t) \sin \omega_k t dt \end{aligned}$$

The integrals may be replaced with a suitable numerical approximation in actual computations; e.g.,

$$\int_0^{TF} x(t) dt = \sum_{n=0}^N x(n\Delta t) \Delta t$$

where $N\Delta t = TF$ and Δt is chosen to be sufficiently small.

The ratio of any two Fourier transforms at a particular frequency may be expressed as an amplitude ratio and a phase angle. For example

$$\frac{X(j\omega_k)}{Y(j\omega_k)} = \left| \frac{X(j\omega_k)}{Y(j\omega_k)} \right| \angle \frac{X(j\omega_k)}{Y(j\omega_k)}$$

where

$$\begin{aligned} \left| \frac{X(j\omega_k)}{Y(j\omega_k)} \right| &= \frac{|X(j\omega_k)|}{|Y(j\omega_k)|} \\ \angle \frac{X(j\omega_k)}{Y(j\omega_k)} &= \angle X(j\omega_k) - \angle Y(j\omega_k) \end{aligned}$$

C. DEFINITIONS OF VARIABLES USED IN SUBROUTINE YPILOT

It is assumed that YPILOT is a subroutine in a much larger digital computer program that simulates the operation of the entire pilot-vehicle system. This program is assumed to be under the executive control of a MAIN program which initializes the program operation, establishes the time step, calls an integration subroutine, passes required information to YPILOT, and performs various final computations. Information is transferred between YPILOT and MAIN by either an argument list or various labeled common blocks. The following variable definitions are used:

1. E and D are any two continuous time signals for which the ratio of Fourier coefficients $D(j\omega_k)/E(j\omega_k)$ is desired. For the pilot-vehicle system shown in figure 1, $E = e$ (system error) and $D = \delta$ (the pilot's control response). Both E and D are available to YPILOT through the argument list.
2. $W(I) = \omega_k$, the input sine wave component frequencies. $W(I)$ is in the labeled common block FREQ. The dimensions of $W(I)$ must be prescribed in both MAIN and YPILOT.
3. $A(I)$ are the amplitudes of the input sine wave components corresponding to $W(I)$. These are in the labeled common block ABC. Not used in YPILOT for computations.
4. C is the value of D actually used in YPILOT for computations. Usually $C = D$. This variable was introduced to permit the scaling of D within YPILOT without affecting corresponding D values in MAIN.
5. DT is a constant time step for the supply of input signals E and D from MAIN to YPILOT. It is the time step for the output of the integration subroutine; i.e. it is the time step for which system response up-dates are available in MAIN. It is available in the argument list.
6. TF is the time over which describing function computations are to be made. Generally, TF is the final time for closed loop system simulation. It is an argument list variable.
7. MSPEC is a control variable for initializing the integrations in YPILOT. It must be initially set to 1 in MAIN and re-set to 1 for each new simulation run. It is an argument list variable.
8. ZKC is the controlled element gain K_c and is used only for the calculation of the open loop system describing function $Y_{OL}(j\omega_k)$.
9. ZLAMBDA is the pole λ for two of the five controlled elements available in YPILOT for the calculation of the open loop describing function. It is available to YPILOT through the argument list.

10. OPTION is an integer variable in the labeled common block ABC prescribed in MAIN and used for the definition of $Y_c(s)$.

11. XC(I) and YC(I) are the arrays for $\cos(\omega_k t)$ and $\sin(\omega_k t)$, respectively. These are computed in MAIN and are available in the labeled common block COMMAND. They are used for the Fourier transform calculations.

12. Z4 is any system time response in MAIN for which the mean-square or root-mean-square value is to be computed in YPILOT. It is in the argument list.

13. MSQBETA = σ_{Z4}^2 ; in labeled common block DENSITY.

14. RMSBETA = σ_{Z4} ; in labeled common block DENSITY.

15. MSQDEL = σ_c^2 ; in labeled common block DENSITY.

16. MSQYE = σ_E^2 ; in labeled common block DENSITY.

17. YEAVG = average value of E (used to determine bias in $E(t)$); in labeled common block DENSITY.

18. AMPYP(I) and PHYP(I) are the amplitude and phase angle arrays, respectively, of the ratio of the Fourier coefficients $D(j\omega_k)/E(j\omega_k)$. Both are available to MAIN in the labeled common block DESFCN. AMPYP(I) is in decibels and PHYP is in degrees following the completion of all calculations.

19. AMPYOL(I) and PHYOL(I) are the amplitude and phase angle arrays, respectively, of the open loop system describing function.

$$\text{AMPYOL}(I) = \text{AMPYP}(I) \times \text{AMPYC}(I)$$

$$\text{PHYOL}(I) = \text{PHYP}(I) + \text{PHYC}(I)$$

The units are decibels and degrees following the completion of all calculations.

20. AMPYC(I) and PHYC(I) are the amplitude and phase arrays, respectively, of the controlled element transfer function $Y_c(s)$ at the frequencies $\omega(I)$.

D. LISTING FOR SUBROUTINE YPILOT

A listing for the subroutine is shown on the following pages. The coding is in Fortran IV and is compatible with the CDC 6600 digital computer systems.

BEST AVAILABLE COPY

```

SUBROUTINE YPILOT (E,D,DT,TF,MSPEC,Z4,ZKC,ZLAMBDA)
  DIMENSION REC(10),XIMC(10),REE(10),XIME(10)
  DIMENSION AMPYC(10),PHYC(10)
  COMMON /COMMAND/ XC(10),YC(10)
  COMMON /ABC/ OPTION,A(10)
  COMMON /FREQ/ W(10)
  COMMON /DENSITY/ MSQDEL,RMSBETA,MSQYE,YEAVG
  COMMON /DESIGN/ AMPYP(10),PHYP(10),AMPYOL(10),PHYOL(10)
  INTEGER OPTION
  REAL MSQDEL,MSQBETA,MSQYE
  C=ZKC*0
  GO TO (5,20,50), MSPEC
5  DO 10 I=1,10
  REC(I)=0.
  XIMC(I)=0.
  REE(I)=0.
  XIME(I)=0.
10 CONTINUE
  MSPEC=2
  CSQ=0.
  YESQ=J.
  YE=0.
  BETASQ=0.
  DT2=2.*DT
20 DO 30 I=1,10
  REC(I)=REC(I)+C*XC(I)
  XIMC(I)=XIMC(I)+C*YC(I)
  REE(I)=REE(I)+E*XC(I)
  XIME(I)=XIME(I)+E*YC(I)
30 CONTINUE
  CSQ=CSQ+C*C
  YE=YE+E
  YESQ=YESQ+E*E
  BETASQ=BETASQ+Z4*Z4
  RETURN
50 DO 60 I=1,10
  REC(I)=DT2*REC(I)
  XIMC(I)=DT2*XIMC(I)
  REE(I)=DT2*REE(I)
  XIME(I)=DT2*XIME(I)
  AMPYP(I)=SQRT(REC(I)**2+XIMC(I)**2)/SQRT(REE(I)**2+XIME(I)**2)
  PHYP(I)=(ATAN2(XIME(I),REE(I))-ATAN2(XIMC(I),REC(I)))*57.3
  GO TO (200,220,240,260,280),OPTION
200 AMPYC(I)=ZKC
  PHYC(I)=0.
  GO TO 300
220 AMPYC(I)=ZKC/W(I)
  PHYC(I)=-9.
  GO TO 300
240 AMPYC(I)=ZKC/(W(I)*W(I))
  PHYC(I)=-19.
  GO TO 300

```

```

260 DX1=SQRT(ZLAMBOA*ZLAMBOA+W(I)*W(I))
    AMPYC(I)=ZKC/DX1
    PHYC(I)=(ATAN2(W(I),ZLAMBOA))*57.3
    GO TO 300
280 DX1=SQRT(ZLAMBOA*ZLAMBOA+W(I)*W(I))
    AMPYC(I)=ZKC/(W(I)*DX1)
    PHYC(I)=57.3*ATAN2(W(I),ZLAMBOA)-90.
300 AMPYOL(I)=AMPYP(I)*AMPYC(I)
    PHYOL(I)=PHYC(I)+PHYC(I)
    AMPYOL(I)=20.*ALOG10(AMPYOL(I))
    AMPYP(I)=20.*ALOG10(AMPYP(I))
60  CONTINUE
    MSQDEL=CSQ*DT/TF
    MSQBETA=BETASQ*DT/TF
    RMSBETA=SQRT(MSQBETA)
    MSQYE=YESQ*DT/TF
    YEAVG=YE*DT/TF
    RETURN
    END

```

BEST AVAILABLE COPY

TABLE 1 - SYSTEM INPUT (FROM REFERENCE 4)

ω_j	Command Input RMS = 0.5"						Command Input RMS = 1.0"					
	1.5		2.5		4.0		1.5		2.5		4.0	
	a_k	b_k	a_k	b_k	a_k	b_k	a_k	b_k	a_k	b_k	a_k	b_k
ω_k												
.157	.2877	.0452	.2667	.0419	.2497	.0392	.5754	.0903	.5334	.0837	.4994	.0784
.262	.2877	.0754	.2667	.0699	.2497	.0654	.5754	.1508	.5334	.1398	.4994	.1308
.393	.2877	.1131	.2667	.1048	.2497	.0981	.5754	.2261	.5334	.2096	.4994	.1963
.602	.2877	.1732	.2667	.1606	.2497	.1503	.5754	.3464	.5334	.3211	.4994	.3006
.969	.2877	.2788	.2667	.2584	.2497	.2420	.5754	.5576	.5334	.5169	.4994	.4839
1.49	.2877	.4287	.2667	.3974	.2497	.3721	.5754	.8573	.5334	.7948	.4994	.7441
2.54	.0288	.0731	.2667	.6774	.2497	.6342	.0575	.1462	.5334	1.355	.4994	1.2685
4.03	.0288	.1159	.0267	.1075	.2497	1.006	.0575	.2319	.0533	.2150	.4994	2.0126
7.57	.0288	.2178	.0267	.2019	.0250	.1890	.0575	.4356	.0533	.4038	.0499	.3780
13.8	.0288	.3970	.0267	.3680	.0250	.3446	.0575	.7941	.0533	.7361	.0499	.6892

$$y_c = \sum_{k=1}^{10} a_k \sin \omega_k t, \quad x_c = dy_c/dt = \sum_{k=1}^{10} b_k \cos \omega_k t, \quad b_k = a_k \omega_k$$

$$\text{RMS Input } \sigma_y = \left[\frac{1}{2} \sum_{k=1}^{10} a_k^2 \right]^{1/2}$$

TABLE 2

LONGITUDINAL DYNAMIC CONFIGURATIONS TESTED IN ARNOLD'S EXPERIMENT

CONF	U_0	$-M_\alpha$	$-M_w$	$-M_g$	$-Z_w$	$-Z_{\delta e}$	$-M_{\delta e}$	$1/T_{\theta z}$	n/α	ω_{SP}^2	CAP	ω_{SP}	S_{SP}	$-M_\alpha$
T-33	422	6.64	.0157	.778	1.590	38.4	14.54	1.55	20.3	7.88	.388	2.81	.495	.358
T-33	591	16.60	.0281	1.187	2.479	81.0	30.08	2.40	44.1	19.54	.443	4.42	.474	.528
1D	422	6.64	.0157	-1.133	1.590	38.4	14.54	1.55	20.3	4.84	.238	2.20	.690	2.579
2D	422	6.64	.0157	10.923	1.590	38.4	14.54	1.55	20.3	24.0	1.183	4.90	.700	-5.653
3A	422	6.64	.0157	54.999	1.590	38.4	14.54	1.55	20.3	94.1	4.63	9.70	.630	-44.367
4A	422	6.64	.0157	11.546	1.590	38.4	14.54	1.55	20.3	25.0	1.23	5.00	.280	-10.336
5A	422	6.64	.0157	12.181	1.590	38.4	14.54	1.55	20.3	26.0	1.28	5.10	.180	-11.935
6C	591	16.60	.0281	2.033	2.479	81.0	30.08	2.40	44.1	11.56	.262	3.40	.670	4.110
7C	591	16.60	.0281	14.81	2.479	81.0	30.08	2.40	44.1	53.3	1.21	7.30	.730	-6.621
8A	591	16.60	.0281	103.1	2.479	81.0	30.08	2.40	44.1	272.2	6.17	16.5	.690	-82.835
9	422	6.64	.0157	-1.850	1.590	38.4	14.54	1.55	20.3	5.29	.261	2.30	1.700	7.080
10	422	6.64	.0157	-1.850	1.590	38.4	14.54	1.55	20.3	5.29	.261	2.30	1.700	4.780
11	422	6.64	.0157	2.672	1.590	38.4	14.54	1.55	20.3	10.89	.247	3.30	1.100	2.999
12	591	16.60	.0281	33.643	2.479	81.0	30.08	2.40	44.1	100.0	2.27	10.0	.450	-27.122
13	591	16.60	.0281	61.48	2.479	81.0	30.08	2.40	44.1	169.0	3.83	13.0	.340	-55.116
14	591	16.60	.0281	91.47	2.479	81.0	30.08	2.40	44.1	243.4	5.52	15.6	.230	-86.776

$$1/T_{\theta z} = (Z_{\delta e} M_w - M_{\delta e} Z_w) \div M_{\delta e}$$

$$n/\alpha = U_0/gT_{\theta z}$$

$$\omega_{SP}^2 = M_g Z_w - M_\alpha$$

$$S_{SP} = -(M_g + M_\alpha + Z_w) \div 2\omega_{SP}$$

$$CAP = \omega_{SP}^2/n/\alpha$$

TABLE 3 - KLEINMAN - DILLOW MODEL PARAMETERS FOR THE ARNOLD DATA

Case	PITCH					PITCH RATE					M_{De}	$^3\sigma_{Aq}$	POR
	$K_{D\theta}$	$K_{F\theta}$	K_{θ}^*	$'\sigma_{\theta}$	$^2\sigma_{\theta}$	K_{Dq}	K_{Fq}	K_{q}^*	$'\sigma_q$	$^2\sigma_q$			
1	.388	.592	-12.2	.269	.348	.1128	.638	-3.39	.635	.681	-14.54	.155	3.50
2	.500	.701	-20.5	.453	.445	.342	.562	-3.47	.996	1.138		.664	3.60
3	.625	.786	-29.6	.593	.613	.595	.542	-2.92	2.17	2.032		2.04	5.17
4	.714	.841	-12.2	.751	.815	.645	.687	-3.45	2.13	2.346		3.26	6.28
5	.762	.860	-10.3	.876	.984	.710	.709	-3.29	2.90	2.889		4.80	7.79
6	.362	.551	-7.19	.295	.329	.1246	.532	-1.68	.657	.703	-30.08	.151	2.82
7	.415	.611	-14.9	.353	.363	.300	.447	-1.68	1.020	1.042		.475	3.63
8	.555	.735	-23.9	.458	.508	.590	.409	-1.35	2.11	1.998		1.42	4.72
9	.377	.568	-23.8	.338	.339	.1128	.671	-3.63	.445	.681	-14.54	.122	2.21
10	.0895	.0924	-20.3	.1053	.1767	0	.496	-3.61	.156	.1631		4_0	1.61
11	.0254	.0857	-25.7	.1015	.1732	0	.375	-3.44	.193	.1856		4_0	1.36
12	.590	.764	-12.4	.543	.555	.588	.511	-1.55	1.92	1.995	-30.08	1.85	6.00
13	.631	.770	-13.1	.586	.623	.695	.503	-1.42	3.40	2.75		3.49	6.33
14	.651	.752	-12.5	.622	.662	.776	.519	-1.33	4.34	3.78		4.81	6.50

1. experimental value

2. model-predicted value

$$3. \sigma_{Aq} = K_{Dq} K_{Fq} K_q^* \sigma_q \left(\frac{M_{De}}{14.54} \right)$$

4. both these values were arbitrarily set to .01 for the plot of Figure 24

TABLE 4 - SUMMARY OF EXPERIMENTAL DATA & KLEINMAN - DILLON MODEL
PARAMETERS FOR THE McDONNELL EXPERIMENT

($M_{8e} = -14.54$)

CASE	$\gamma_c (s)$	$K_{D\theta}$	$K_{F\theta}$	K_{θ}^*	K_{Dq}	K_{Fq}	K_q^*	σ_L	NO. RUNS	σ_{θ}^1	σ_q^2	T_L^3	$\sigma_{\beta q}$	POR ⁴	POR ⁵	POR ⁶
1								.5	3	.37/.50	.68	3.67	1.72	4.8	5.3	5.8
2	$1/5^2$.966	.929	5.34	.944	.838	3.21	1.0	9	.73/.85	1.35	2.26	3.43	7.2	6.4	7.5
3								1.5	3	1.10/1.18	2.03	3.17	5.15	8.0	7.1	10.1
4	$1/5(5+4)$.926	.913	11.5	.894	.812	3.26	1.0	3	.43/.55	1.05	.84	2.48	5.5	5.9	5.0
5								.5	3	.22/.30	.47	0	.85	2.8	4.3	2.9
6	$1/5$.941	.905	84.0	.923	.783	2.50	1.0	7	.44/.59	.95	0	1.71	4.1	5.3	4.8
7								1.5	6	.65/.75	1.42	0	2.56	5.1	5.9	6.0
8	$1/5(5+1)$.936	.921	7.56	.902	.825	3.54	1.0	5	.50/.47	1.15	1.0	3.03	6.1	6.2	4.7
9	$1/5[7.78]$.927	.900	11.07	.913	.738	2.80	1.0	3	.44/.49	1.29	0	2.43	5.3	5.9	4.4
10	$1/5[7.16]$.932	.891	105.8	.929	.607	1.15	1.0	5	.47/.50	1.57	1.0	1.02	4.6	4.5	5.0
11	$1/5(5+2)$.930	.917	8.39	.897	.818	3.19	1.0	1	.46/.55	1.08	.5	2.53	4.5	5.9	4.9
12	$1/5-2$.985	.926	134.	.977	.813	3.11	1.0	1	2.15/.87	4.92	0	12.13	9.	8.4	8.2
13	$1/5(5-1)$.978	.935	4.21	.961	.860	3.42	1.0	1	1.44/?	2.83	0	8.00	10.	7.8	10.6

1. PREDICTED/EXPERIMENTAL AVERAGE

4. AVERAGE OF EXPERIMENTAL VALUES (COOPER-HARPER)

2. MODEL PREDICTED

5. POR = POR ($\sigma_{\beta q}$) ~ FIG. 24

3. APPROXIMATE AVERAGE (REF. 17)

6. POR FROM EQUATION 21 OF REF. 18 :

$$POR = 5.8 \sigma_{\theta} + .43 \sigma_q + .43 T_L + 1.0$$

TABLE 5 - PAPER PILOT PARAMETERS FOR THE ONSTOTT DATA (AFTER JOHNSON [20])

case	Paper Pilot Values				Onstott Experiment
	K_p	T_L	σ_z	M_{be}	$\sigma_{\theta z} = K_p T_L \frac{g}{154} \frac{M_{be}}{154}$
25	- 2.92	.3	.65	- 8.19	.22
26	- 3.91	1.0	1.14	- 8.19	2.51
					POR
					4.2
					6.15

TABLE 6 - KLEINMAN-DILLOW MODEL PARAMETERS FOR THE
ARNOLD/NEAL-SMITH CONFIGURATIONS

Case	K_{Fq}	K_q^*	σ_q	$M_{\delta e}$	$\sigma_{\rho q}$	${}^2_{POR}$	${}^3_{POR}$	${}^4_{POR}$
				-14.54				
9	.916	3.53	.319	↓	1.03	4.5	5.5	2.2
10	.918	3.83	.083		.292	3.3	4.0	1.6
11	.919	3.46	.1255		.399	3.5	2.7	1.4

1. predicted from the K-D model
2. from figure 24 with $\sigma_{\rho q}$ -- predicted
3. from flight test (reference [19]) -- average
4. from fixed-base simulator (reference [18]) --average
- 5.

$$\sigma_{\rho q} = K_{Fq} K_q^* \sigma_q \frac{M_{\delta e}}{14.54} \sim \text{deg}$$

TABLE 7 - PERFORMANCE COMPARISONS: MEASURED VS KLEINMAN-DILLOW
MODEL PREDICTIONS (MILLER-VINJE [23])

Case	Miller-Vinje Experiment				Kleinman-Dillow Prediction			
	σ_u	σ_t	σ_θ	σ_x	σ_u	σ_t	σ_θ	σ_x
PH1	.351	1.40	.730	.575	.371	1.399	.732	.588
PH2	.570	1.84	1.19	.950	.682	2.11	1.343	1.082
3	.836	2.6	1.80	1.24	.971	2.754	1.962	1.544
4	1.285	3.46	2.85	2.16	1.453	3.77	3.09	2.32
5	1.635	3.80	3.56	3.235	1.827	4.52	4.10	2.92
6	.781	1.98	1.63	1.28	.643	1.466	1.400	1.038
7	.824	2.25	1.72	1.37	.861	2.22	1.744	1.381
9	.837	3.05	1.92	1.35	1.088	3.26	2.19	1.722
10	.894	3.48	2.03	1.34	1.290	3.88	2.53	2.05
12	.784	2.43	1.75	1.21	.872	2.36	1.784	1.390
13	.524	1.40	1.08	.97	.532	1.490	1.056	.852
16	1.22	4.39	2.76	1.805	1.440	4.08	2.92	2.29
17	.879	3.82	2.00	1.18	1.264	4.30	2.47	1.986
18	1.606	5.52	3.65	2.455	1.961	5.70	3.97	3.11
19	.725	3.22	1.64	1.04	.974	3.30	1.917	1.533
20	1.475	4.81	3.31	2.415	1.670	4.73	3.48	2.65
21	.733	3.01	1.56	1.095	.859	2.92	1.700	1.355
22	1.44	4.72	3.30	2.37	1.566	4.41	3.31	2.49
28	.506	1.36	.93	.840	.540	1.655	1.088	.860
29	.972	2.38	1.86	1.42	1.044	2.97	2.09	1.662
30	.734	2.05	1.54	1.17	.876	2.47	1.813	1.392
31	.792	1.86	1.52	1.40	1.055	2.87	2.07	1.692
32	1.29	4.42	2.62	1.88	1.87	6.25	3.65	2.94
34	1.06	3.18	2.17	1.51	1.25	3.97	2.45	1.97
35	1.29	2.74	2.45	1.97	1.44	3.75	2.85	2.31
36	.900	2.26	1.94	1.51	1.02	2.63	2.21	1.65

TABLE 8 - CONVERSION OF MILLER-VINJE POR TO THE COOPER-HARPER SCALE

Conversion equations :	<u>Cooper (C)</u>	<u>Cooper-Harper (C-H)</u>
	$0 \leq C \leq 3.5$	C
	$3.5 < C \leq 5.5$	$3.5 + 1.5 (C - 3.5)$
	$5.5 < C \leq 7.6$	$6.5 + 1.67 (C - 5.5)$

<u>Case</u>	<u>Cooper POR</u>	<u>Cooper - Harper POR</u>
PH 1	2.5	2.5
PH 2	2.75	2.75
PH 3	3.12	3.12
PH 4	4.0	4.25
PH 5	4.75	5.38
PH 6	3.37	3.37
PH 7	4.25	3.0
PH 9	3.75	3.88
PH 10	4.25	4.63
PH 12	3.12	3.12
PH 13	2.50	2.50
PH 16	4.75	5.38
PH 17	4.36	4.79
PH 18	5.0	5.75
PH 19	3.62	3.68
PH 20	4.25	4.63
PH 21	3.62	3.68
PH 22	4.12	4.43
PH 28	2.0	2.0
PH 29	4.0	4.25
PH 30	3.5	3.5
PH 31	3.5	3.5
PH 32	6.5	8.17
PH 34	5.0	5.75
PH 35	5.0	5.75
PH 36	3.5	3.5

TABLE 9
KLEINMAN-DILLOW MODEL PARAMETERS FOR THE VINJE-MILLER DATA

CASE	$-K_u^*$	K_{Fu}	$-K_x^*$	K_{Fx}	K_g^*	K_{Fg}	K_θ^*	$K_{F\theta}$	$M_{\delta e}$
PH 1	12.8	.949	5.98	.969	3.30	.866	8.55	.937	.285
2	8.2	.953	4.08	.976	3.22	.908	5.64	.958	.415
3	9.47	.947	5.00	.977	2.70	.929	6.68	.969	.371
4	6.53	.937	3.86	.978	2.06	.950	4.87	.979	.467
5	5.35	.930	3.54	.979	1.85	.961	4.22	.984	.511
6	11.8	.893	5.87	.972	3.09	.982	7.78	.981	.300
7	9.02	.931	4.61	.976	2.47	.954	6.19	.977	.360
9	6.57	.954	3.58	.978	1.94	.914	4.80	.964	.451
10	6.24	.959	3.33	.979	2.50	.916	4.58	.961	.369
12	8.53	.937	4.47	.976	1.88	.940	5.90	.974	.493
13	8.44	.937	4.47	.973	2.38	.929	5.93	.965	.396
16	6.71	.951	3.54	.979	1.91	.930	4.76	.970	.476
17	5.50	.964	2.89	.979	2.19	.895	4.08	.951	.416
18	4.23	.957	2.67	.980	1.97	.919	3.44	.966	.458
19	6.08	.958	3.16	.977	2.26	.888	3.10	.953	.369
20	5.03	.945	3.16	.979	2.19	.918	2.77	.973	.418
21	6.75	.953	3.54	.976	2.42	.882	2.53	.955	.343
22	5.04	.939	3.16	.978	2.10	.912	2.00	.975	.445
28	8.05	.933	4.08	.972	1.57	.890	3.03	.963	.585
29	9.26	.968	4.47	.978	2.44	.932	6.18	.969	.394
30	6.41	.945	4.08	.977	2.16	.924	5.12	.970	.433
31	8.00	.948	4.08	.978	3.07	.938	5.65	.968	.277
32	5.97	.966	2.77	.980	2.12	.902	4.02	.954	.444
34	7.18	.960	3.33	.978	1.83	.905	4.75	.957	.480
35	7.62	.943	3.78	.979	2.85	.949	5.27	.972	.305
36	6.04	.937	4.47	.977	3.18	.941	5.24	.975	.279

Table 10 - Kleinman-Dillow Model Predictions of Signal Cross-Correlations

case	$E[ux]$	$E[uq]$	$E[u\theta]$	$E[x\theta]$	$E[xq]$	$E[\theta q]$
PH1	0	.301	0	0	0	0
PH2	↓	.930	.0041	1.091	-.041	↓
3	↓	1.183	.081	2.47	-.081	↓
4	↓	3.93	.042	6.29	-.042	↓
5	↓	6.15	-.230	10.89	-.230	↓
6	↓	.721	.102	1.295	-.102	↓
7	↓	1.35	.095	2.04	-.095	↓
9	↓	2.34	.035	2.98	-.065	↓
10	↓	3.28	.022	3.97	-.022	↓
12	↓	1.43	.092	2.08	-.092	↓
13	↓	.536	.0175	.720	-.017	↓
16	↓	4.00	.193	5.48	-.193	↓
17	↓	3.37	.0037	3.31	-.0037	↓
18	↓	7.48	-.346	10.10	.346	↓
19	↓	2.00	.0366	2.07	-.0366	↓
20	↓	5.41	-.081	7.86	.0814	↓
21	↓	1.55	.0443	1.66	-.0443	↓
22	↓	4.76	-.0027	7.14	.0027	↓
28	↓	.578	.0434	.740	-.043	↓
29	↓	2.09	.170	2.79	-.170	↓
30	↓	1.48	-.0374	2.11	.037	↓
31	↓	2.07	.069	2.83	-.069	↓
32	↓	7.30	.221	7.32	-.221	↓
34	↓	3.16	.186	3.53	-.186	↓
35	↓	3.76	.234	5.47	-.234	↓
36	↓	1.91	-.248	3.19	.248	↓

note: units are ft, ft/sec, deg, deg/sec

Table II - Estimated Rate Control Activity Metrics for
Miller-Vinje Cases

Case	$\sigma_{\beta g}$	$\sigma_{\beta u}$	$\sigma_{\beta x}$	$\sigma_{\beta g} + \sigma_{\beta u}$	POR (C-H).
PHI	.079	.084	.146	.163	2.5
2	.106	.127	.226	.233	2.75
3	.169	.191	.307	.360	3.12
4	.217	.253	.456	.470	4.25
5	.237	.286	.522	.523	5.38
6	.124	.170	.253	.294	3.37
7	.131	.171	.281	.302	3.0
9	.179	.174	.345	.353	3.88
10	.202	.136	.342	.338	4.63
12	.145	.212	.335	.357	3.12
13	.084	.113	.184	.197	2.50
16	.255	.255	.476	.510	5.38
17	.214	.133	.347	.347	4.79
18	.315	.205	.500	.520	5.75
19	.164	.106	.261	.270	3.68
20	.279	.202	.451	.481	4.63
21	.151	.111	.242	.262	3.68
22	.277	.209	.447	.486	4.43
28	.077	.153	.221	.230	2.0
29	.147	.231	.369	.378	4.25
30	.122	.132	.253	.254	3.5
31	.102	.114	.237	.216	3.5
32	.258	.227	.517	.488	8.17
34	.174	.241	.408	.415	5.75
35	.155	.194	.355	.349	5.75
36	.130	.098	.224	.228	3.5

1. degrees

$$2. \sigma_{\beta x}^2 = \sigma_{\beta g}^2 + \sigma_{\beta u}^2 + 2 K_g^* K_F K_u^* K_{Fu} \left(\frac{Mg}{14.54} \right)^2 E [ug]$$

TABLE 12 - AIRCRAFT STABILITY DERIVATIVE SET; CASE 1

$$\frac{1}{T_{\theta_2}} = 2.0 \quad CAP = 0.16 \quad \zeta_{sp} = 0.35$$

Conf	n/ α	ω_{sp}	U_0	$M_{\delta e}$	$Z_{\delta e}$	M_w	Z_w	M_q	$M_{\dot{\alpha}}$
1	1	0.400	16.1	-14.54	-16.	-0.02	-2.022	.080	1.662
2	5	0.894	80.5					.401	.995
3	10	1.265	161.					.801	.335
4	50	2.828	805.					4.006	-3.964
5	100	4.000	1610.					8.012	-8.79

$$\frac{1}{T_{\theta_2}} = 2.0 \quad CAP = 0.28 \quad \zeta_{sp} = 0.50$$

Conf	n/ α	ω_{sp}	U_0	$M_{\delta e}$	$Z_{\delta e}$	M_w	Z_w	M_q	$M_{\dot{\alpha}}$
6	1	0.529	16.1	-14.54	-16.	-0.02	-2.022	.021	1.472
7	5	1.183	80.5					.104	.735
8	10	1.673	161.					.208	.141
9	50	3.742	805.					1.309	-2.759
10	100	5.292	1610.					2.077	-5.347

TABLE 12 - CONTINUED

$\frac{1}{T_{\theta_2}} = 2.0 \quad CAP = 3.6 \quad \zeta_{sp} = 0.5$										
Conf	n/α	ω_{sp}	U_o	$M_{\delta e}$	$Z_{\delta e}$	M_w	Z_w	M_q	$M_{\dot{\alpha}}$	
11	1	1.897	16.1	-14.54	-16.	-.02	-2.022	-1.621	1.746	
12	5	4.243	80.5					-8.106	5.885	
13	10	6.0	161.					-16.212	12.234	
14	50	13.416	805.					-81.058	69.664	
15	100	18.974	1610.					-162.117	145.165	

$\frac{1}{T_{\theta_2}} = 0.2 \quad CAP = 3.6 \quad \zeta_{sp} = 0.35$										
Conf	n/α	ω_{sp}	U_o	$M_{\delta e}$	$Z_{\delta e}$	M_w	Z_w	M_q	$M_{\dot{\alpha}}$	
16	1	1.9	161.	-14.54	-16	-.02	-.222	-1.712	.604	
17	5	4.24	805				-.218	-8.716	5.96	
18	10	6.0	1610				-.266	-14.29	10.36	
19	50	13.42	8050				-.338	-56.2	47.15	
20	100	18.97	16100				-.888	-42.8	30.41	

TABLE 12 - CONCLUDED

$$\frac{1}{T_{\theta_2}} = 2.0 \quad \text{CAP} = 10.0 \quad \Sigma_{sp} = 0.35$$

Conf	n/ α	ω_{sp}	U_0	M_{se}	Z_{se}	M_w	Z_w	M_g	$M_{\dot{\alpha}}$
21	1	3.162	16.1	- 14.54	- 16.	- .02	- 2.022	- 4.786	4.594
22	5	7.071	80.5					-23.932	21.004
23	10	10.0	161					- 47.864	42.886
24	50	22.361	805					- 239.318	225.688
25	100	31.623	1610					- 478.635	458.521

TABLE 13 - AIRCRAFT STABILITY DERIVATIVE SET; CASE 2

$$\frac{1}{T_{\theta_2}} = 0.2 \quad \omega_{sp} = 0.5 \quad \zeta_{sp} = 0.35$$

Conf	n/ α	CAP	U _o	M δ_e	Z δ_e	M _w	Z _w	M _q	M $\dot{\alpha}$
26	1	.25	161	- 14.54	- 32.	-.01	-.222	6.13	- 6.258
27	5	.05	805		- 32	-.002	-.204	6.67	- 6.816
28	10	.025	1610		- 32	-.001	-.202	6.73	- 6.878
29	50	.005	8050		- 64	-.0005	-.202	18.69	- 18.84
30	100	.0025	16100		- 100	-.0005	-.203	38.42	- 38.57

$$\frac{1}{T_{\theta_2}} = 0.2 \quad \omega_{sp} = 3.0 \quad \zeta_{sp} = 0.35$$

Conf	n/ α	CAP	U _o	M δ_e	Z δ_e	M _w	Z _w	M _q	M $\dot{\alpha}$
31	1	9.	161	- 14.54	- 16.	-.01	-.211	-35.02	33.13
32	5	1.8	805			-.01	-.211	- 4.50	2.61
33	10	.9	1610			-.002	-.202	- 28.61	26.72
34	50	.18	8050			-.002	-.202	35.15	-37.05
35	100	.09	16100			-.001	-.269	26.39	-28.22

TABLE 14 - AIRCRAFT STABILITY DERIVATIVE SET; CASE 3

$$n\alpha = 2. \quad \omega_{sp} = 2. \quad \zeta_{sp} = 0.35$$

Conf	$\frac{1}{T_{\theta z}}$	U_0	$M_{\delta e}$	$Z_{\delta e}$	M_w	Z_w	M_q	$M_{\dot{\alpha}}$
36	.05	1288	-14.54	-200	-.06	-.875	83.75	-84.27
37	.10	644		-100	-.01	-.169	14.44	-15.67
38	.20	322		-20		-.214	-3.64	2.45
39	.50	128.8		-20		-.514	-5.28	4.39
40	2.0	32.2		-10		-2.007	-1.88	2.44

$$n\alpha = 50 \quad \omega_{sp} = 5. \quad \zeta_{sp} = 0.35$$

Conf	$\frac{1}{T_{\theta z}}$	U_0	$M_{\delta e}$	$Z_{\delta e}$	M_w	Z_w	M_q	$M_{\dot{\alpha}}$
41	.05	32200	-14.54	-500	-.10	-3.49	915.5	-915.5
42	.10	16100				-3.54	447.7	-447.7
43	.20	8050				-3.64	214.3	-214.2
44	.50	3220				-3.94	75.4	-75.0
45	2.0	805				-5.44	10.2	-8.26

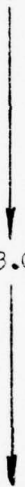

TABLE 15 - KLEINMAN-DILLOW MODEL PARAMETERS & PREDICTED POR;
CASE 1, $\sigma_{wg} = 10$ f/s

Conf	$ K_q^* $	K_{Fq}	σ_q	σ_{Pq}	POR ¹	n/ α	CAP	$\frac{1}{T_{02}}$	ξ_{SP}
1	3.43	.858	1.82	5.35	7.1	1	.16	2.0	.35
2	3.25	.855	1.45	4.06	6.7	5			
3	3.38	.847	1.33	3.80	6.6	10			
4	3.25	.829	1.45	3.90	6.7	50			
5	3.37	.807	1.74	4.73	6.9	100			
6	1.80	.851	1.33	2.03	5.6	1	.28		.5
7	2.54	.842	.91	1.95	5.5	5			
8	6.17	.901	1.55	8.61	7.9	10			
9	.849	.815	1.22	.84	4.2	50			
10	.353	.783	1.55	.43	3.5	100			
11	1.38	.836	.83	.96	4.4	1	3.6		
12	.660	.794	1.31	.68	4.0	5			
13	.168	.743	1.55	.19	3.1	10			
14	.045	.609	2.61	.07	2.6	50			
15	no convergence					100			
16	3.46	.836	.82	3.38	6.4	1		0.2	.35
17	3.42	.800	1.95	5.34	7.1	5			
18	3.66	.766	2.49	6.97	7.6	10			
19	3.50	.627	3.78	8.28	7.9	50			
20	3.68	.559	4.47	9.21	8.1	100			
21	.81	.818	1.50	.99	4.5	1	10.	2.0	
22	.19	.742	2.50	.35	3.4	5			
23	.08	.678	2.96	.15	3.0	10			
24	no convergence					50			
25	.01	.451	5.58	.02	1.9	100			

1. from σ_{Pq} & figure 24

TABLE 16 - KLEINMAN-DILLOW MODEL PARAMETERS & PREDICTED POR;
CASE 2, $\sigma_{wg} = 10$ f/s

$$\xi_{SP} = 0.35 \quad \frac{1}{T_{O_2}} = 0.2$$

Conf	$ K_q^* $	K_{F_q}	σ_q	σ_{A_q}	POR ¹	n/α	ω_{SP}
26	3.77	.847	.098	.313	3.3	1	.5
27	3.52	.850	.096	.287	3.3	5	
28	3.29	.848	.098	.273	3.3	10	
29	3.29	.851	.096	.269	3.3	50	
30	3.30	.849	.098	.275	3.3	100	
31	2.75	.820	1.42	3.20	6.3	1	3.0
32	3.28	.821	1.42	3.82	6.6	5	
33	3.28	.821	1.42	3.82	6.6	10	
34	3.27	.821	1.42	3.81	6.6	50	
35	3.57	.822	1.41	4.14	6.7	100	

1 - from σ_{A_q} & figure 24

TABLE 17 - KLEINMAN-DILLOW MODEL PARAMETERS & PREDICTED POR;
CASE 3, $\sigma_{wg} = 10 \text{ f/s}$

$$\xi_{sp} = 0.35$$

Conf	$ K_q^* $	K_{Fq}	σ_q	$\sigma_{\beta q}$	POR ¹	n/α	ω_{sp}	$\frac{1}{T_{\theta z}}$
36	38.3	.838	.838	26.8	9.8	2	2.0	.05
37	4.02	.901	.901	3.02	6.2	2	↓	.10
38	3.56	.831	.836	2.62	6.0	2		.20
39	3.58	.834	.834	2.49	5.9	2		.50
40	3.40	.837	1.28	3.64	6.5	2		2.0
41	176.	.790	2.27	315.6	10.	50	5.0	.05
42	95.6	.790	2.26	170.7	10.	50	↓	.10
43	51.5	.790	2.29	93.2	10.	50		.20
44	20.1	.790	2.40	38.1	10.	50		.50
45	7.63	.790	3.23	19.5	9.3	50		2.0

1 - from $\sigma_{\beta q}$ & figure 24

TABLE 18 - KLEINMAN-DILLOW MODEL PARAMETERS & PREDICTED POR;
CASE 1, $\sigma_{w_3} = 16$ f/s

Conf	$ K_q^* $	K_{Fq}	σ_q	σ_{Pq}	POR ¹	n/ α	CAP	$\frac{1}{T_{02}}$	ξ_{sr}
1	3.43	.859	2.88	8.49	7.9	1	0.16	2.0	0.35
2	3.25	.855	2.33	6.47	7.5	5	↓	↓	↓
3	3.33	.848	2.13	6.01	6.9	10	↓	↓	↓
4	3.25	.828	2.32	6.24	7.4	50	↓	↓	↓
5	3.37	.809	2.79	7.61	7.7	100	↓	↓	↓
16	3.46	.835	1.32	3.81	6.6	1	3.6	0.2	↓
17	3.42	.800	3.12	8.54	7.	5	↓	↓	↓
18	3.66	.766	3.	11.2	8.3	10	↓	↓	↓
19	3.50	.627	6.05	13.3	8.6	50	↓	↓	↓
20	3.68	.559	7.15	14.7	8.8	100	↓	↓	↓

1--from σ_{Pq} and figure 24

TABLE 19 - KLEINMAN-DILLOW MODEL PARAMETERS & PREDICTED POR;
CASE 2, $\sigma_{w3} = 16$ f/s

$$\zeta_{sp} = 0.35 \quad \frac{1}{T_{\theta z}} = 0.2$$

Conf	$ K_q^* $	K_{Fq}	σ_q	$\sigma_{\rho q}$	POR ¹	n/α	ω_{sp}
26	3.77	.847	.157	.501	3.7	1	0.5
27	3.52	.850	.153	.458	3.6	5	
28	3.29	.849	.156	.436	3.5	10	
29	3.29	.854	.151	.424	3.5	50	
30	3.30	.855	.152	.429	3.5	100	
31	2.75	.821	2.27	5.12	7.1	1	3.0
32	3.28	.822	2.27	6.12	7.4	5	
33	3.28	.821	2.28	6.14	7.4	10	
34	3.27	.822	2.28	6.13	7.4	50	
35	3.57	.822	2.25	6.60	7.5	100	

1 - From $\sigma_{\rho q}$ & figure 24

TABLE 20 - KLEINMAN-DILLOW MODEL PARAMETERS & PREDICTED POR;
CASE 3, $\sigma_{w_3} = 16$ f/s

$$S_{sr} = 0.35$$

Conf	$ K_q^* $	K_{Fq}	σ_i	σ_{p_2}	POR ¹	n/α	ω_{sr}	$\frac{1}{T\theta_s}$
36	38.3	.835	1.34	42.9	10.	2.	2.	.05
37	4.02	.832	1.44	4.82	7.	↓	↓	.10
38	3.56	.829	1.42	4.19	6.7	↓	↓	.20
39	3.58	.828	1.35	4.00	6.7	↓	↓	.50
40	3.40	.838	2.05	5.84	7.3	↓	↓	2.0
41	176	.790	3.62	503.	10.	50.	5.	.05
42	75.6	.790	3.62	273.	10.	↓	↓	.10
43	51.5	.790	3.66	149.	10.	↓	↓	.20
44	20.1	.791	3.84	61.	10.	↓	↓	.50
45	7.63	.791	5.17	31.2	10.	↓	↓	2.0

1 - from σ_{p_2} & figure 24

TABLE 21 - KLEINMAN-DILLOW MODEL PARAMETERS & PREDICTED POR;
CASE 1, $\sigma_{wg} = 5$ f/s

Conf	$ K_q^* $	K_{Fq}	σ_q	σ_{pq}	POR ¹	n/ α	CAP	$\frac{1}{T_{02}}$	k_{sp}
6	1.80	.852	.661	1.01	4.5	1	.28	2.0	.5
7	2.54	.843	.452	.97	4.4	5			
8	6.17	.901	.775	4.31	6.8	10			
9	.849	.815	.609	.42	3.5	50			
10	.353	.784	.773	.21	3.1	100			
11	1.38	.835	.416	.48	3.6	1	3.6		
12	.660	.794	.652	.34	3.4	5			
13	.168	.743	.775	.097	2.7	10			
14	.045	.609	1.304	.036	2.2	50			
15	no convergence					100			
21	.805	.818	.749	.49	3.7	1	10.		.35
22	.198	.742	1.252	.18	3.1	5			
23	.075	.678	1.478	.075	2.6	10			
24	no convergence					50			
25	.0084	.452	2.791	.011	1.6	100			

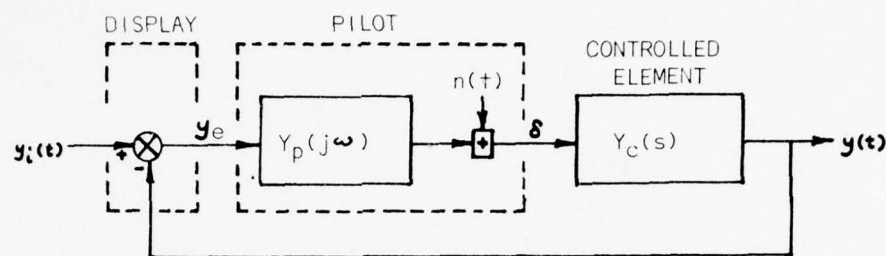
1 - from σ_{pq} & figure 24

TABLE 22 - PREDICTED VARIATION OF POR WITH ω_{sp} AT CONSTANT $\frac{1}{T_{0c}}$ & ζ_{sp} ;
 $\sigma_{wg} = 10 \text{ f/s}$

$\frac{1}{T_{0c}} = 0.2$ $\zeta_{sp} = 0.35$			$\frac{1}{T_{0c}} = 2.0$ $\zeta_{sp} = 0.35$			$\frac{1}{T_{0c}} = 2.0$ $\zeta_{sp} = 0.50$		
Conf	ω_{sp}	POR	Conf	ω_{sp}	POR	Conf	ω_{sp}	POR
26	.5	3.3	1	.4	7.1	6	.529	5.6
16	1.9	6.4	2	.894	6.7	7	1.183	5.5
38	2.0	6.0	3	1.265	6.6	8	1.673	7.9 ✓
31	3.0	6.3	40	2.0	6.5	11	1.897	4.4
17	4.24	7.1	4	2.828	6.7	9	3.742	4.2
43	5.0	10. ✓	21	3.162	4.5 ✓	12	4.243	4.0
18	6.0	7.6	5	4.0	6.9	10	5.292	3.5
19	13.42	7.9	45	5.0	9.3 ✓	13	6.0	3.1
20	18.97	8.1	22	7.071	3.4	14	13.416	2.6
			23	10.0	3.0			
			24	22.361	-			
			25	31.623	1.9			

TABLE 23 - EFFECTS OF M_α ON PREDICTED POR

Conf	M_α	POR
17	-16.1	7.1
43	-805.	10. ✓
18	-32.2	7.6
4	-16.1	6.7
21	-.3	4.5 ✓
5	-32.2	6.9
45	-80.	9.3 ✓
22	-1.62	3.4
7	-1.6	5.5
8	-3.2	7.9 ✓
11	-.32	4.4



$y_i(t)$ = random command input, low amplitude, low bandwidth.

$y_e(t)$ = displayed system error.

$\delta(t)$ = pilot's control output.

$y(t)$ = controlled element response.

$Y_c(s)$ = controlled element dynamics, transfer function representation.

$Y_p(j\omega)$ = portion of pilot's dynamic response that is linearly correlated with system input, describing function representation.

$n(t)$ = portion of pilot's response that is not linearly correlated with system input; the remnant.

$\delta(j\omega) = Y_p(j\omega)e(j\omega) + n(j\omega)$

$$Y_p(j\omega) = K_p K_T \left[\frac{a_T}{\sigma_T} \right] e^{-j\omega\tau} \left(\frac{T_L j\omega + 1}{T_I j\omega + 1} \right) \left(\frac{T_K j\omega + 1}{T_K' j\omega + 1} \right) \left\{ \frac{\left(\frac{j\omega}{\omega_{sp}} + 1 \right) e^{-j\omega\tau_{NM}}}{(T_{N1} j\omega + 1) \left[\left(\frac{j\omega}{\omega_N} \right)^2 + \frac{2\zeta_N}{\omega_N} j\omega + 1 \right]} \right\}$$

---- The "Precision Pilot Model"

Figure 1--- The Servo Model for Pilot Dynamics (The Precision Pilot Model)

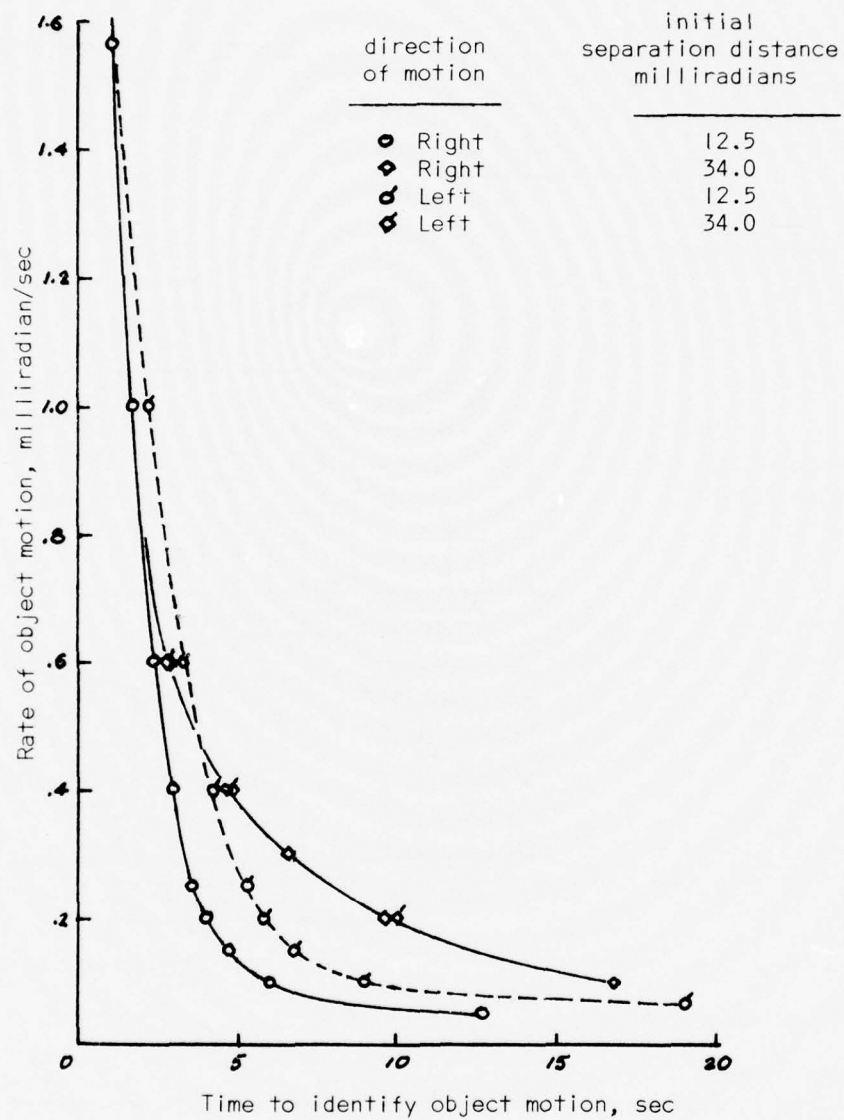
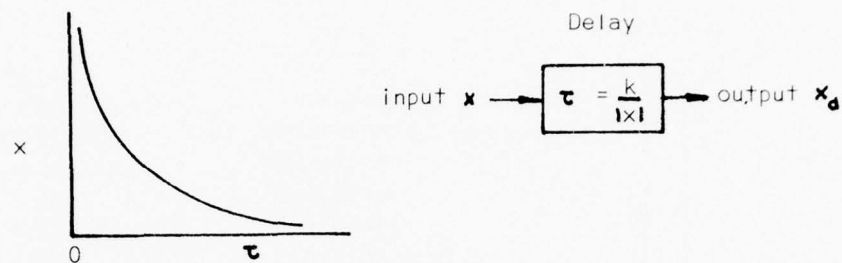
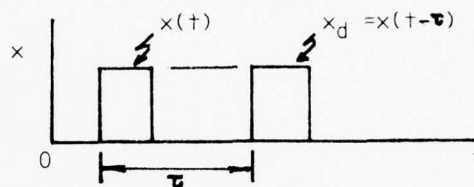


Figure 3--- Latency Time Delay for Visual Rate Detection vs. Rate of Object Motion (From Brissenden [8])

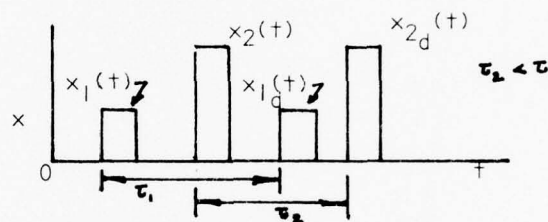


1. Pulse response:

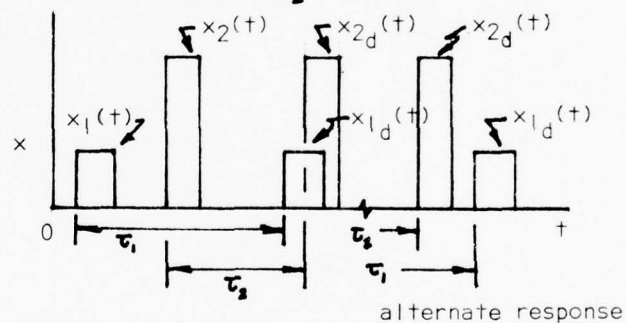


2. Response to pulse train:

a.



b.



3. Sinusoidal response:

$$x = A \sin \omega t$$

$$x_d = A \sin(\omega t + \phi)$$

$$\phi = \omega \tau$$

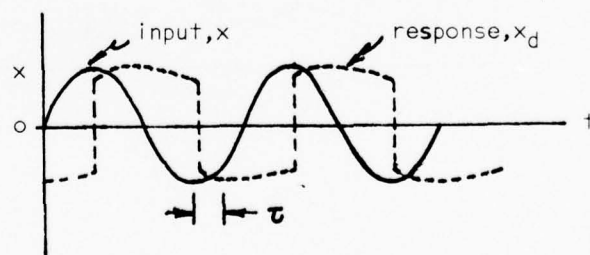
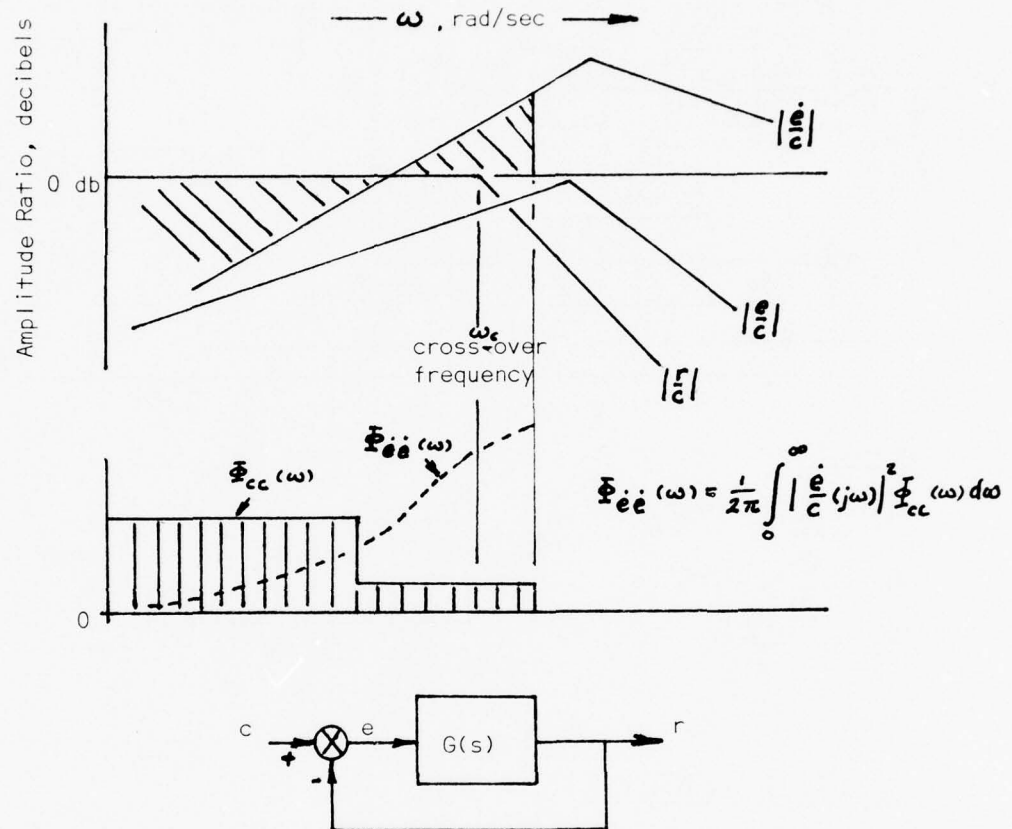


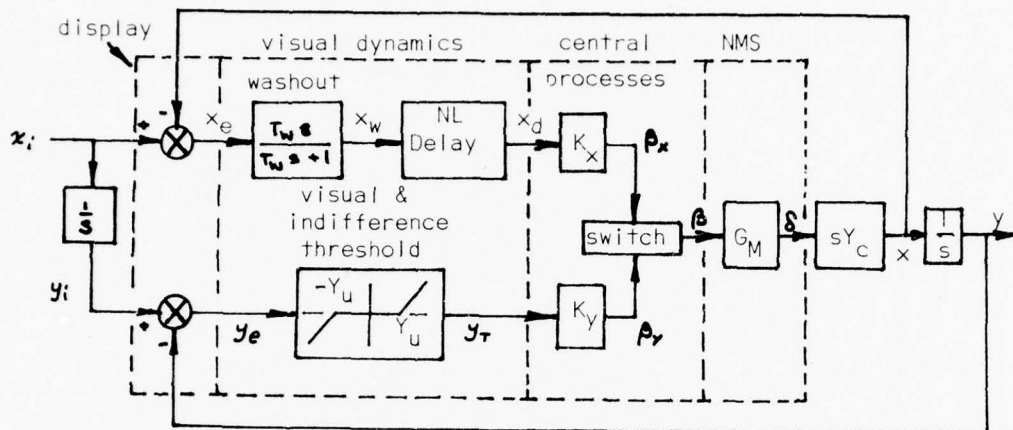
Figure 4--- Time Response Properties-- Nonlinear Delay



$$\frac{r}{c}(s) = \frac{G(s)}{1 + G(s)} \quad \frac{e}{c}(s) = \frac{1}{1 + G(s)} \quad \frac{\dot{e}}{c}(s) = \frac{s}{1 + G(s)}$$

Figure 5--- Generic Amplitude Properties of Closed Loop System Dynamics

Pilot-Vehicle System Model

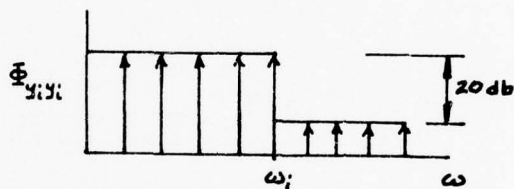


System Input

$$x_i(t) = \sum_{k=1}^{10} b_k \cos \omega_k t$$

$$y_i(t) = \sum_{k=1}^{10} a_k \sin \omega_k t$$

$$\sigma_{y_i}^2 = 1/2 \sum_{k=1}^{10} a_k^2$$



Switch

$$SF = P_I X_d^2 - Y_T^2$$

$$\beta = \begin{cases} \beta_x, & SF > 0 \\ \beta_y, & SF < 0 \end{cases}$$

Neuromuscular System Dynamics

$$G_M(s) = \frac{(\frac{s}{30} + 1) e^{-1.5}}{(\frac{s}{10} + 1) [(\frac{s}{15})^2 + \frac{2(.1)}{15} s + 1]}$$

Parameters Used for Study of Nonlinear Delay Dynamics

$$\tau = 0.16 / |x_w|, K_x = K_y = 0.3, P_I = 2.75, Y_U = 0.06, T_w = 3.33$$

Figure 6--- Model for Evaluation of Nonlinear Delay Dynamics

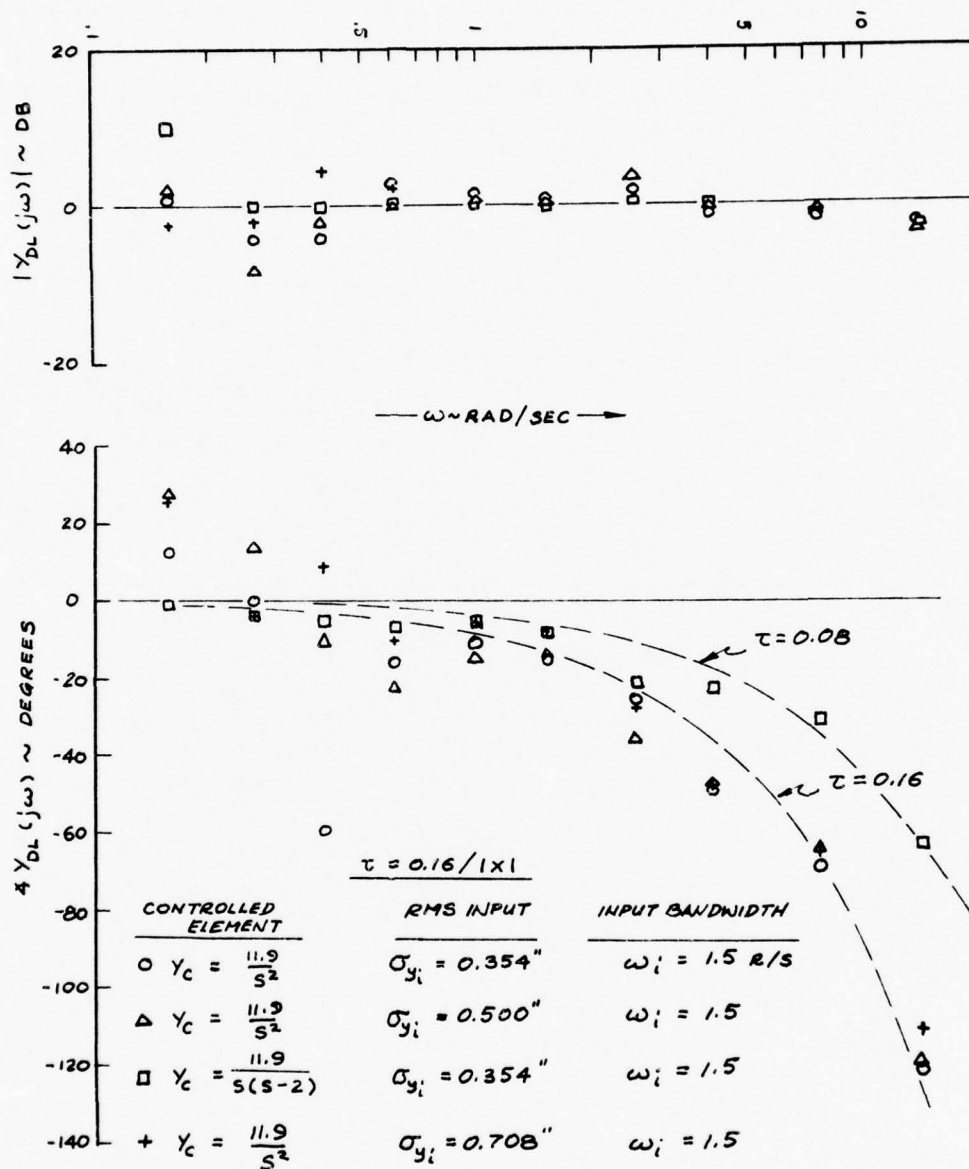


Figure 7 --- Measured Describing Functions for a Nonlinear Delay:
Effects of σ_{y_c} & $Y_c(s)$

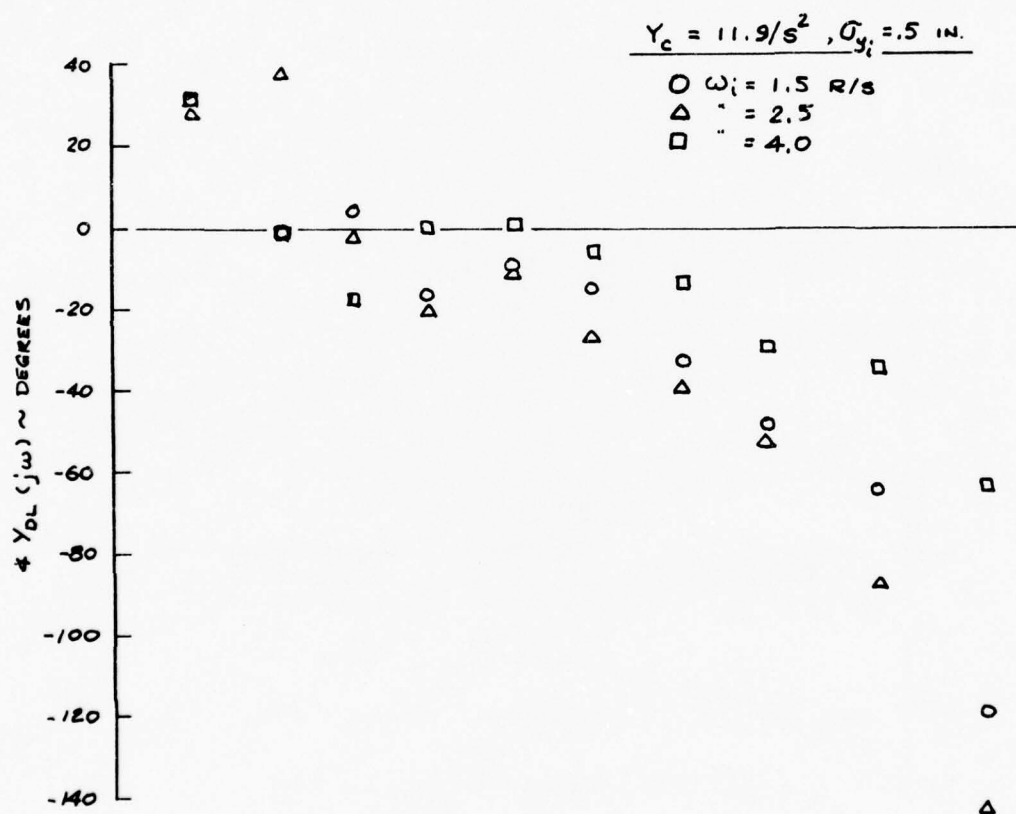
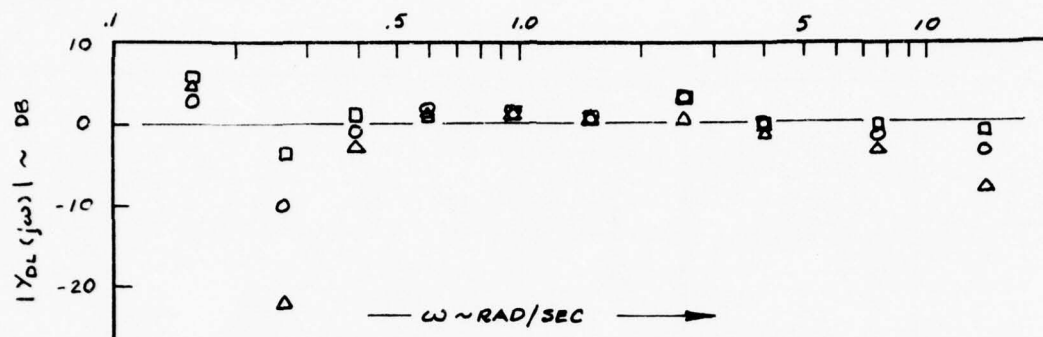
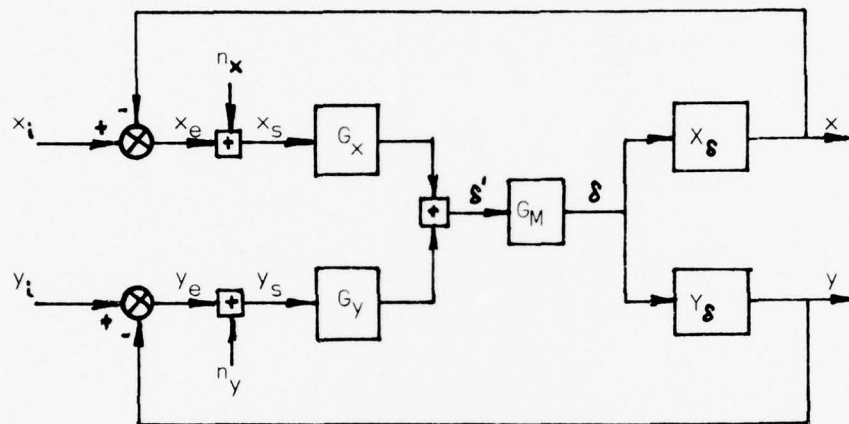


Figure 8--- Measured Describing Functions for a Nonlinear Delay:
Effect of Input Bandwidth



Linear elements: G_M , X_δ , Y_δ

Describing functions: G_x , G_y

Figure 10--- A Special Closed Loop System

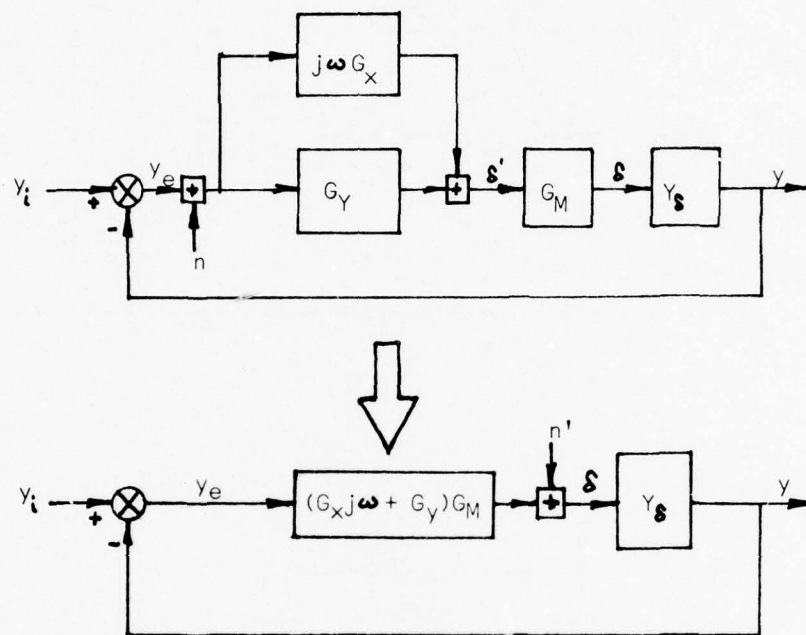
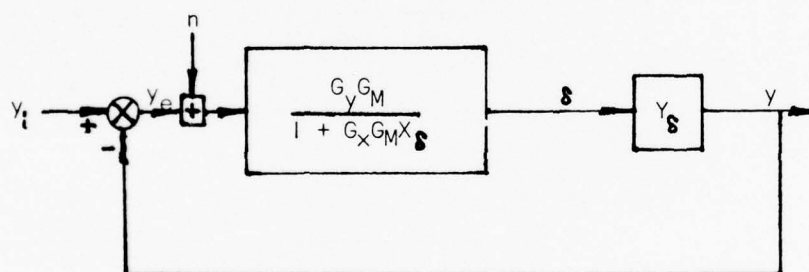
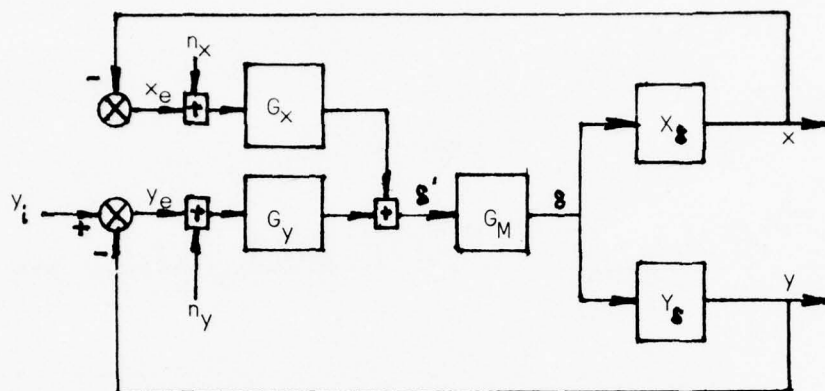


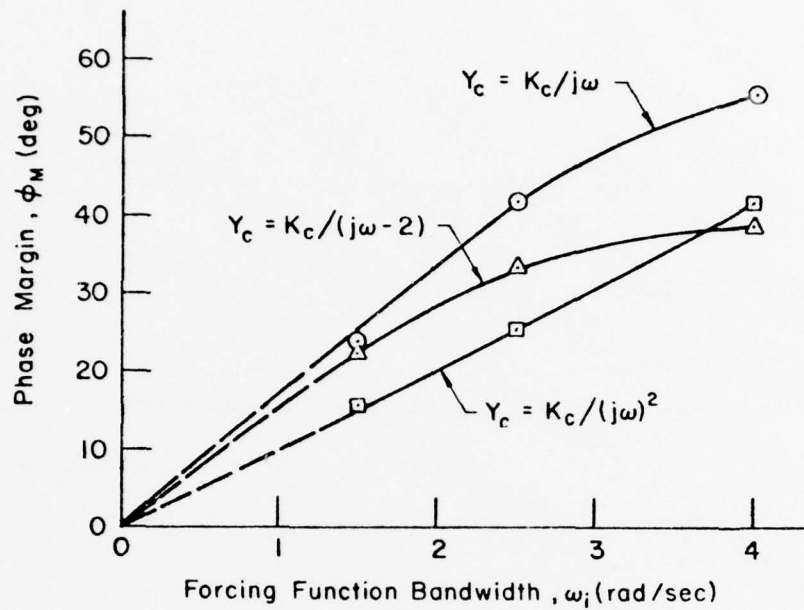
Figure 11--- Special Case #1; Block Diagram Reduction
 ($x_i = dy_i/dt$, $x = dy/dt$)



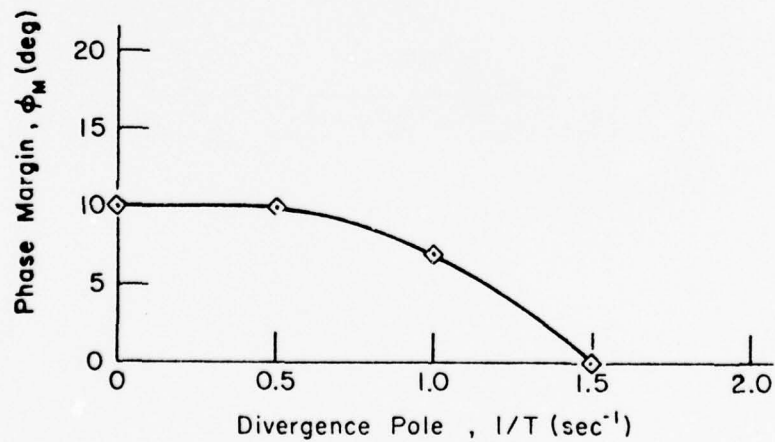
Describing Function;

$$\frac{\delta}{y_e}(j\omega) = \frac{\bar{\Phi}_{y_i} \delta}{\bar{\Phi}_{y_i} y_e} = \frac{G_y G_M}{1 + G_x G_M X_s}$$

Figure 12--- Special Case #2; Block Diagram Reduction
($x_i = 0$)



(a) Phase Margin Variation with Forcing Function Bandwidth for $Y_c = K_c/j\omega$, $K_c/(j\omega)^2$, and $K_c/(j\omega - 2)$



(b) Phase Margin Variation with $1/T$ for $Y_c = K_c/j\omega(j\omega - 1/T)$
 $\omega_1 = 1.5, 1/4''$

Figure 13--- Phase Margin Variations; From Reference 4

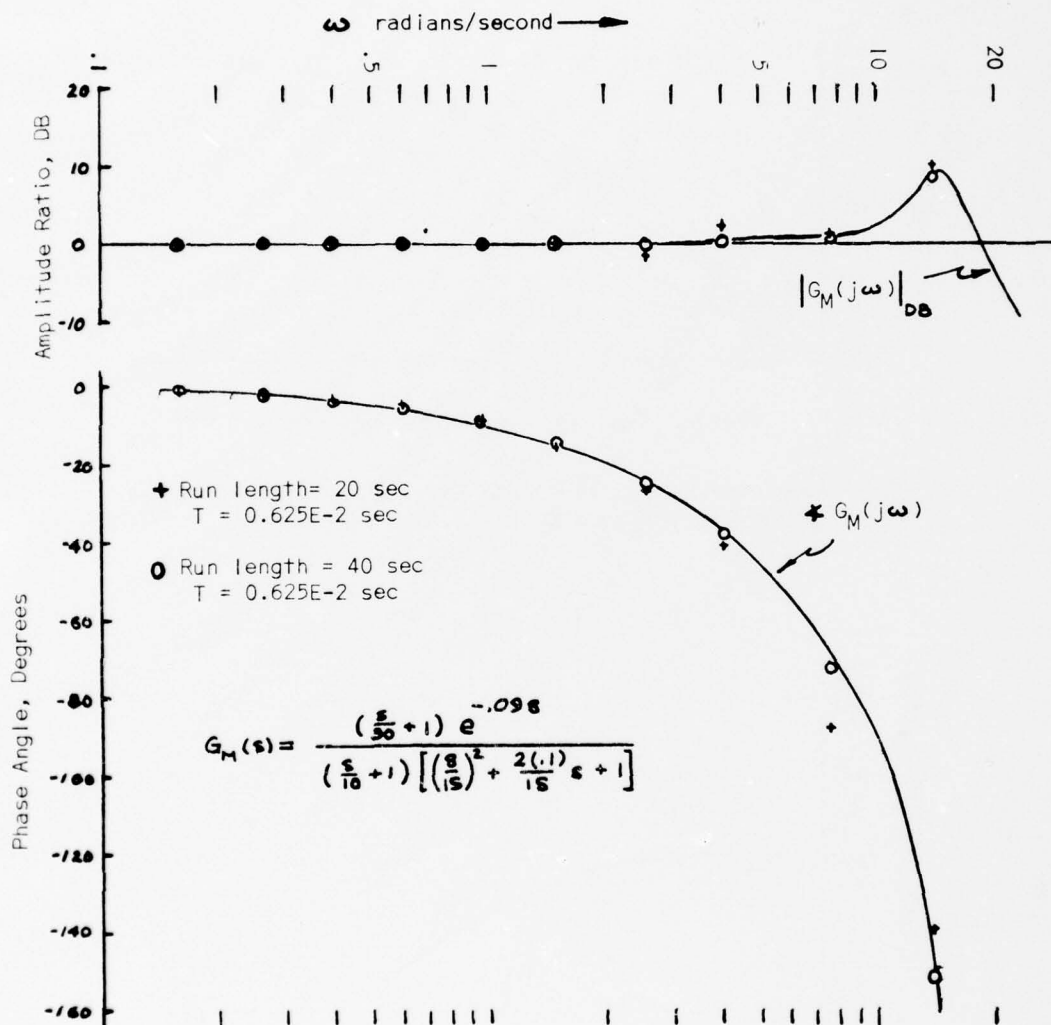


Figure 14--- Computer-Measured Neuromuscular System Dynamics

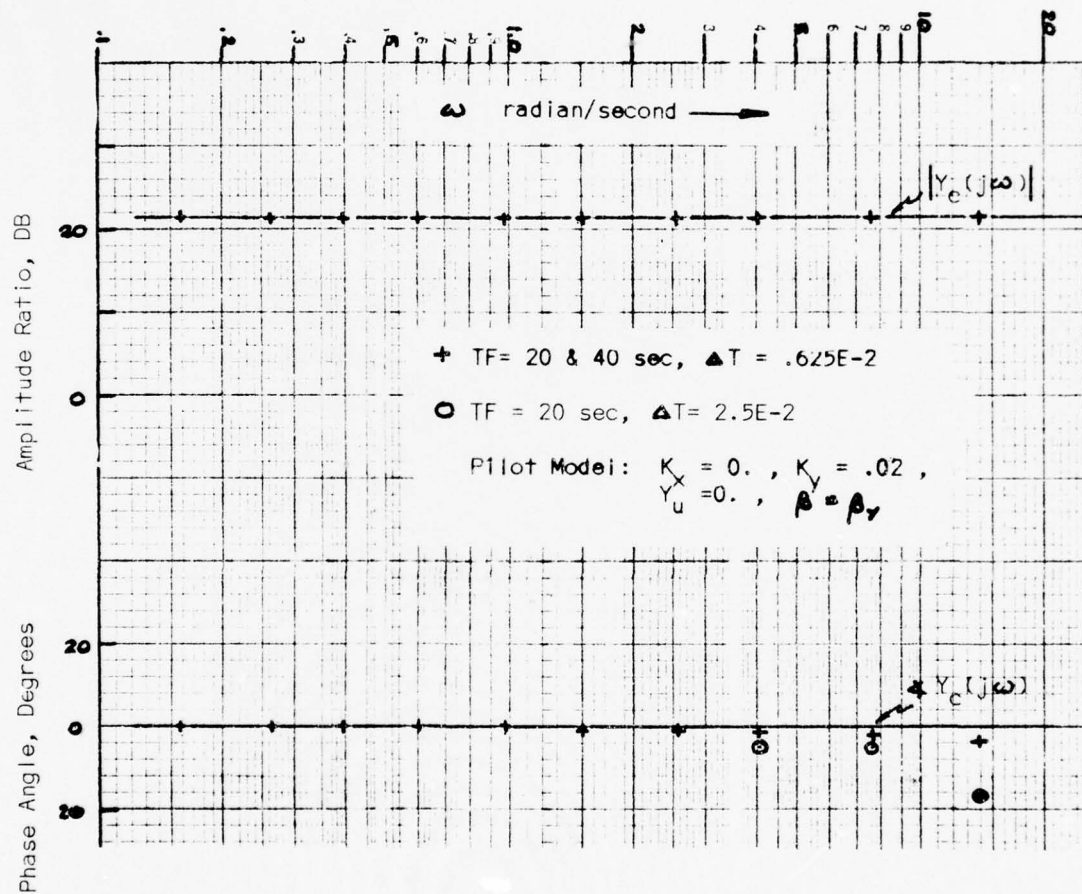


Figure 15--- Measured Controlled Element Dynamics, $Y_c = 11.9$

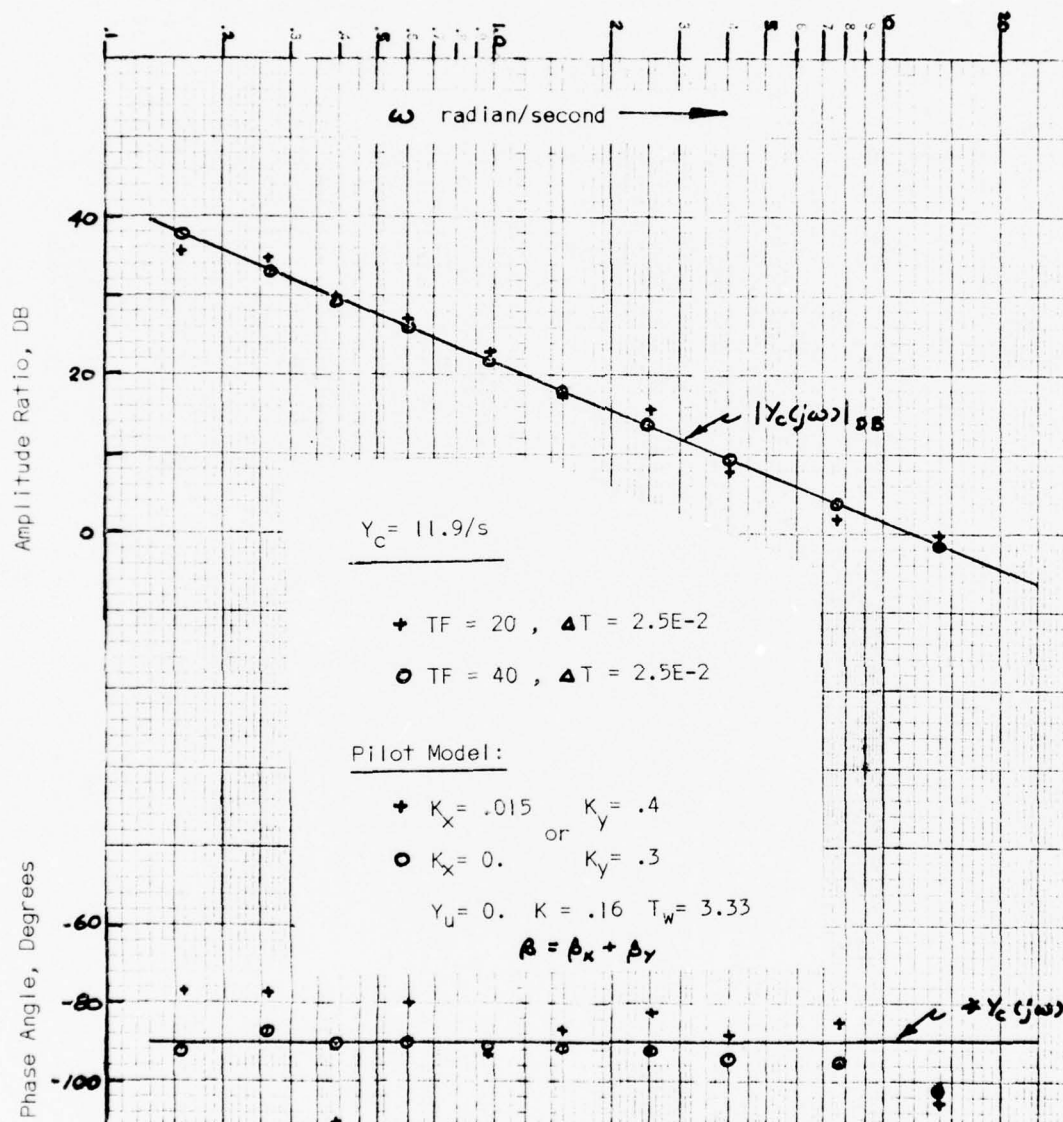


Figure 16--- Measured Controlled Element Dynamics, $Y_C(s) = 11.9/s$

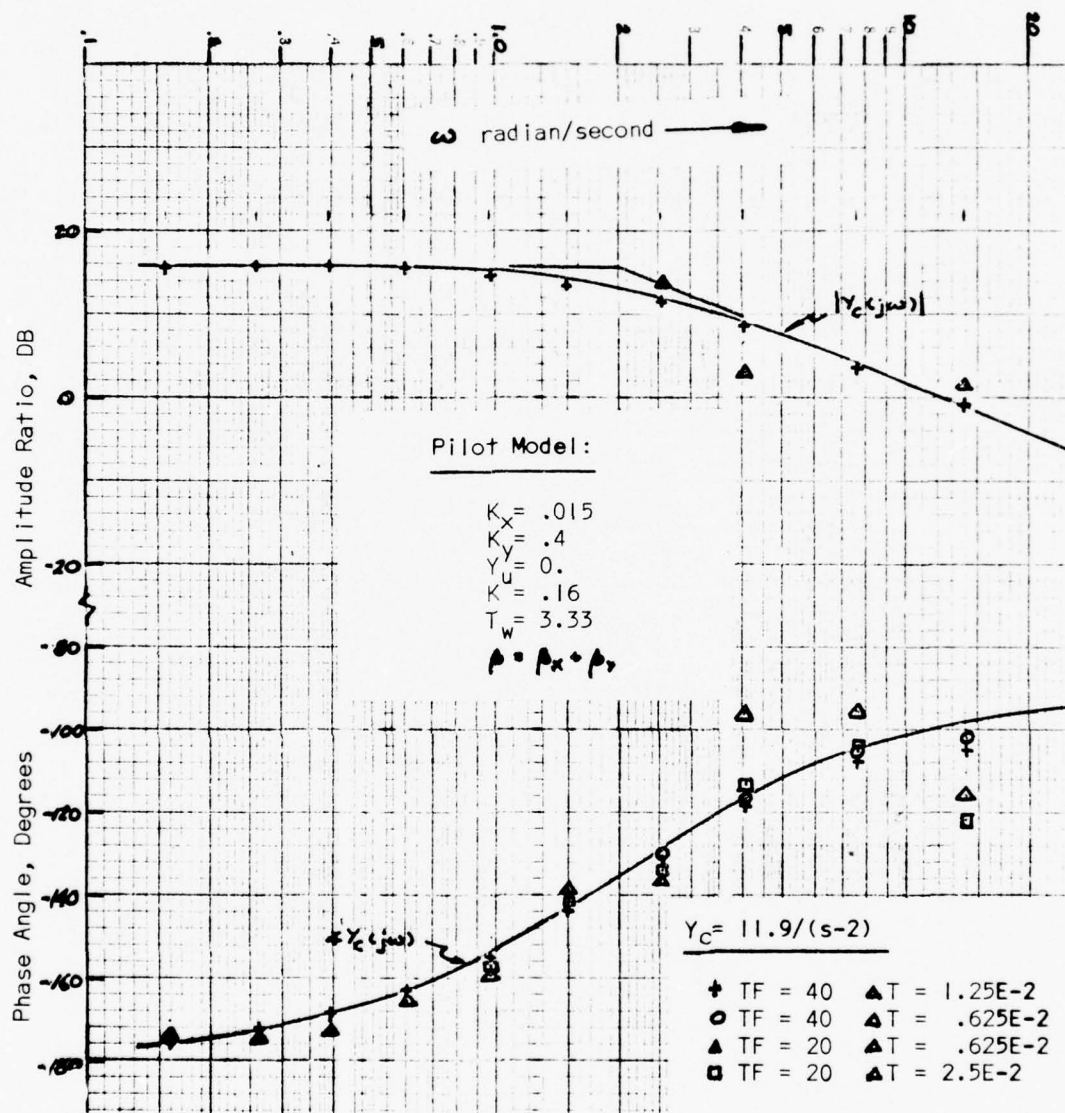


Figure 17--- Measured Controlled Element Dynamics, $Y_c(s)=11.9/(s-2)$

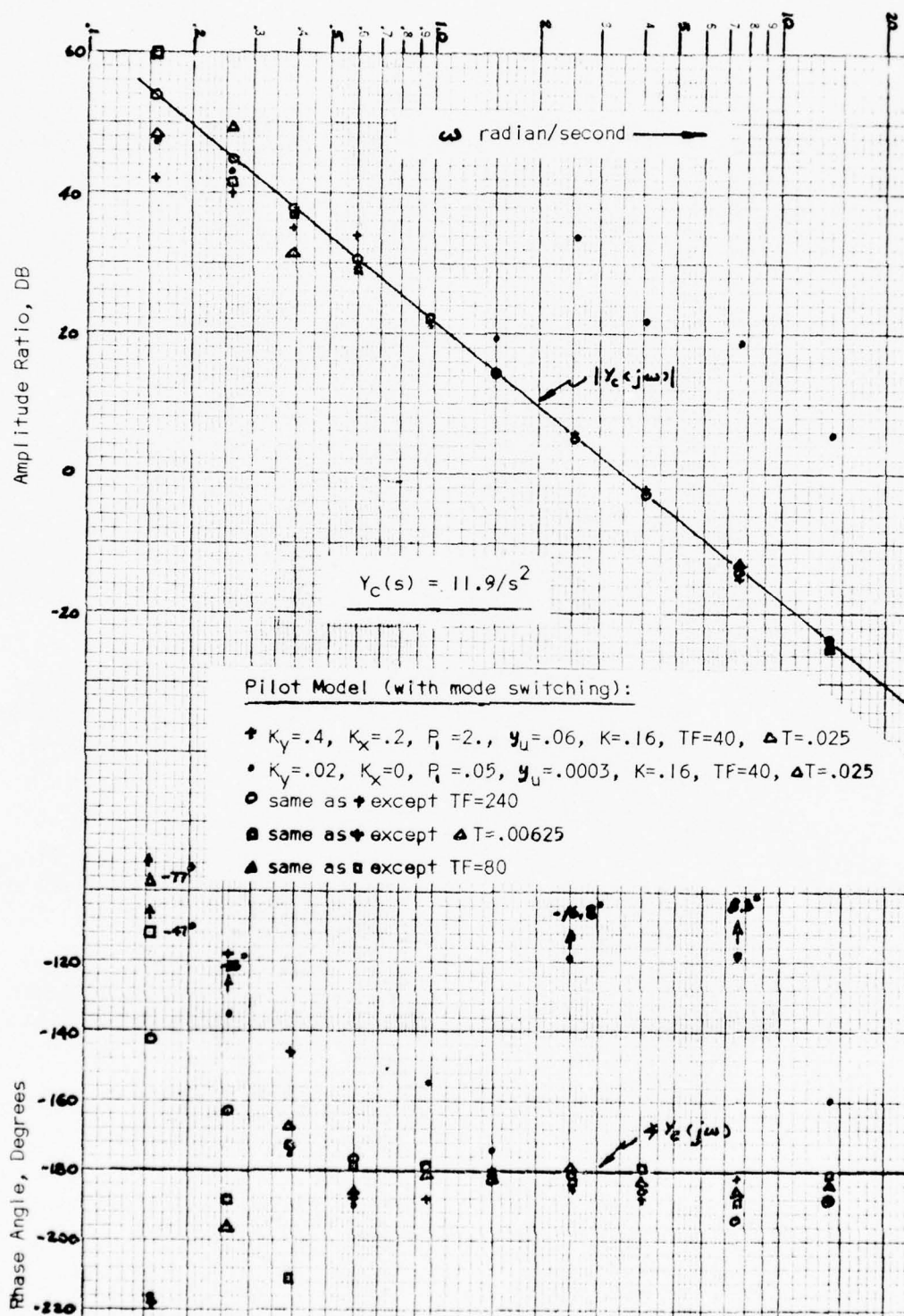


Figure 18--- Measured Controlled Element Dynamics, $Y_C(s)=11.9/s^2$

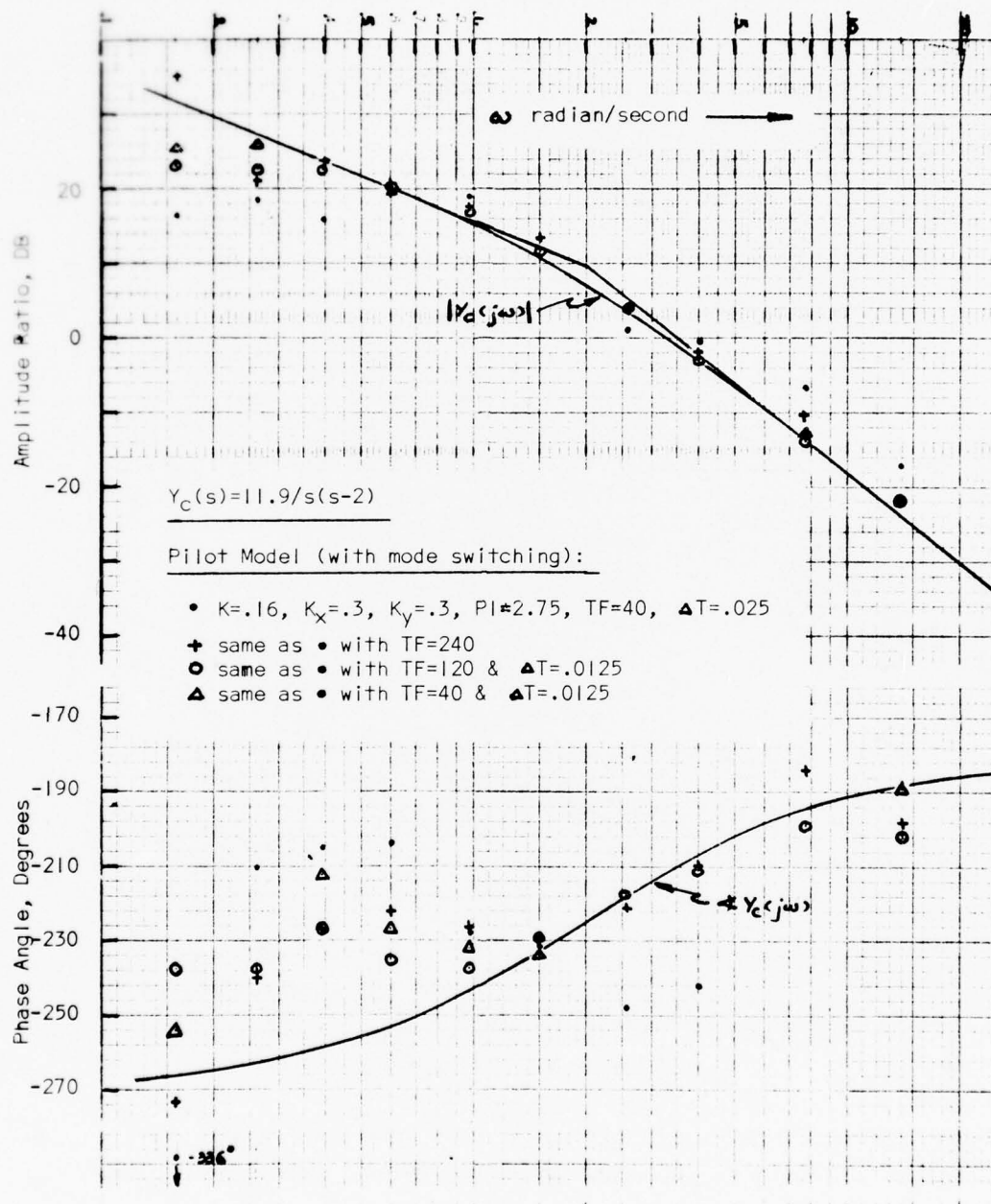


Figure 19--- Measured Controlled Element Dynamics, $Y_C(s) = 11.9/s(s-2)$

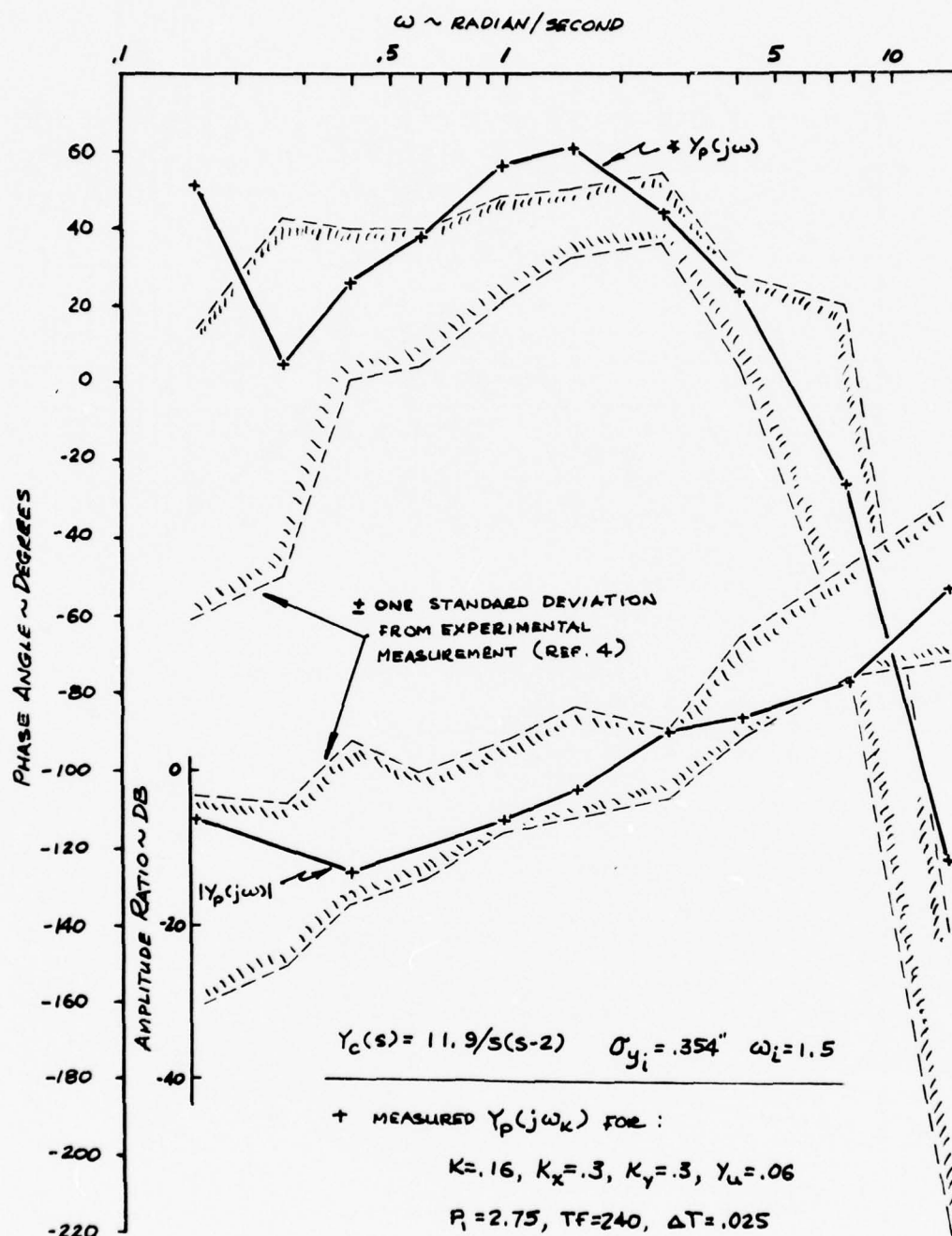


Figure 20--- Comparison of Measured and Experimental $Y_p(j\omega)$

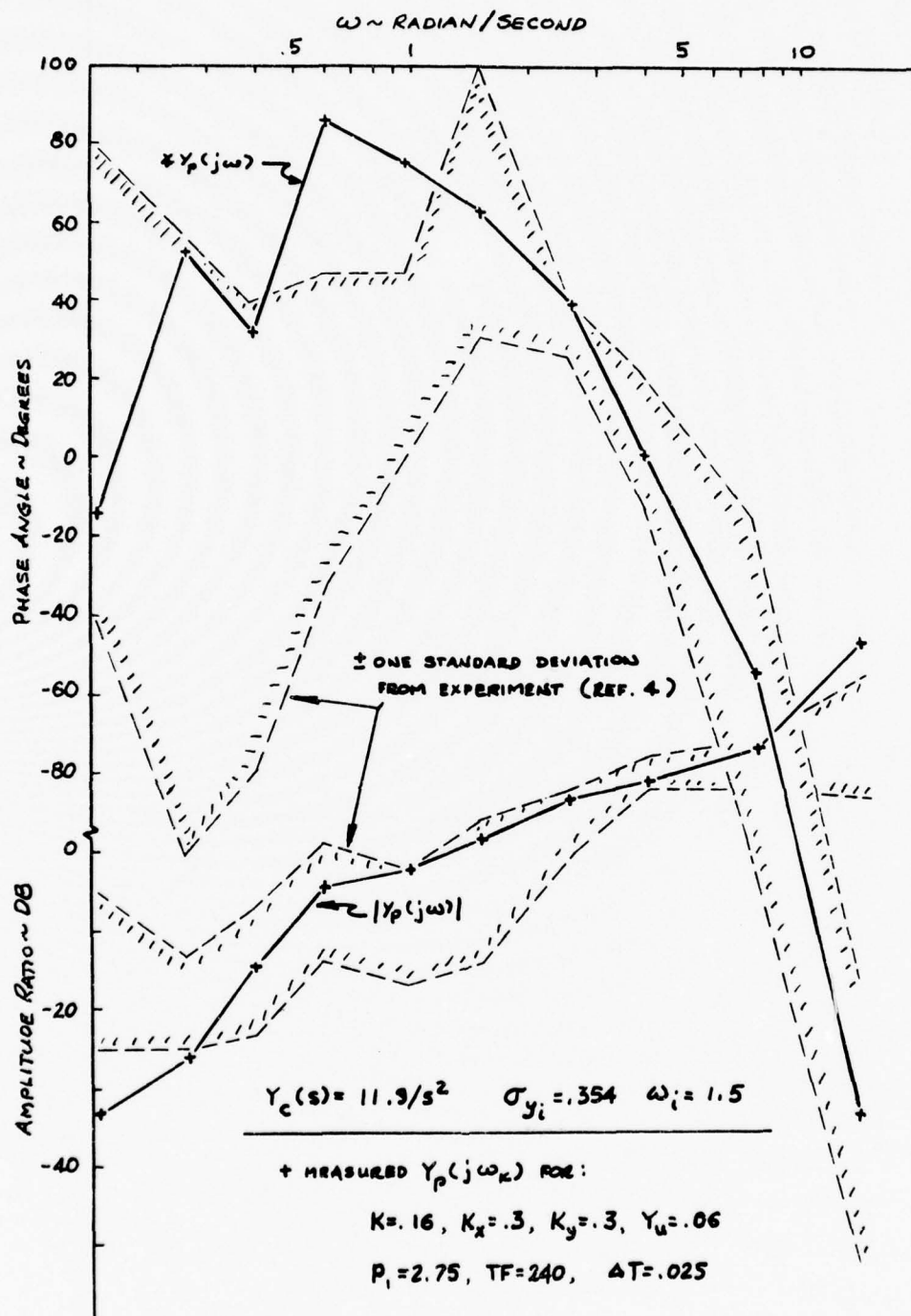


Figure 21--- Comparison of Measured and Experimental $Y_p(j\omega)$

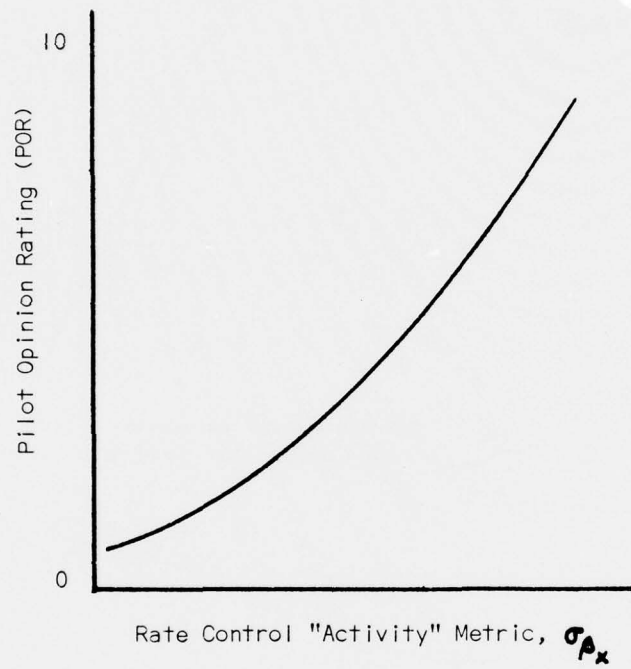
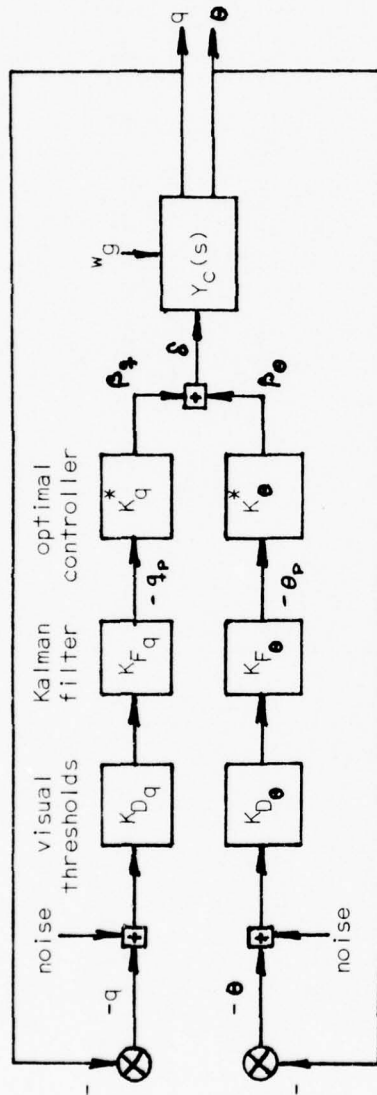


Figure 22--- Pilot Rating vs. σ_{ρ_x} -- Generic



$$q = d\theta/dt$$

K_{Dq} = visual rate threshold describing function

$K_{D\theta}$ = visual position threshold describing function

K_{Fq} & $K_{F\theta}$ are the equivalent Kalman Filter gains for the rate and position channels, respectively

K_q^* & K_θ^* are feedback gains which minimize the cost functional:

$$J = 70\sigma_{\theta_p}^2 + 7\sigma_{\dot{q}_p}^2 + R\sigma_\delta^2$$

R is selected to create a first order "neuromuscular" lag time constant of 0.1 seconds

and θ_p are \dot{q}_p as perceived by the human pilot

Figure 23--- Equivalent Kleinman-Dillow Model (Converged) for the Arnold Experiment

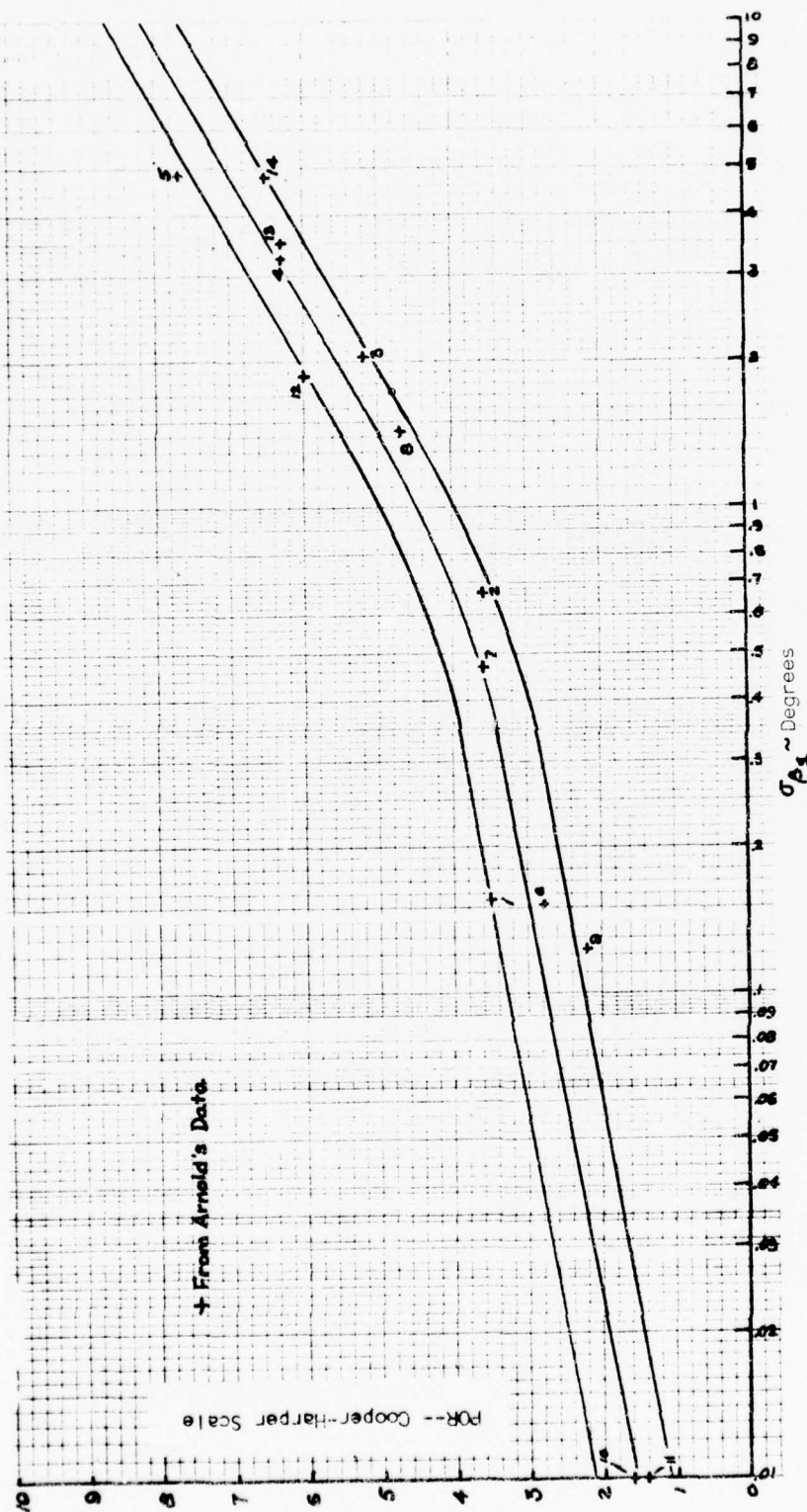


Figure 24--- Variation of Pilot Opinion Rating With Proposed Rating Metric

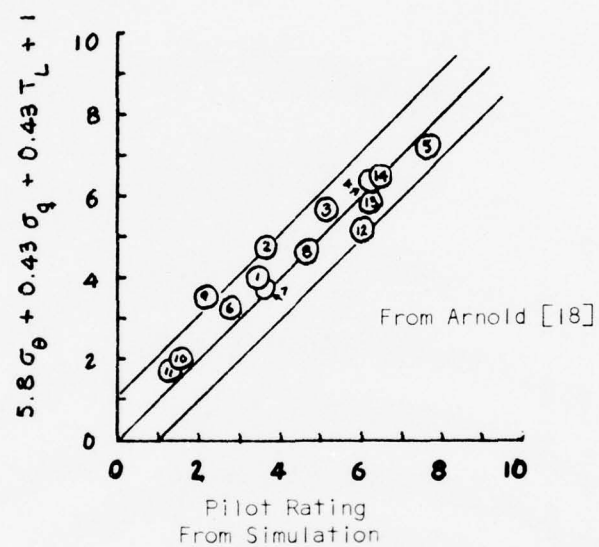


Figure 25--- Correlation of Pilot Opinion Rating With
Arnold's Rating Expression

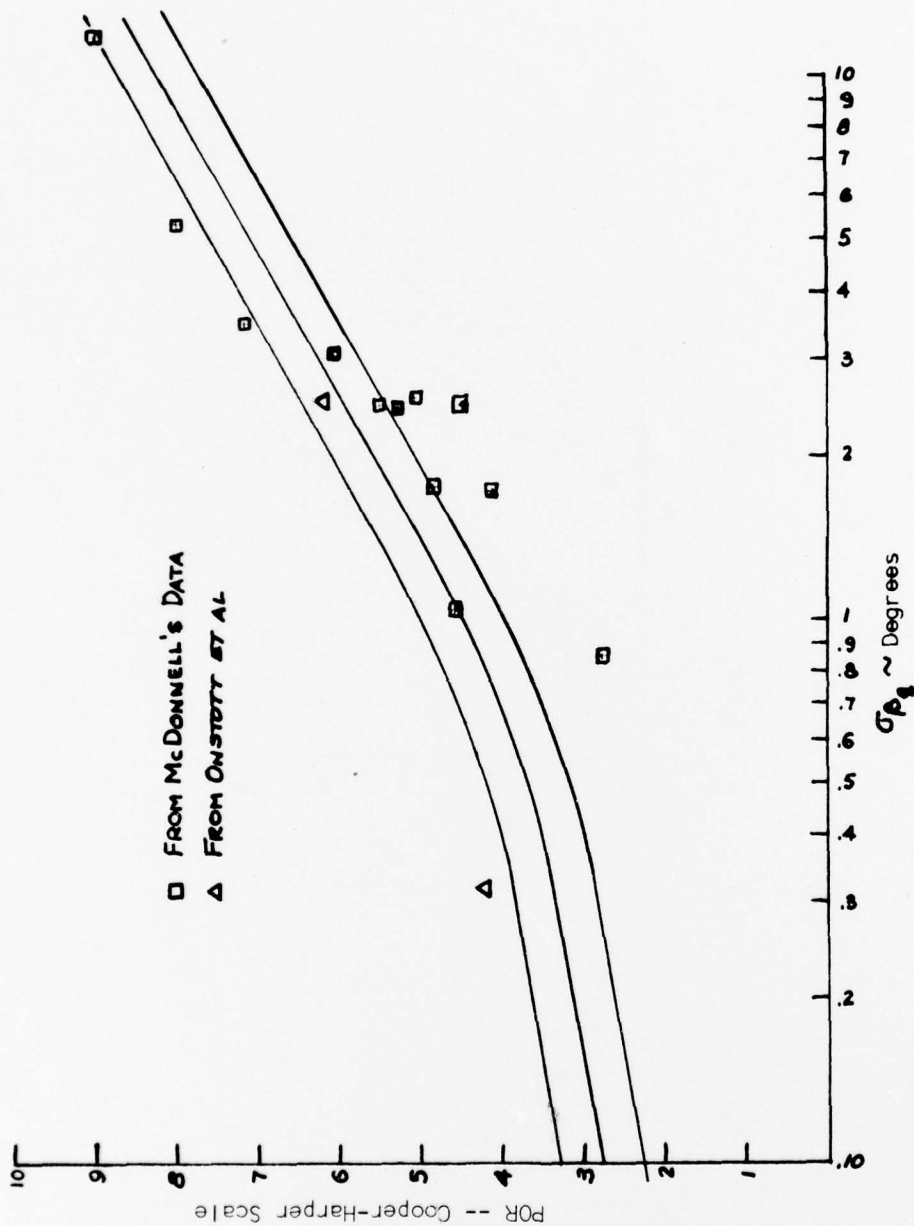


Figure 26-- Variation of McDonnell's and Onstott's, et al, Rating Data
With the Proposed Rating Metric

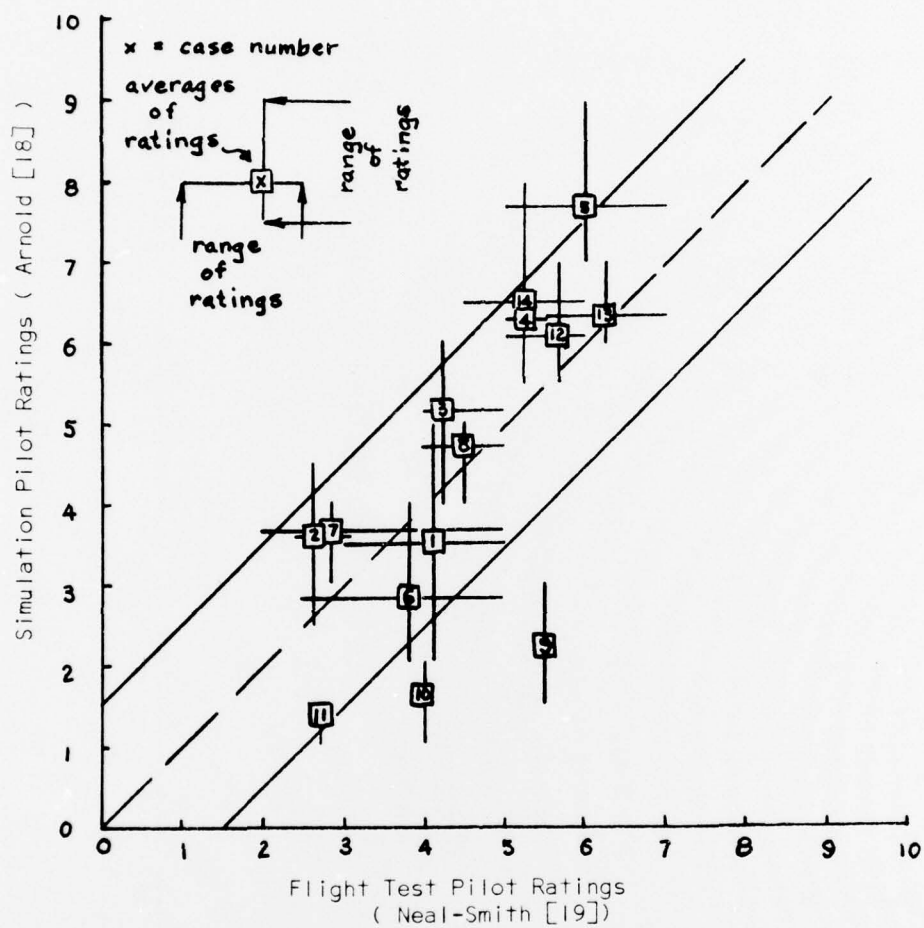


Figure 27--- Comparison of Simulator and Flight Test Pilot Ratings
 (Figure 4 of Reference [18])

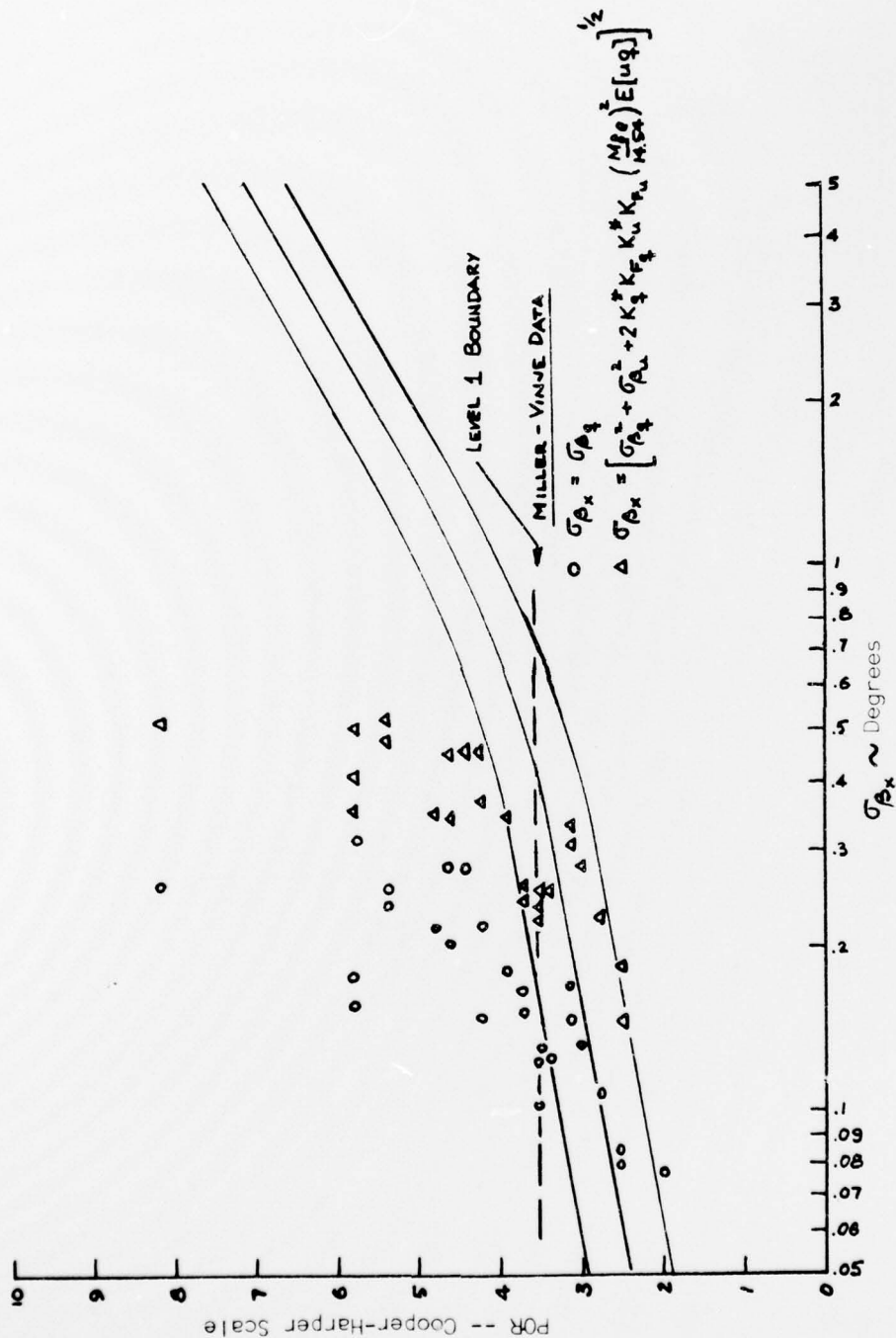


Figure 28--- Variations of Pilot Opinion Rating with σ_{β_x} & σ_{β_q} for Multiple Loop Tracking (Miller- Vinje Data)

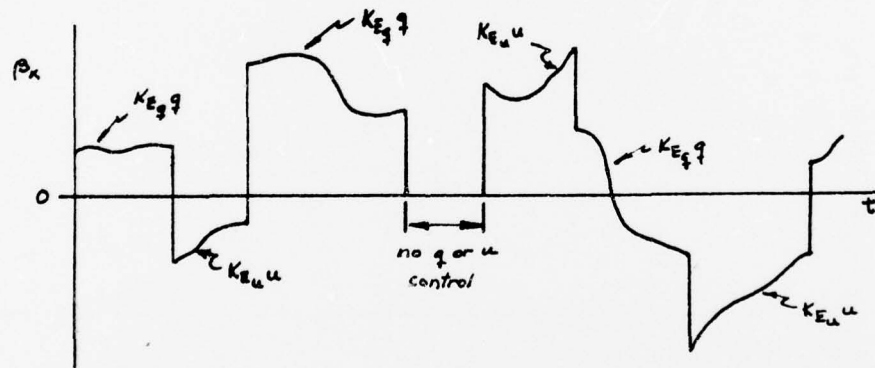
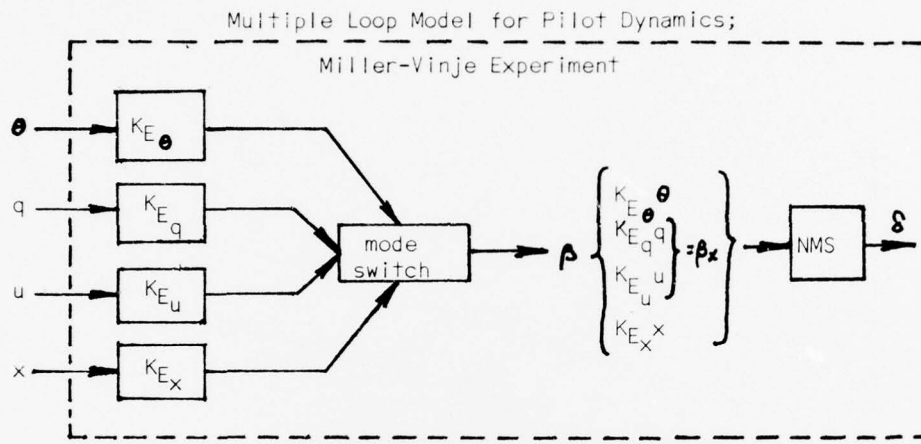


Figure 29--- Rate Signal activity Measure With a Mode-Switching Model for Pilot Dynamics -- Multiple Loop

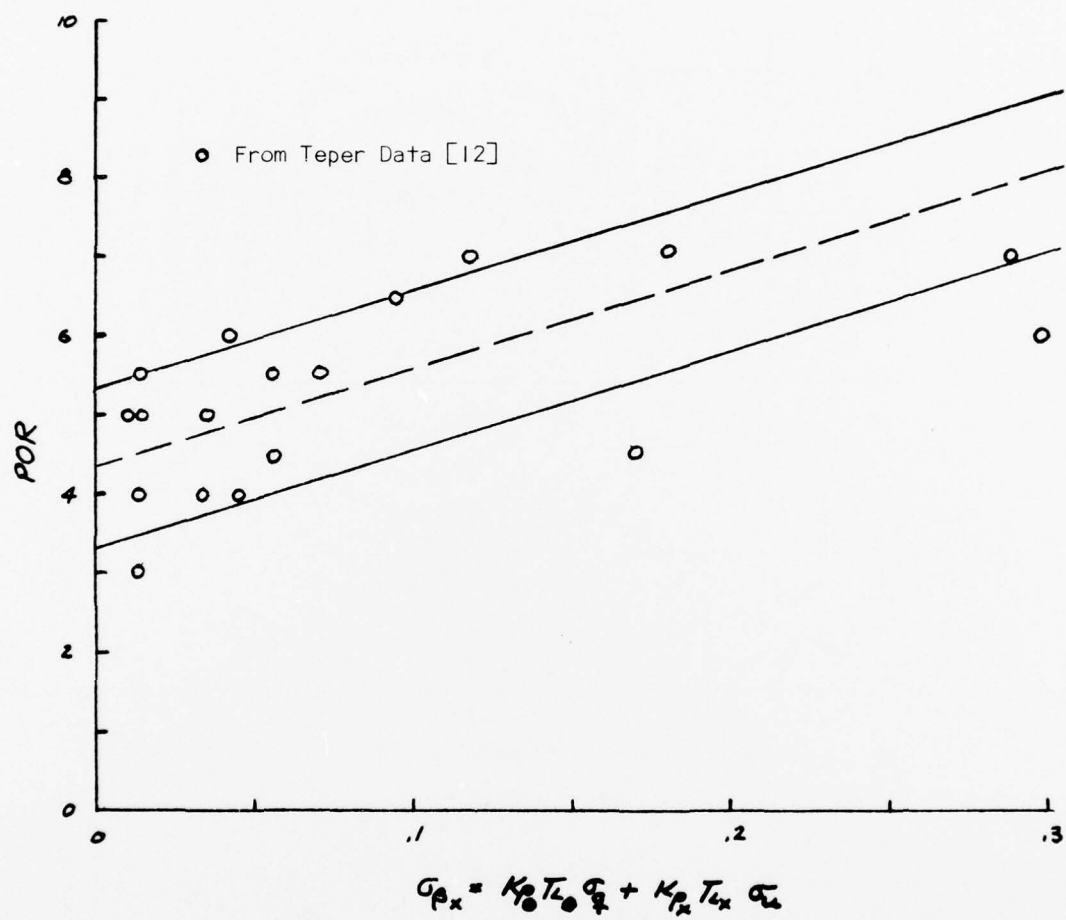


Figure 30--- Variation of Pilot Opinion Rating With σ_{px} for Multiple Loop Tracking (From Teper [12])

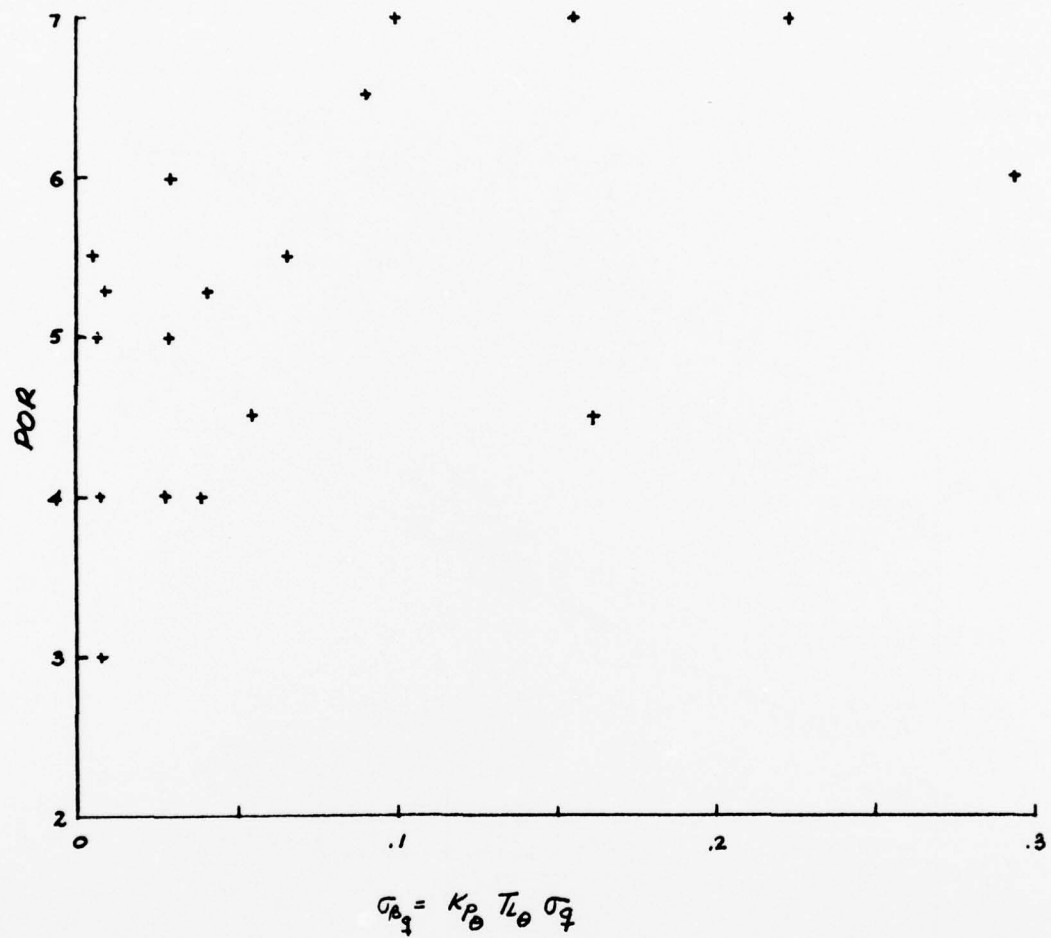


Figure 31--- Variation of Pilot Opinion Rating With σ_{P_3} for Multiple Loop Tracking (Teper Data [12])

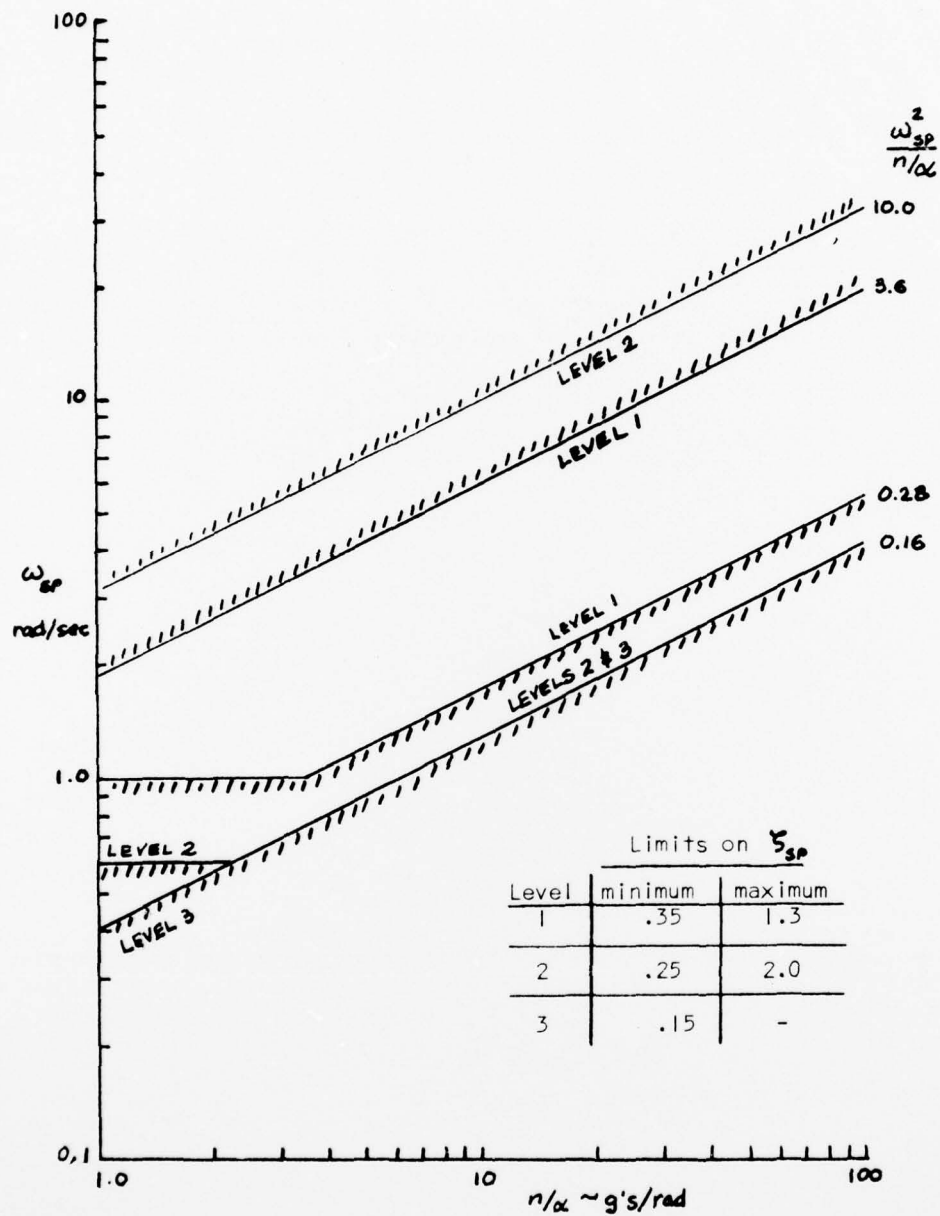


Figure 32--- Short-Period Frequency and Damping Requirements:
MIL-F-8785B; Category A

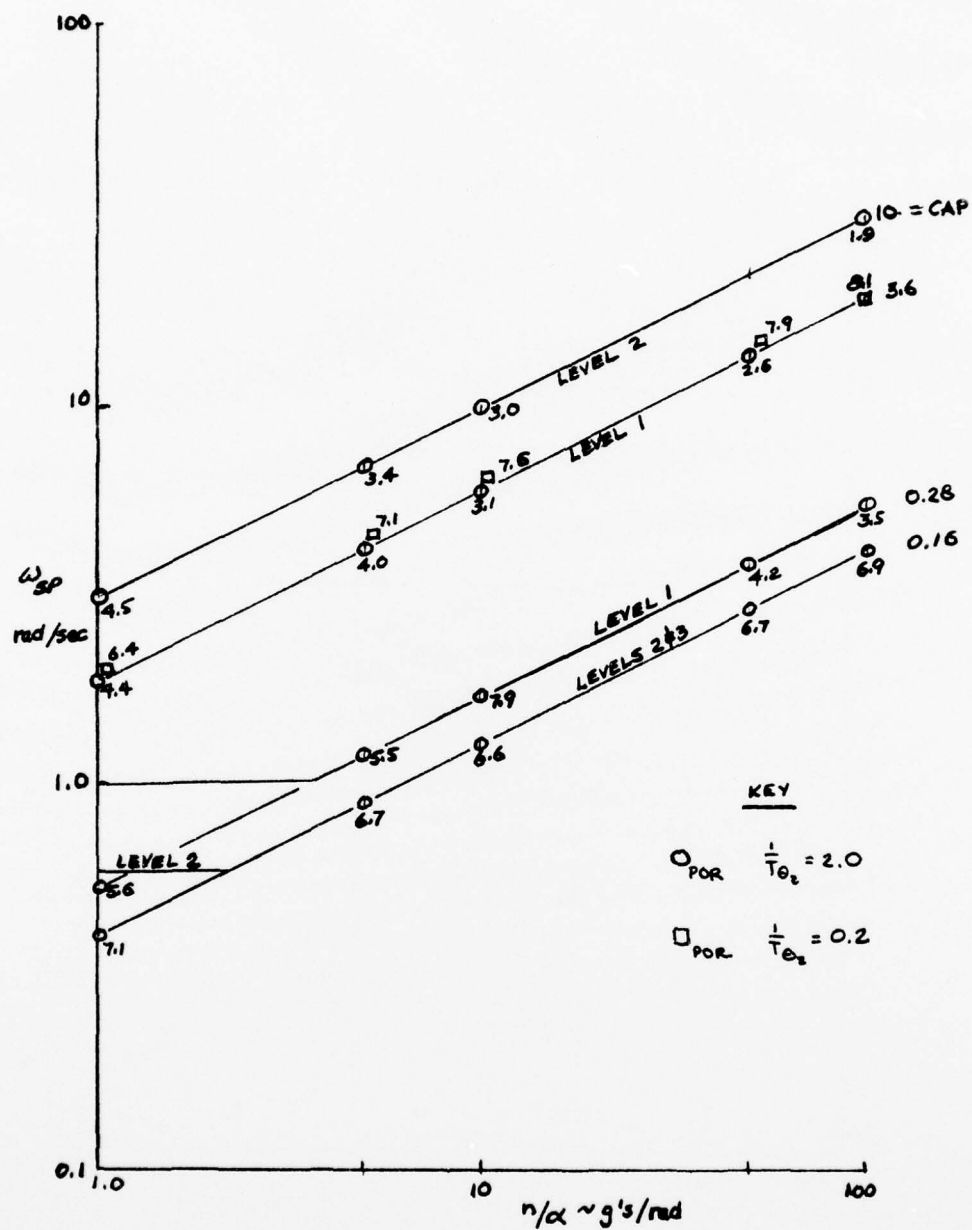


Figure 33--- Comparison of Predicted POR with MIL-F-8787B;
Case I (CAP= Parameter); $\sigma_{wg} = 10$ f/s

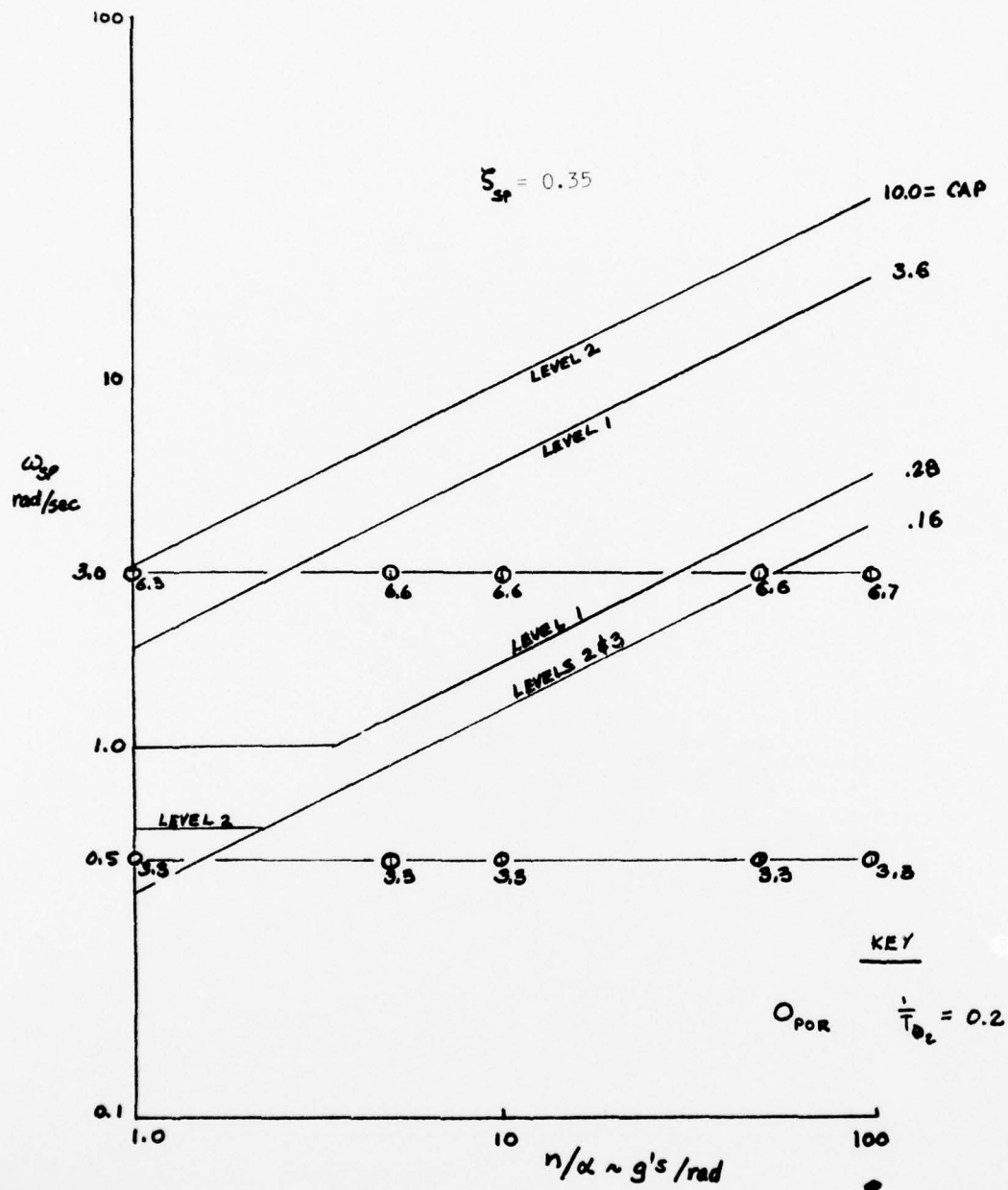
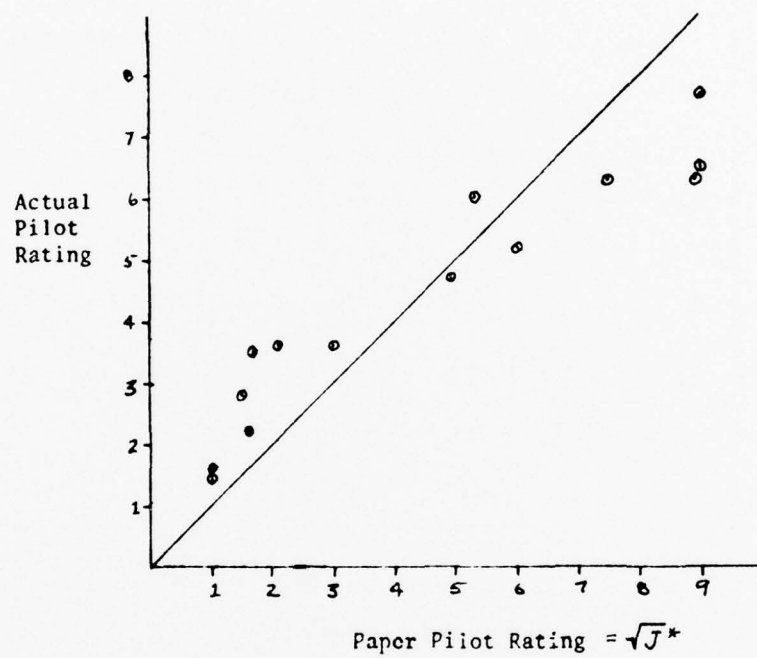
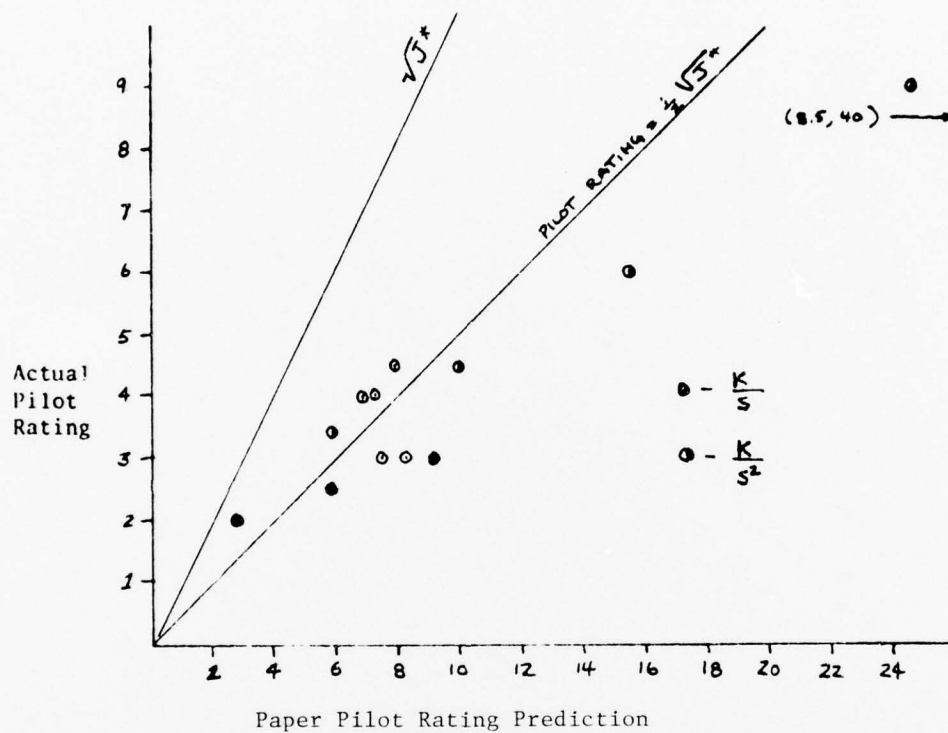


Figure 34--- Comparison of Predicted POR With MIL-F-8785B;
Case 2 (ω_{sp} = Parameter); $\sigma_{wg} = 10$ f/s



(from Dillow & Picha, reference 25, page 56)

Figure 35 -- Comparison of Paper Pilot Rating Prediction and Actual Pilot Rating for Arnold's Experiment.



(from Dillow & Picha, reference 25, page 88)

Figure 36 -- Comparison of Paper Pilot Rating Prediction and Actual Pilot Rating for McDonnell's Experiment.

REFERENCES

1. Anonymous, Military Specification, Flying Qualities of Piloted Airplanes, MIL-F-8785B (ASG), 7 August 1969.
2. Chalk, C.R., T.P. Neal, T.M. Harris, F.E. Pritchard and R.J. Woodcock, "Background Information and User Guide for MIL-F-8785B (ASG) 'Military Specification - Flying Qualities of Piloted Airplanes,'" AFFDL-TR-69-72, August 1969.
3. Anderson, R.O., "A New Approach to the Specification and Evaluation of Flying Qualities," AFFDL-TR-69-120, May 1970.
4. McRuer, Duane, Dunstan Graham, Ezra Krendel, William Reisener, Jr., "Human Pilot Dynamics in Compensatory Systems: Theory, Models and Experiments With Controlled Element and Forcing Function Variations," AFFDL-TR-65-15, July 1965.
5. Baron, Sheldon, David L. Kleinman, Duncan C. Miller, William H. Levison, and Jerome I. Elkind, "Application of Optimal Control Theory to the Prediction of Human Performance in a Complex Task," AFFDL-TR-69-81, March 1970.
6. McRuer, Duane, "Development of Pilot-in-the-Loop Analysis," J. Aircraft, Vol. 10, No. 9, Sept. 1973, pp. 515-524.
7. Stapleford, R.L., D.T. McRuer and P. Magdaleno, "Pilot Describing Function Measurements in a Multiloop Task," NASA CR-542, Aug. 1966.
8. Brissenden, Roy F., "A Study of the Human Pilot's Ability to Detect Angular Motion with Application to Control of Space Rendezvous," NASA TN D-1498, Dec. 1962.
9. McRuer, D.T., et al, "New Approaches to Human-Pilot/Vehicle Dynamic Analysis," AFFDL-TR-67-150, Feb. 1968.
10. Magdaleno, R.E. and D.T. McRuer, "Experimental Validation and Analytical Elaboration for Model's of the Pilot's Neuromuscular Subsystem in Tracking Tasks," NASA CR-1757, April 1971.
11. McRuer, D.T., R.E. Magdaleno and G.P. Moore, "A Neuromuscular Actuation System Model," paper presented at the USC-NASA Annual Manual Control Conference, March 1967.
12. Teper, Gary L., "An Assessment of the 'Paper Pilot' - An Analytical Approach to the Specification and Evaluation of Flying Qualities," AFFDL-TR-71-174, June 1972.

13. Onstott, Edward D., "Multi-Axis Pilot-Vehicle Dynamics," Proc. of the 10th Annual Conference on Manual Control, Wright-Patterson Air Force Base, Ohio, 9-11 April 1974.
14. Elkind, J.I., "Characteristics of Simple Manual Control Systems," MIT, Lincoln Laboratory, TR-111, 6 April 1956.
15. Levison, William H., Sheldon Baron and David L. Kleinman, "A Model for Human Controller Remnant," 5th Annual NASA-University Conference on Manual Control, MIT, March 27-29, 1969, NASA SP-215, pp. 171-198.
16. Jex, Henry R. and Raymond E. Magdaleno, "Corraborative Data on Normalization of Human Operator Remnant," IEEE Trans. on M-MS, p. 137-140, Dec. 1969. (reference 15 is also in this journal issue)
17. McDonnell, John D., "Pilot Rating Techniques for the Estimation and Evaluation of Handling Qualities," AFFDL-TR-68-76, December 1968.
18. Arnold, John D., "An Improved Method for Predicting Aircraft Longitudinal Handling Qualities Based on the Minimum Pilot Rating Concept," MSE Thesis GGC/MA/73-1, Air Force Institute of Technology, Wright-Patterson AFB, Ohio, June 1973.
19. Neal, T.P., and R.E. Smith, "An In-Flight Investigation to Develop Control System Design Criteria for Fighter Airplanes," Vols. I and II, AFFDL-TR-70-74, June 1970.
20. Johnson, Robert B., "Predicting Pitch Task Flying Qualities Using Paper Pilot," MSE Thesis GGC/MA/73-2, Air Force Institute of Technology, Wright-Patterson AFB, Ohio, June 1973.
21. Onstott, E.D., E.P. Salmon and R.L. McCormick, "Prediction and Evaluation of Flying Qualities in Turbulence," AFFDL-TR-71-162, Feb. 1972.
22. Naylor, Flynoy R., "Predicting Roll Task Flying Qualities with 'Paper Pilot'," MSE Thesis GAM/MA/73-1, Air Force Institute of Technology, Wright-Patterson AFB, Ohio, June 1973.
23. Miller, David P. and Edward W. Vinje, "Fixed-Base Flight Simulation Studies of VTOL Aircraft Handling Qualities in Hovering and Low-Speed Flight," AFFDL TR-67-152, January 1968.
24. Taylor, Calvin R., "Predicting Heading Task Flying Qualities With Paper Pilot," MSE Thesis GE/MA/73-1, Air Force Institute of Technology, Wright-Patterson AFB, Ohio, June 1973.

25. Dillow, James D. and Douglas G. Picha, "Application of the Optimal Pilot Model to the Analysis of Aircraft Handling Qualities," Air Force Institute of Technology, AFIT-TR-75-4, Wright-Patterson AFB, Ohio, August 1975.
26. Ashkenas, I. L. and D. T. McRuer, "A Theory of Handling Qualities Derived from Pilot-Vehicle System Considerations," Aerospace Eng. Rev., Vol. 21, No. 2, February 1962.
27. Pirsig, Robert M., Zen and the Art of Motorcycle Maintenance, Bantam Books, Toronto/New York/London, April 1975.